Use Authorization

In presenting this thesis in partial fulfillment of the requirements for an advanced degree at Idaho State University, I agree that the Library shall make it freely available for inspection. I further state that permission to download and/or print my thesis for scholarly purposes may be granted by the Dean of the Graduate School, Dean of my academic division, or by the University Librarian. It is understood that any copying or publication of this thesis for financial gain shall not be allowed without my written permission.

Signature ________________________________

Date ____________________________________

IMPLEMENTATION OF THERMOELECTRIC MODULES IN BRAYTON CYCLE FOR ELECTRIC POWER GENERATION

By

Dhiraj Tripathi

A thesis submitted in partial fulfillment of the requirements for the degree of

MASTER OF SCIENCE

IN

MECHANICAL ENGINEERING

IDAHO STATE UNIVERSITY

Spring, 2014

COMMITTEE APPROVAL

To the Graduate Faculty:

The members of the committee appointed to examine the thesis of DHIRAJ TRIPATHI find it satisfactory and recommend that it be accepted.

Dr. Richard Wabrek

Dr. Alba Perez

Dr. Mikle Ellis, Graduate Faculty Representative

ACKNOWLEDGEMENTS

I would like to express my sincere gratitude to all those who made this thesis possible. I would like to express my heartfelt thanks to my advisor, Dr. Richard Wabrek, for his continued guidance and answers to all of my questions and my co-advisors Dr. Alba Perez, who gave me this wonderful opportunity to learn and work under them. I would also like to acknowledge Dr. Brian Williams for his endless support and guidance throughout my master's degree here at Idaho State University. Without their knowledge, motivation, and support this research would not have been possible.

Lastly, I would like to express my deep appreciation to my parents and family for their motivation and support.

Table of Contents

List of Figures

List of Tables

ABSTRACT

The cost of energy harvesting processes can be optimized by increasing the efficiency of the system and reutilizing waste energy. One concept of waste heat utilization from the 10KW baseline Brayton cycle using semiconductor-based thermocouples for power generation, is demonstrated here. Bismuth Telluride-based material was selected which is suitable for tapping power from average temperature differences across the thermo elements. Each thermocouples is incorporated in a flat plate heat exchanger. The chosen material is capable of functioning under low temperatures (ranging from 300K to 400K). Exhaust heat from the Brayton cycle at 550K, 600K and 700K is reused as a heat reservoir in a flat plate heat exchanger. The flow of cooling water on the other side of the plate acts as a heat sink, thus creating a temperature gradient. The flat plate heat exchanger consists of thermocouples, which generate power by the phenomenon know as the Seebeck effect. The number of thermocouples that can be incorporated inside the plate is determined for all three different turbine exhaust temperatures. Two different approaches (to determine the overall heat transfer coefficient for the heat exchanger to obtain area of heat exchanger and heat input required for ‘n’ number of thermocouples when thermocouple is treated as a heat engine) are utilized to verify the results. Overall efficiency of the cycle is shown to improve by a small percentage, which could have real significance when utilized in larger power plants. Although some power generating plants have been built, further improvement of materials will lead to an increased figure of merit, ‘Z’, of chosen material and will help implement such technology for commercial power generation.

Chapter 1: Introduction

1.1 Background

Kelvin states in the second law of thermodynamics that it is impossible to develop a heat engine that extracts energy from a high-temperature reservoir and converts all of the energy into work[1]. A considerable portion of this energy has to be discarded to a low temperature reservoir and is known as *waste heat.* This is becoming an increasing problem in our society. The world's energy consumption has increased from 300 EJ/y in 1980 to 498.1 EJ/y in 2008. With this growth rate, the projected energy consumption will increase to 715 EJ/y by 2030, which means more energy will be wasted to fulfill our future energy needs [2]. Increased fuel costs also illustrate the need to explore better and cheaper technologies to harvest the energy in demand.

Another major concern for human beings is the rapid growth of greenhouse gases due to the industrialization and urbanization of the world in the last century. Some believe this has caused the average global surface temperature to rise from -0.33 ˚C in 1850 to 0.3 ˚C in 2000[2]. With the current rate of CO_2 emission, the projected earth's surface temperature by 2100 will be approximately 3˚C. Such anomalies in climate temperature could lead to rise in sea levels, precipitation changes, hurricanes , typhoons, and other unwanted changes in climate.

Along with the above-mentioned concerns, current technologies used in heat engines are bulky, produce noise, require periodic maintenance, and are impractical for use in hostile environments such as deep sea water, underground mines, and spacecrafts, or in rural areas where no transportations is available.

Reference Table 1.1 shows the temperature range for various processes in the Brayton, Ranking, and Combine cycles. A good source of waste heat can be found in the Brayton cycle. It gives off medium temperature exhaust gas ranging from 500-550K [3]. The General Brayton cycle has thermodynamic efficiencies of about 33% and a large amount of combustion products (gas streams exiting the turbine leave with the fuel heating value was and are not converted to work). Waste heat produced from this cycle is large enough to qualify for selection for further research on utilizing waste heat. With the use of heat exchangers, it increases to about 37%[2] but the device occupies more space, costs more, and requires more maintenance.

Table 1.1 Thermodynamic Comparison of Power Cycle [3]

	Gas Turbine	Steam Power Plant		Combined Cycle Power Plant
		With Reheat	Without Reheat	
Average temperature of the heat supplied (K)	950-1000	640-700	550-630	950-1000
Average temperature of exhaust heat (K)	500-550	320-350	320-350	320-350
Carnot efficiency(%)	42-47	45-54	37-50	63-68

1.2 Motivation

Various types of commercial equipment such as recuperators, regenerators, heat wheels, heat pipe, economizers, heat exchangers, heat recovery boilers, heat pumps, and thermo-compressors have been used to improve the efficiency of a thermodynamic cycle and recover the energy lost in waste heat. Application of such equipment has improved the efficiency of heat engines from 3% in 1821 to 60% in the present day. This suggests huge potential to apply other approaches to challenge the limit given by the second law of thermodynamics as well as overcome other problems such as bulkiness, noise, and maintenance inherited by conventional technologies [4,5].

Among such devices, the thermoelectric device is a promising technology. These devices generate electricity when exposed to temperature difference, and are thus called hence called Thermoelectric Generators (TEGs). They work on the principle known as the Seebeck effect, which states that junction of two different materials (metal/semiconductor), when exposed to temperature difference, would generate voltage signal. The open circuit voltage signal is given as:

$$V_{oc} = \alpha\,(T_h - T_c) \tag{1.1}$$

where, α is called the Seebeck coefficient. The Seebeck coefficient depends on the property of the material used and is expressed in Seebeck voltage per unit temperature (volt/Kelvin or microvolts/Kelvin). T_h is the temperature of waste heat, and T_c is the temperature of the ambient air or coolant used to retain the temperature difference. Thermoelectric devices are created by adding a number of thermoelectric modules in a specific pattern. Thermoelectric modules are built from thermocouples combined electrically in series a thermally in parallel fashion. An individual thermocouple consists of two thermo elements, which can be a combination of metals or semiconductors. The basic layout of a thermoelectric module is as shown in Table 1.2.

Table 1.2 Layout of TEG Heat Exchanger

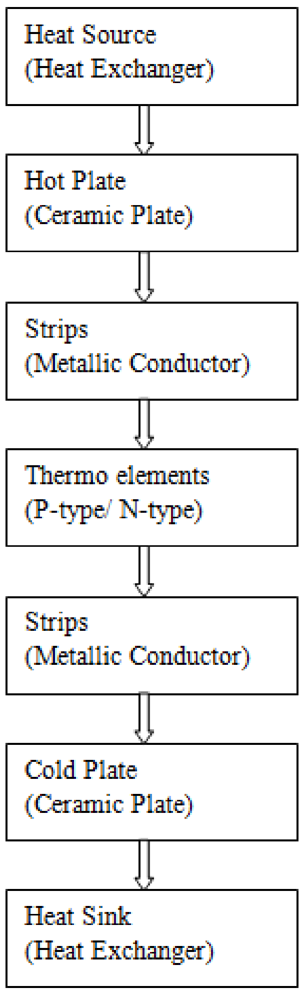

The phenomenon of the Seebeck effect was discovered back in 1821 by Thomas Johann Seebeck. He experimented with a number of metals and metal oxides, eventually developing the Seebeck series. The power generated by combining these metals listed in the Seebeck series is very low compared to power generated by semiconductor material used in the present day. Table 1.3 illustrates the Seebeck coefficient relative to platinum material, which has 5 μV/K for both metal and semiconductors. This shows the importance of using semiconductors as thermoelectric material.

Table 1.3 Seebeck Coefficients [6]

Seebeck Coefficients for Some Metals and Alloys

Metals	Seebeck Coefficient
	μV/K
Antimony	47
Nichrome	25
Molybdenum	10
Cadmium	7.5
Tungsten	7.5
Gold	6.5
Silver	6.5
Copper	6.5
Rhodium	6.0
Tantalum	4.5
Lead	4.0
Aluminum	3.5
Carbon	3.0
Mercury	0.6
Platinum	0
Sodium	-2.0
Potassium	-9.0
Nickel	-15
Constantan	-35
Bismuth	-72

Seebeck Coefficients for Some Semiconductors

Semiconductors	Seebeck Coefficient
	μV/K
Se	900
Te	500
Si	440
Ge	300
n-type Bi_2Te_3	-230
p-type $Bi_{2-x}Sb_xTe_3$	300
p-type Sb_2Te_3	185
PbTe	-180
$Pb_{03}Ge_{39}Se_{58}$	1670
$Pb_{06}Ge_{36}Se_{58}$	1410
$Pb_{09}Ge_{33}Se_{58}$	-1360
$Pb_{13}Ge_{29}Se_{58}$	-1710
$Pb_{15}Ge_{37}Se_{58}$	-1990
$SnSb_4Te_7$	25
$SnBi_4Te_7$	120
$SnBi_3Sb_1Te_7$	151
$SnBi_{2.5}Sb_{1.5}Te_7$	110
$SnBi_2Sb_2Te_7$	90
$PbBi_4Te_7$	-53

Further research in semiconductor materials has led to the creation of thermoelectric modules, which are compact, silent, and reliable, and require minimum maintenance. These devices can operate continuously for a longer period of time, are flexible power sources, and can achieve high figures of merit for material suitable for lower temperature ranges[7]. Emerging fields are beginning to use thin films, nanostructures, super lattice structures formed from quantum wells, and quantum wires. This allows for better control of the material properties, thus increasing the power output compared to bulk materials being used conventionally[8]. The performance of materials in use is given by figure of merit ‘Z’ as given in equation 1.2:

$$Z = \frac{\sigma\,\alpha^2}{\kappa} \tag{1.2}$$

where σ is the electrical conductivity (siemens/m), $K$is the thermal conductivity (W/m^{2}K), and α (μV/K) is the Seebeck coefficient. These properties are material-dependent, and semiconductors in use today are altered in their material properties and named as negative/positive type, depending on the majority charge carrier (electron/hole) obtained after doping intrinsic (natural) semiconductors. Suitable thermoelectric material must demonstrate high electrical conductivity and Seebeck coefficient, but low thermal conductivity. Table 1.4 provides some basic parameters used to select thermo elements to form TEGs.

Table 1.4 Properties of Thermoelectric Material

Material	Composition	Material Type	Applicable Temperature (°C)	Optimum ZT	Refer
Oxide-based	$NaCo_2O_4$	p	30-500	1.20	[9]
PbTe-based	PbTe	n	230-577	0.70	
Zn_4Sb_3-based	$Zn_4(Sb_{0.97}Sn_{0.03})_3$	p	230 – 480	1	
	Zn_4Sb_3	p	230 – 480	1.22	
ZnSb-based	$Zn_{0.346}Sb_{0.643}Sn_{0.01}Ag_{0.001}$	p	60-177	0.8-1.22	[10]
MnTe	$Na_{0.01}Mn_{.99}Te$	p	500-550	1.5-1.75	
PbTe-based	PbTe $Na_{0.3}$	p	45-100	1.3	
Bi_2Te_3-based	$(Sb_{0.8}Bi_{0.2})_2 Te_3$	p	25-75	1.1	[11]
	$Bi_2(Te_{0.8}Se_{0.2})_3$	n	25-150	0.8	

Application of such thermoelectric modules, in conjunction with conventional heat recovery technologies, has the potential to further improve the Brayton cycle efficiency. Thus, it is worth considering the application of thermoelectric modules on freely available exhaust heat sources to improve the efficieny of the Brayton cycle. This thesis aims to explore the material requirements, sizing, cost benefits, and ergonomics of this application.

1.3 Objective

The objective of this thesis is to investigate the use of practical thermoelectric power generation devices for waste-heat recovery from traditional thermodynamic cycle power plants. This effort will include the selection of candidate thermoelectric materials, thermodynamic analysis of the overall plant efficiency, and sizing of the thermoelectric module at various exhaust temperature.

1.4 Method and Approach

- Survey of waste heat sources will be demonstrated through reference to published data. It includes the classification of waste heat sources as high, medium, and low quality heat. Justification for the selection of exhaust heat from the Brayton cycle is given.
- Examination of various technologies used to recover waste heat leads to the selection of thermoelectric devices as a convenient technology for present study.
- Survey of thermoelectric materials with reference to published data will be conducted. This survey will include the study of applicable temperature ranges of these materials, the study of properties such as the Seebeck coefficient, electrical conductivity, and thermal conductivity, and changes in materials associated with changes in temperature of the heat source.
- Based on the reference data, an exemplary bismuth telluride (BiTe) based thermoelectric material is chosen for recovery of waste heat from the Brayton cycle.
- Recovery of waste heat from the Brayton cycle using the BiTe-based thermoelectric material accounts for changes in overall efficiency of the Brayton cycle. Further

calculation will help estimate overall efficiency of the cycle along with the power produced by each TEG module.

- With confirmation of the technology and material used to improve the efficiency of the Brayton cycle, the temperature profile across the BiTe-based thermoelectric plate will be obtained. This will help to estimate the electrical power generated across the plate, based on the variation of the temperature profile. Thus, with the knowledge of electrical power output from individual thermoelectric couples, sizing of the thermoelectric device for this particular case is obtained.

1.5 Sources of Waste Heat and Recovery Device in Use

Waste heat is the remaining source of heat released into the atmosphere due to the combustion of fuel or any chemical reaction which could not be utilized during a process. Huge amounts of waste heat are produced from kilns, cooling towers, boilers, engine exhaust and nozzles. Tables 1.5, 1.6, and 1.7 shows the industrial sources of waste heat along with their temperature ranges and classify them as high, medium, or low sources of heat.

Table 1.5 Sources of High temperature Waste Heat [12]

Types of Devices	Temperature (^0C)
Nickel refining furnace	1370 – 1650
Aluminium refining furnace	650 –760
Zinc refining furnace	760 – 1100
Copper refining furnace	760 – 815
Steel heating furnace	925 – 1050
Copper reverberatory furnace	900 – 1100
Open hearth furnace	650 – 700
Cement kiln (Dry process)	620 – 730
Glass melting furnace	1000 – 1550
Hydrogen plants	650 – 1000
Solid waste incinerators	650 – 1000
Fume incinerators	650 – 1450

Table 1.6 Sources of Medium Temperature Waste Heat [12].

Types of Devices	Temperature (^0C)
Steam boiler exhaust	230 – 480
Gas turbine exhaust	370 – 540
Reciprocating engine exhaust	315 – 600
Reciprocating engine exhaust (turbo charged)	230 – 370
Heat treatment furnace	425 – 650
Drying & baking ovens	230 – 600
Catalytic crackers	425 – 650
Annealing furnace cooling systems	425 – 650

Table 1.7 Sources of Low Temperature Waste Heat [12].

Source	Temperature ^{0}C
Process steam condensate	55-88
Cooling water from: Furnace doors	32-55
Bearings	32-88
Welding machines	32-88
Injection molding machines	32-88
Annealing furnaces	66-230
Forming dies	27-88
Air compressors	27-50
Pumps	27-88
Internal combustion engines	66-120
Air conditioning and refrigeration condensers	32–43
Liquid still condensers	32-88
Drying, baking and curing ovens	93-230
Hot processed liquids	32-232
Hot processed solids	93-232

Various devices are used to recover the heat being wasted from these sources depending on the quality of heat, medium of heat flow, and cost of installing heat recovery equipment. As discussed in sections 1.1 and 1.2, the need for a more energy-efficient device has motivated researchers to come up with cheap, easy-to-maintain, efficient, energy-recovering devices. Some of the typical heat recovering devices used in industries at present are recuperators – (work as heat exchangers), regenerators, and heat wheels (wheels rotate between high and low temperature ducts and heat pipes), as well as other devices such as economizers, heat exchangers, and heat pumps. All of these devices have a limitation of recirculation of the low grade heat source and do not produce any other form of energy (chemical, electrical, potential, kinetic) which could have been harnessed and used more conveniently.

Other technologies, such as thermionic emission, convert heat sources into electricity but are only efficient at temperatures of about 1000˚C and are only capable of producing high power density. Recently, physicists at the University of Utah have developed a device that is capable of turning heat into sound and sound into electricity [13]. Furthermore, the radioisotope-thermoelectric generator (RTG) has been used to power satellites and space probes. This technology uses a thermoelectric material which receives heat from radioactive decay and had been used in the space probe Voyager 1. Thus, in general thermoelectric materials have been studied and most extensively used as direct energy conversion tools. Applications of these materials can be found in cooling electronic equipment (chips), power vehicle accessories (for recovering waste heat from the exhaust pipe), and Radioisotope-Powered TEGs for power supply in hostile regions (for durations too long to be supplied by cell power), gas-heated power supplies for radio receivers, radiation measuring thermocouples, and thermopiles. Other applications include a small thermoelectric power plant installed in Japan which utilizes the heat from an incinerator.

1.6 Concept of TEG in Brayton Cycle

The Brayton cycle is an ideal cycle for gas-turbine engines. Exhaust gas from the cycle is a source of medium temperature heat which can be circulated through a heat exchanger consisting of thermoelectric modules to generate electricity. It can also operate as an open or closed cycle.

Open Brayton cycle:

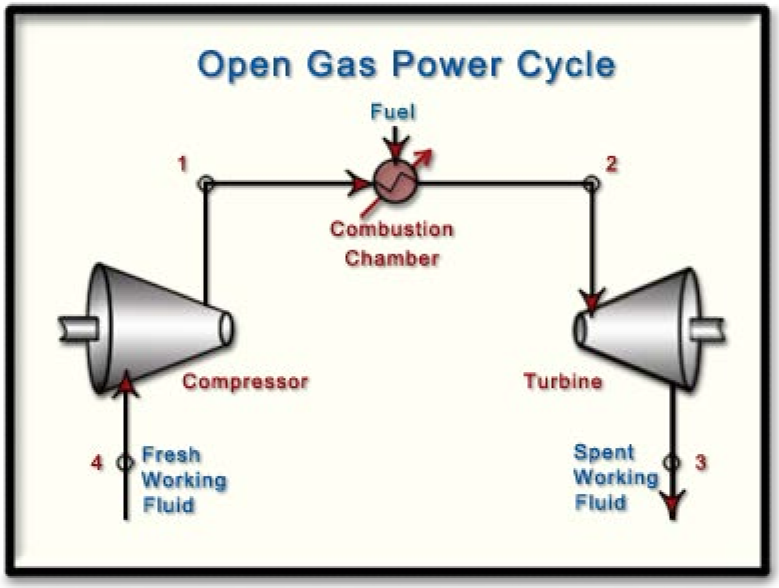

Figure 1.1 Open Brayton Cycle [14]

In this cycle air at ambient temperature undergoes compression which causes the air temperature and pressure to rise. After compression the air flows into a combustion chamber where fuel is burned at constant pressure, which results in high temperature combustion gas. This gas is then passed through the turbine, which expands to the atmospheric pressure. This change in pressure imparts kinetic energy to the turbine, thus producing shaft work. At the end stage, the combustion gas is exhausted from the turbine.

Closed Brayton cycle:

Working fluid in the closed Brayton cycle undergoes the same process as that in the open cycle, except that the heat addition to the working fluid in the combustion chamber is a constant pressure process with an external heat source and heat exchanger. In addition, the exhaust gas from the turbine is passed through a heat exchanger which rejects heat to the ambient air at constant pressure.

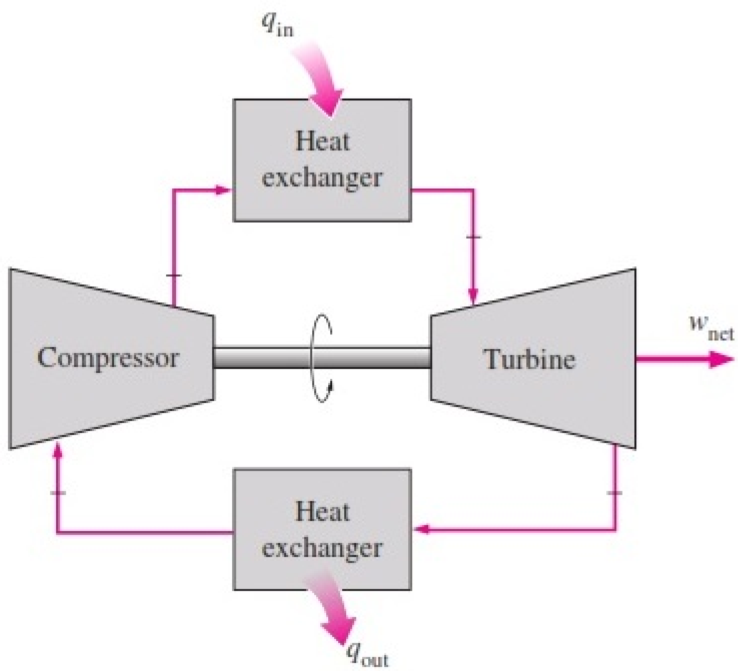

Figure 1.2 Closed Brayton Cycle [15]

In the present study, a closed Brayton cycle was selected, in which the exhaust gas circulates through the heat exchanger and has a temperature of 550K on the hot side. This temperature is a general industrial operation thumb rule, as temperatures below 423K are likely to cause corrosion due to condensation [12]. As an example, flat plate heat exchangers can be used to release exhaust heat into the cooling fluid. These flat plate heat exchangers consist of thermoelectric couples built and arranged into the flat plate. The flat plate is exposed to hot exhaust gas on one side and cooling water on the other side, thus creating a temperature difference. Also, closed Brayton cycles have been used in combination with combined cycle gas turbines for electric power generation. In the future, closed Brayton cycles may be used in tandem with high temperature solar panel and space exploration. Illustration of the thermoelectric heat exchanger plate is shown in Figures 1.3 and 1.4.

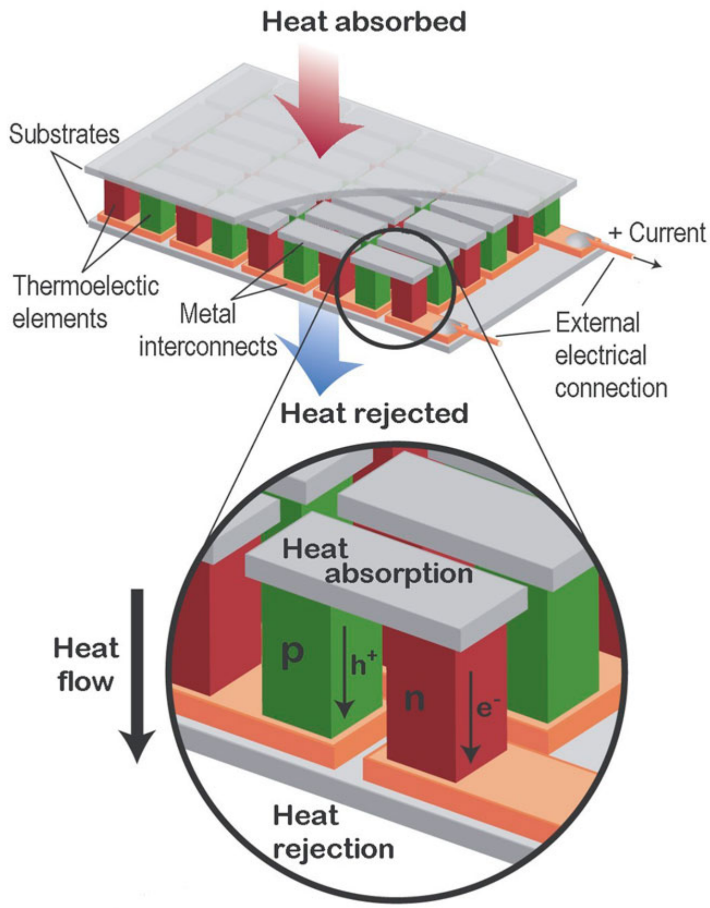

Figure 1.3 Flat Plate Inbuilt With Series of TEG[7]

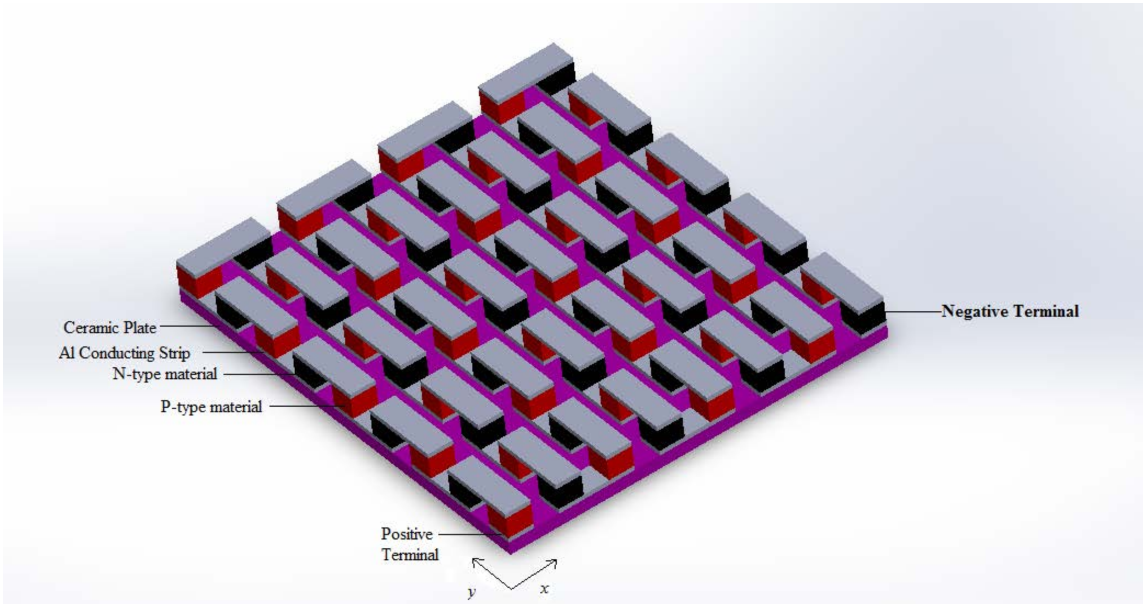

Figure 1.4 Isometric View of a Module without Top Ceramic Plate

As shown in Figure 1.4, the TEG heat exchanger is built from a ceramic insulator/plate followed by conducting metallic strips, semiconducting material, another layer of conducting metallic strip and a second ceramic insulator/plate on the top to cover the module. An array of thermoelectric elements have been sandwiched between two ceramic plates, with hot exhaust gas on one side and cold water flowing on the other side. The number of thermocouples used is 71. The cross sectional area of each thermo element, including an air gap is :- $a = 1.4mm \times 1.4mm$. A close view of each thermocouple along with dimension is shown in Figure 1.5.

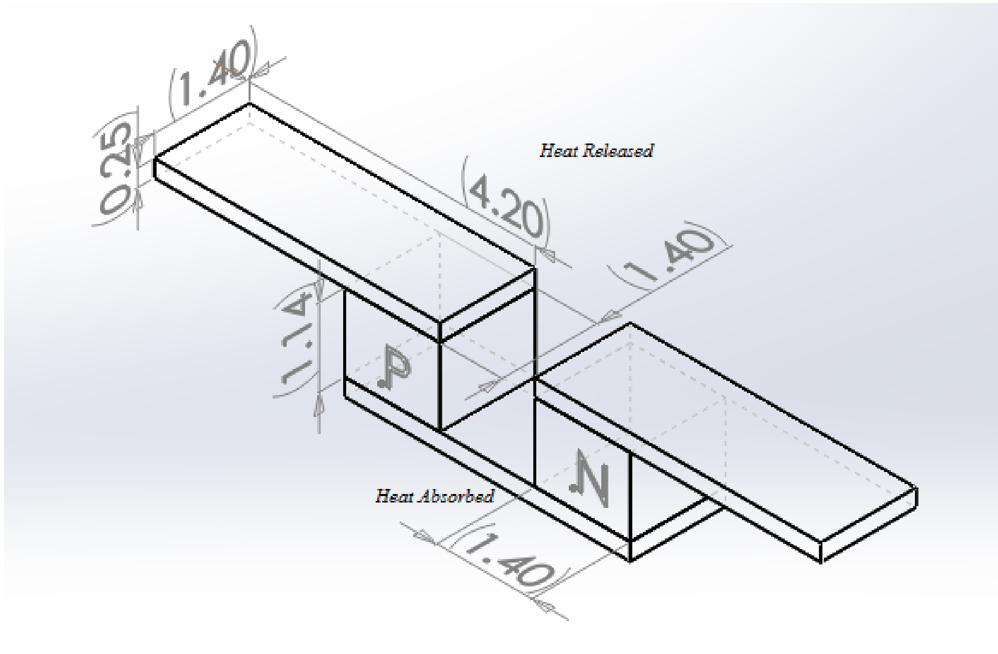

Figure 1.5 Dimension of Thermo Electric Elements

Chapter 2: Selection of Thermoelectric Materials

2.1 Semiconductor as TEG

Material having a high figure of merit (def. section 1.2) are ideal candidate for use as TEGs. Some of the requirements for conduction of heat in solid material are:

1. Free electrons or holes.
2. Phonons – caused by lattice vibration (motion of atoms in a solid/crystal structure around an equilibrium position)
3. Electron-hole pairs
4. Excitons (electron hole pair in motion caused by absorption of photons; pairs are bounded within each other's electrostatic field)

In the case of solid semiconductors used as TEGs, the dominant means of heat transfer is due to conduction/scattering of free electrons or holes and phonon conduction.

In the case of solid metals, the dominant requirement for heat conduction is free electrons, which contributes to both electrical and thermal conductivity, as suggested by the Wiedemann-Franz-Lorenz law. This law is based on experimental observation, and states that the ratio of thermal conductivity, κ(due to conduction electron), to the electrical conductivity, σ, is constant in the case of large numbers of metals and metal alloys within fixed temperature ranges. In addition, this ratio is proportional to the absolute temperature T. The proportionality constant is called the Lorenz number. The Lorenz number is given as $\frac{\kappa}{\sigma T} = 2.45 \times 10^{-8} watt - ohm/°K^2$. Some metals shows deviation from the Wiedemann-Franz-Lorenz law at room temperatures. Solid state theory considers the interaction of electrons with lattice vibration, which explains the reason for deviation from the Wiedemann-Franz-Lorenz law. For example, Beryllium (Be) at room temperature does not follow the law due to the higher Debye temperature for this metal. At temperatures below the Debye temperature, quantum effects can be observed. Further discussion regarding the causes of violation of the Wiedemann-Franz-Lorenz law is omitted here as it deals more with treatment of electrons and phonons in solid state physics.

A general observation of equation 1.2 shows that in the case of metal, increase in the Seebeck coefficient(s) leads to increase in figure of merit, which is about 100 microvolts per degree Kelvin, whereas κ/σ is constant at a given temperature, as suggested by the Wiedemann-Franz-Lorenz law, with of the exception of some metals[10]. Thus, the possible increase of figure of merit is limited in the case of metals.

In the case of semiconductors, the absolute value of the Seebeck coefficient (consisting of one type of charge carrier p-type or n-type) can reach approximately 1000 microvolts per degree Kelvin, which gives a high figure of merit compared to any other metal. However, this comes at the cost of increasing the ratio of thermal conductivity (κ) to electrical conductivity (σ) . All three properties defining figure of merit depend on density of conduction electron and holes. This dependence is well illustrated by Figure1.6 as the Seebeck coefficient decreases, electrical conductivity increases, and total thermal conductivity increases with increase in charge carrier density. In general, the figure of merit can be optimized by varying three basic conduction electron and hole density-dependent parameters.

The total thermal conductivity in the case of semiconductors consists of two parts: an electronic thermal conductivity, and conduction due to lattice vibration: $\kappa = \kappa_{el} + \kappa_l$.

Conduction due to lattice vibration is same as in insulators or metals. However, electronic thermal conductivity depends on free electron density, and this density is more abundant in highly doped semiconductors compared to insulators/metals thus increasing the total thermal conductivity.

The electrical conductivity (σ) also depends on the density of the charge carriers, as given in equation 2.1[16]:

$$\sigma = ne^2 < \tau > / m^* \tag{2.1}$$

where,

$n =$ number of charge carriers per unit cube

$e =$ charge of carrier

$< \tau > =$ average relaxation time

$m^* =$ effective mass of the carrier

Thus, doped semiconductors with approximate carrier concentration of 10^{19}cm^3 have all the carrier density-dependent parameters at optimum values, and provide the best figure of merit compared to metals/insulators [16]. This value of carrier concentration can be tuned by controlled doping of the semiconductor, thus making the semiconductor suitable to be used as a TEG.

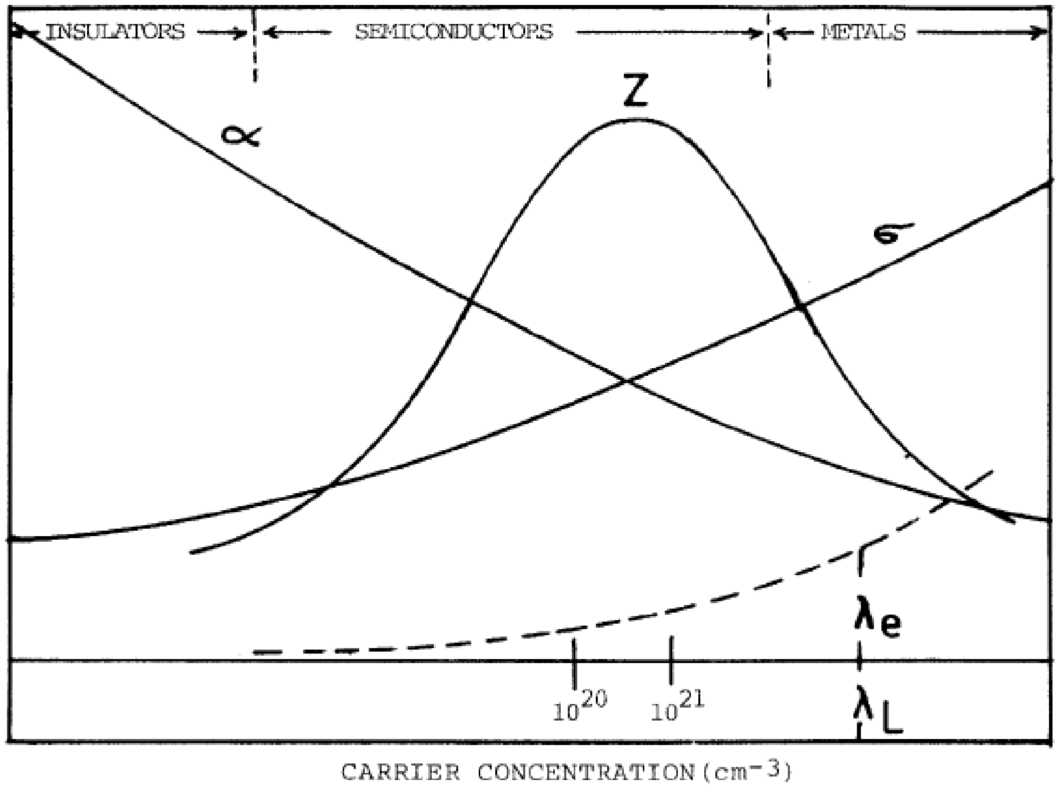

Figure 2.1 Schematic of how Seebeck Coefficient, Electrical Conductivity, Thermal Conductivity Depend on Concentration of Charge Carriers [8].

2.2 Properties of Thermoelectric Material

TEGs produce electricity based on temperature difference across the TEG module. Thus, we must direct attention to the changes occurring in the properties of the materials used, as well as electricity produced through changes in the temperature profile across the module surface. The changes associated with such devices depend on the specific nature of the charge carrier, which depends on the atomic structure of the material in use. Thus it is necessary to understand changes in material properties within a given temperature range.

Other parameters such as the type of semiconductor (intrinsic/extrinsic, level of doping), material used to solder adjunct parts (electrodes), operating environment (condensation at cooling side, corrosive property), thermal stress during operation, and arrangement of TEG modules (single array/cascaded array of TEG module) all contribute to changes in material properties and optimum power produced. But, our discussion will be confined to changes in electrical conductivity (σ), thermal conductivity (κ), and the Seebeck coefficient(α) resulting from change in temperature.

2.2.1 Effect of Temperature on Electrical Conductivity

Recent TEGs in use are extrinsic semiconductors, and the doping level is optimized in every possible way to result in highest figure of merit 'Z' for that particular material at a given temperature. Thus our focus will be on the effect of temperature on extrinsic semiconductors.

Introducing external impurities (atoms/dopant), consisting of donor valence electrons, produces additional electrons in the valence band of that substance and forms an n-type extrinsic semiconductor. Because donor electrons are attracted by impure parent atom, the force required to excite these electrons is much less than that required by electrons in the valence bond. This force is called "donor activation energy". It can be illustrated using the band structure/energy level of electrons, as shown in Figure 2.2.

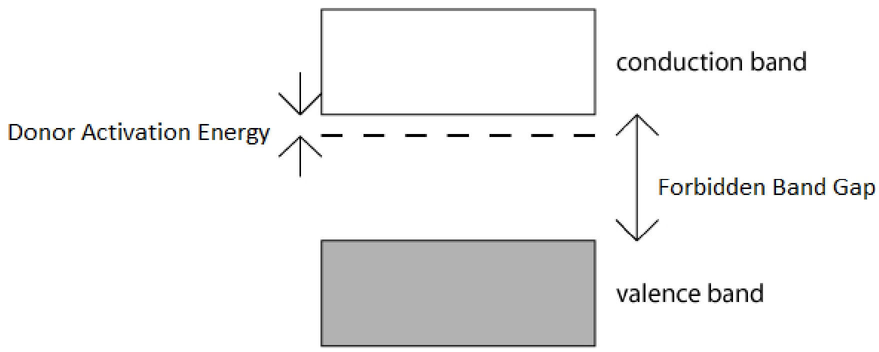

Figure 2.2 Band Structure for N-Type Semiconductor

Before doping (intrinsic semiconductor) the valence band is completely filled at absolute zero. With the increase in temperature, thermal excitation causes some electrons to jump into conduction bands with an equal number of holes in the valence band.

After doping, the energy level of the extra electrons is in the forbidden band, and very close to the bottom of the conduction band. Thus, minimal thermal excitation can promote electrons to the conduction band. In this case, donor electrons contributing to conduction electrons do not create electron deficiencies (holes) in the valence band, as none of the electrons in the intrinsic semiconductor bond structure are altered. Thus, without any vacancy in the bond structure, other bond electrons cannot move in (i.e. the donor electron does not create a hole as it leaves its position, creating an n-type extrinsic semiconductor).

Introducing external impurities (atoms/dopant) consisting of deficient elements, as compared to the valence electrons of the substance being doped, produces an electron deficiency (hole) in the valence band of that substance. This forms a p-type extrinsic semiconductor. Due to presence of a hole, electrons from neighboring bonds can move into this hole, creating another hole in the atomic structure. Thus, a hole moves in the opposite direction of the electron, and the energy required to move the electron to the hole is called “acceptor activation energy”. It can be illustrated using the band structure/energy level of hole, as shown in Figure 2.3:

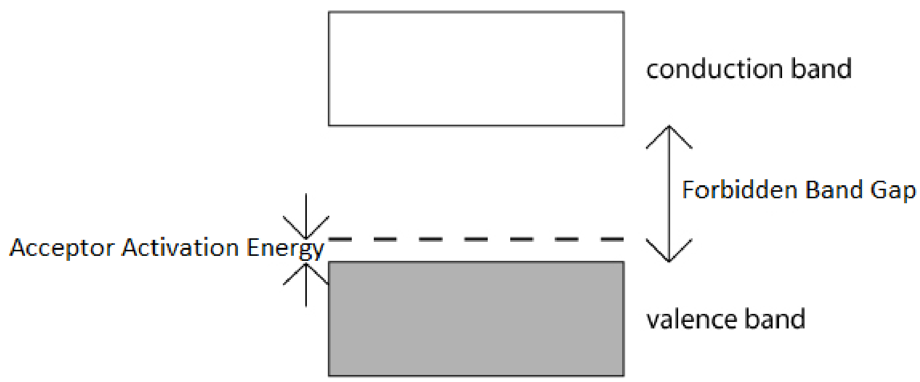

Figure 2.3 Band Structure for P-Type Semiconductor

After doping, the energy level of the hole is in the forbidden band and is close to the top of valence band. Thus, minimal thermal excitation can promote holes to the valence band. Such material is called a “p-type extrinsic semiconductor”. In addition, note that holes do not create electrons in the conduction band. As mentioned earlier, donor energy levels (n-type) and acceptor energy levels (p-type) lie in the forbidden energy gap. The energy level in the forbidden band, which has a 50% probability of being occupied, is called the “Fermi level”. The location of the Fermi level can be determined based on the number of charge carriers and their dependence on temperature. In the case of p-type semiconductors, electrons in the valence band can be excited into the acceptor level at temperatures much lower than the temperature required for excitation into the conduction band. Thus, at lower temperatures, the number of holes in the valence band in p-type semiconductors will be much higher than the number of electrons in the conduction band. Lower temperatures in this case refer to limiting the temperature beyond which both the impurity levels and valence electrons are ionized (atom/molecule with a net electric charge due to the loss or gain of one or more electrons). Furthermore, ionization or increase in temperature causes the material to behave like intrinsic material. This is due to lack of acceptor energy levels (p-type) and electrons in the valence band at high temperatures. Both the carriers being ionized and the material itself go to intrinsic temperature range.

Below the intrinsic temperature range, the Fermi level must be in the bottom half of the forbidden band gap in the case of p-type semiconductors. In addition, the net charge of the material in use per unit volume must be maintained. Thus, in case of p-type semiconductor,

Number of holes per unit volume in valence band = Number of electrons per unit volume in acceptor level+ Number of electrons per unit volume in the conduction band.

$$p = 2N_v\left[1 - \frac{1}{exp\left[-\frac{\epsilon_f}{KT}+1\right]}\right] = \left[\frac{N_a}{exp[(\epsilon_a - \epsilon_f)/(KT)]+1}\right] + \left[\frac{2N_c}{exp[(\epsilon_g - \epsilon_f)/(KT)]+1}\right] \qquad (2.2.1.1)$$ [16]

$\epsilon_a = energy\ level\ of\ acceptor\ in\ forbidden\ band$

$\epsilon_g = energy\ level\ at\ the\ bottom\ of\ the\ conduction\ band$

$N_a = number\ of\ acceptor\ level$

$N_v = number\ of energy\ level\ in\ valence\ band$

$N_c = number\ of energy\ level\ in\ conduction\ band$

$\epsilon_f = fermi\ level\ energy$

$K = Boltzmann\ constant\ (8.617\,3324(78) \times 10^{-5} eV/K)$

$T = Absolute\ temperature$

Note: Assume energy level (ϵ) at the top of the valence band is zero as the band diagram represents only the energy difference in the valence shell of an atom.

Equation 2.2.1.1 [16] can be solved for Fermi energy level. This equation depends on various energy levels in the band, number of charge carriers at various energy bands and temperature applied to the material. Thus, the Fermi level changes based on characteristics of the material after doping and temperature. When the temperature is significantly below the intrinsic range for p-type material, the number of electrons in the conduction band will be negligible compared to number of holes in the valence band. It can be assumed that if the temperature is high enough, but just below the intrinsic range, an expression for Fermi level as a function of temperature and number of acceptor state per unit volume can be obtained. If the temperature is increased, the hole concentration becomes equivalent to the acceptor level (i.e. more of the acceptor level is occupied). When the Fermi level has increased to $4KT$greater than the acceptor energy level the material reaches a saturation point: i.e. small percentage of acceptor states will be available. Thus at this temperature the material enters a transition range between extrinsic and intrinsic conduction.

Increase in temperature causes the Fermi level to move halfway between the energy gap and the top of the valence band and acceptor state for p-type semiconductors. The above discussion can also be seen in Figure 2.4, which shows the temperature dependence of the Fermi level with specific impurity concentration (n-type/ p-type).

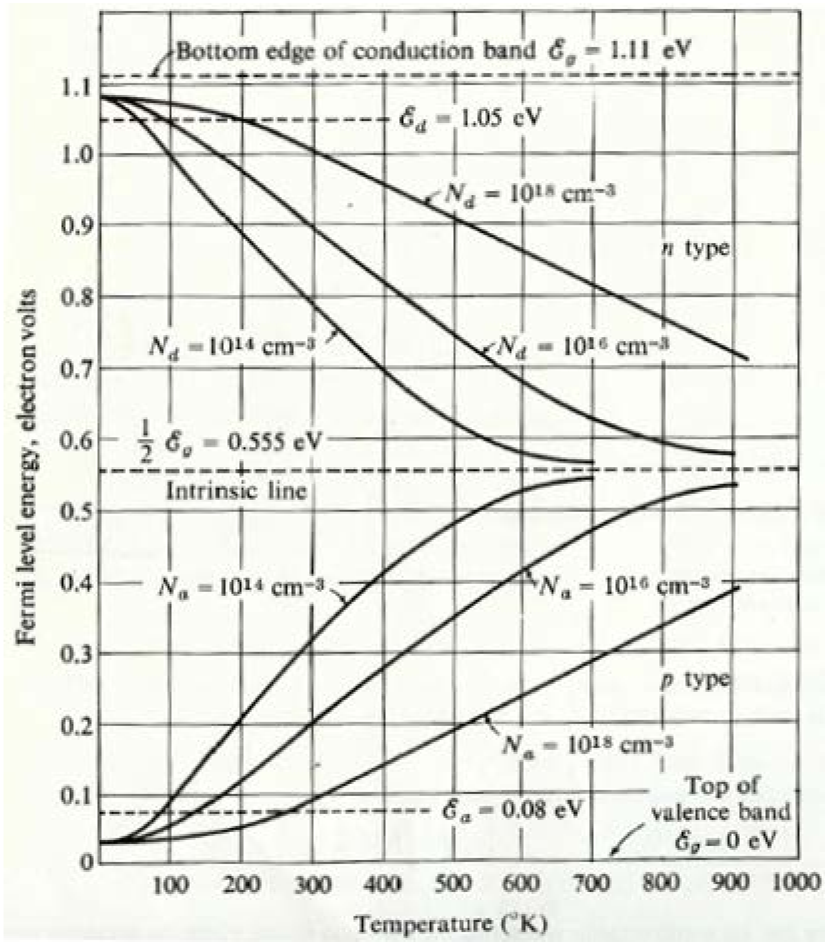

Figure 2.4 Variation of the Fermi Level with Temperature for Silicon as a Function of Impurity Level [16]

In sum, in the case of intrinsic types, the number of electrons is equal to the number of holes, and Fermi level is at the center of the forbidden gap. In the case of an n-type semiconductor, the number of electrons is greater and number of holes is less than in intrinsic types, causing the Fermi level to move toward the upper half of the conduction band. In the case of p-type semiconductors, the number of electrons is lesss while number of holes is greater than in intrinsic types, causing the Fermi level to move downward closer to the valence band.

In n-type semiconductors, donor electrons are the source for intrinsically produced electrons, which increase with an increase in temperature and reach a saturation level. This causes the material to behave like intrinsic material which causes the Fermi level to move down to the intrinsic Fermi level line. Similarly, for p-type semiconductors, as the temperature increases, material becomes more intrinsic and the Fermi level moves up to the intrinsic Fermi level line. Thus both n- and p-type semiconductors become more and more intrinsic at higher temperatures. The temperature range limits for extrinsic semiconductors are shown in Figure 2.5. This saturation level in extrinsic semiconductors also shows that the conductivity below the intrinsic temperature range is high for an extrinsic semiconductor. This is because of the maximum donor level available for conduction in this range.

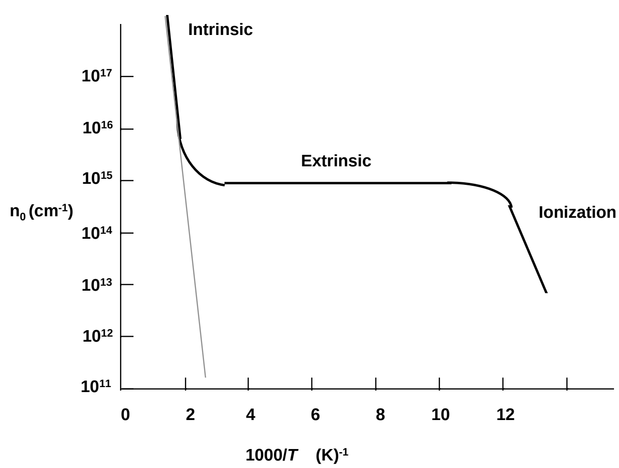

Figure 2.5 Temperature Dependence of ‘n’ for Doped Semiconductor [16]

In the case of mixed types of extrinsic semiconductors, conductivity is defined by equation 2.2.1.2, which is derived using transport theory [16].

$$\sigma = e(n\mu_n + p\mu_p) \tag{2.2.1.2}$$

where,

$\sigma =$electrical conductivity (S/m)

$e =$ charge of carrier (C)

$n =$ number of electrons per unit volume in conduction band

$\mu_n =$ mobility of n-type carriers (m^2/(V.s))

$p =$ number of hole per unit volume in valence band

$\mu_p =$ mobility of p-type carriers (m^2/(V.s))

Note: Mobility indicates the rate of flow of the charge carrier when an electric field is applied. It is given as the ratio of average drift velocity of charge carrier per unit electric field.

If the semiconductor is n-type left term, $\sigma \approx e(n\mu_n)$ and if it is p-type right term, $\sigma \approx e(p\mu_p)$ electrical conductivity is defined by equation 2.2.1.2. This is due to the dominance of electrons and holes in respective types of material. Various theoretical/experimental data based on the above discussion can be found the literature. Some of the plots on electrical conductivity vs. temperature will be presented in section 2.3.

2.2.2 Effect of Temperature on Thermal Conductivity

Thermal conductivity in a semiconductor is due to two factors: electronic thermal conduction and conduction due to lattice vibration (Refer section 2.1). Electronic thermal conductivity depends on carrier concentration, unlike lattice vibration, thus contributing to an increase in total thermal conductivity of semiconductors (Refer figure2.1). Carrier concentration (electron/holes) in the conduction band and valence band also depends on temperature the material is exposed to. Thus total thermal conductivity depends on the Fermi level in the forbidden band, which depends on the temperature applied to the material.

2.2.3 Effect of Temperature on Seebeck effect

The Seebeck effect can be observed when heat is applied to one of the two different metal/extrinsic semiconductor junctions, creating temperature difference. It produces direct current between the two materials due to the flow of electrons towards the cooler thermo element. TEGs requires a large Seebeck coefficient and low thermal conductivity to achieve higher temperature differences between the two junctions. Also, minimum electrical resistivity reduces joule heating along the thermo elements.

These thermocouples can be arranged in series to meet the required voltage or in a parallel pattern to increase the current available. The Seebeck coefficient increases with increase in extrinsic charge carrier (Refer Figure2.1). Again, the Fermi level will depend on the temperature of each number of charge carriers (Refer figure 2.4). The temperature to which the semi-conductor materials are exposed can transform them from extrinsic to intrinsic types, depending on the material properties. Thus, the Seebeck effect depends on the temperature applied to the material.

2.3 Selection of TEG module

Tremendous research has been conducted to improvise the three parameters (Refer section 2.2) of TEG material. In general commercially promising TEG materials have been classified based on applicable temperature ranges as shown in figure 2.6. where 'ZT' defines the capacity of a given material to efficiently produce thermoelectric power. It is also called "figure of merit" which is a dimensionless quantity to describe the performance of thermoelectric material. Based on the temperature profile for exhaust gas obtained in section 3.3, the average temperature across TEG plates lies from $20°C$ to $100°C$.

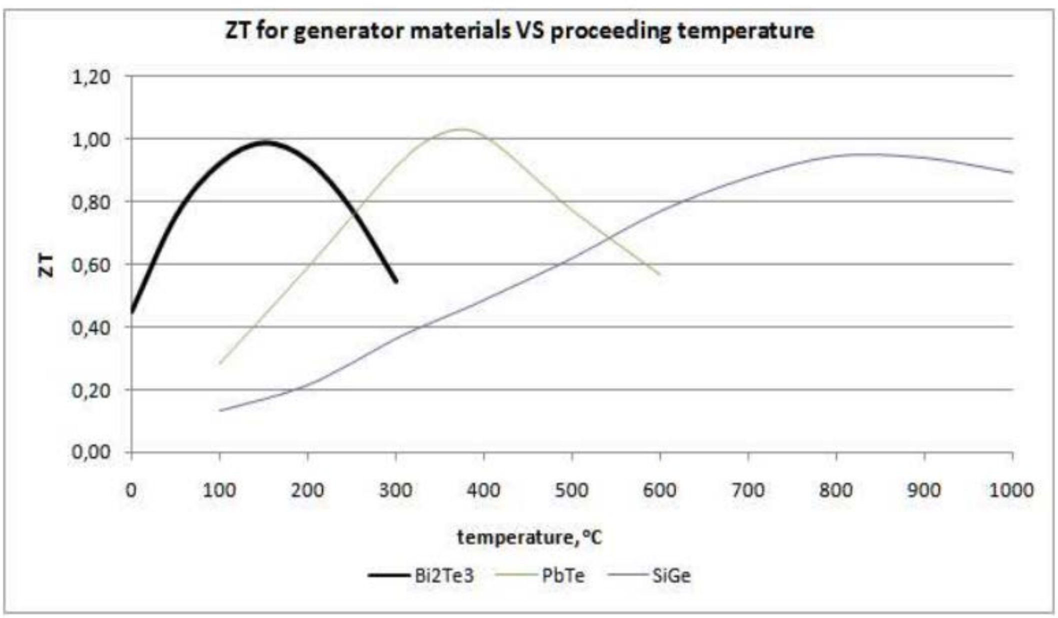

Figure 2.6 Optimum ZT for Material Depending on Temperature

Figure 2.6 demonstrates that bismuth telluride-based material has a high figure of merit for temperatures below $300°C$, whereas for temperature from $100°C$ to $600°C$ Lead Telluride-based material can be useful. Silicon Germanium-based material can be useful for temperature ranging between $100°C$ and $1000°C$. Thus bismuth (Bi) telluride (Te) based material has been selected in this study as a TEG heat exchanger, as its average working temperature is low. Hence, it can be concluded that bismuth telluride based materials are suitable for power generation in a lower temperature range.

Properties of Selected TEG material

The majority of thermoelectric properties are temperature dependent. Analytical methods can be used to obtain a differential equation that defines the behavior of material specific TEG. But obtaining exact solutions from those equations requires a computational method. Thus all the properties are obtained at average temperatures across the heat exchanger plate and treated as temperature independent quantities. All of the properties were obtained from figure 2.7 for p-type BiTe-based material and from figure 2.8 for n-type BiTe-based material. For further details about the fabrication process of the material and its effect on thermo-electric properties, refer to Reference [17].

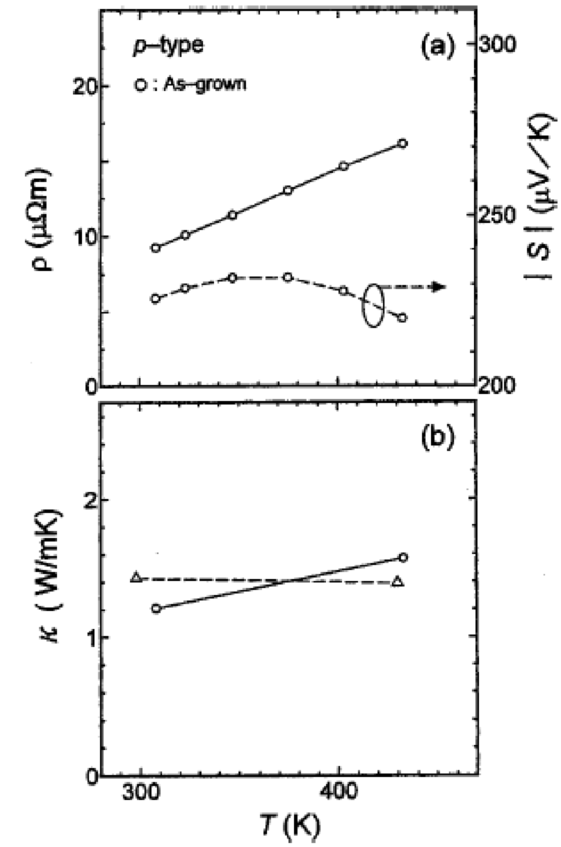

Figure 2.7 Electrical Resistivity"ρ", Seebeck Coefficient “α” and Thermal Conductivity "K" for P-type$(Bi_{0.250}Sb_{0.75})_2Te_3$ Doped with 8 wt% Excess Te[17]

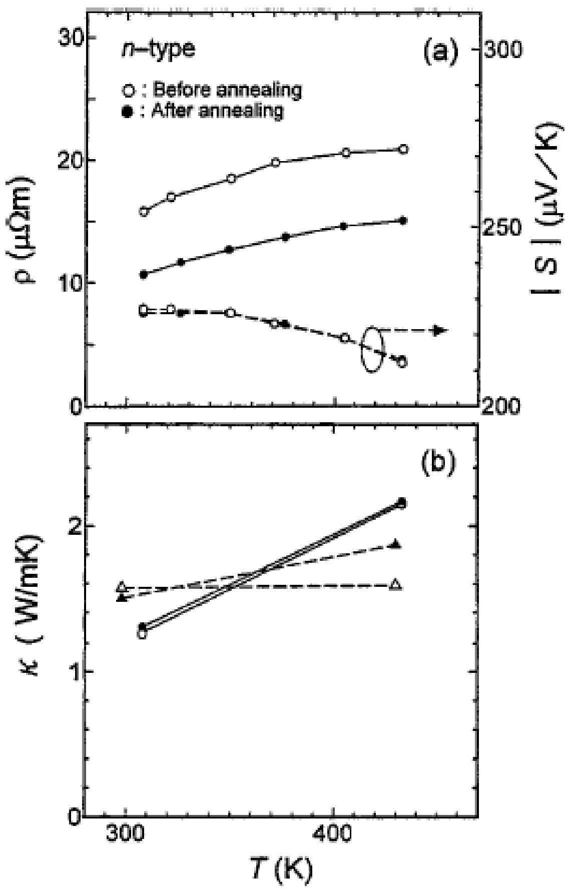

Figure 2.8 Electrical Resistivity “ρ”, Seebeck Coefficient “α” and Thermal Conductivity “K” for N-type $Bi_2(Te_{0.94}Se_{0.06})_3$ Doped with 0.07 wt% I, 0.02 wt % Te, and 0.03 wt % CuBr[17]

Table 2.1 Properties of P-type BiTe Material at 550K

x(m)	$T_{avg,plate}(K_p)$	$\rho_p(\Omega.m)$	$\alpha_p(V/K)$	$Z_p(K^{-1})$	$K_p\left(\frac{W}{m.K}\right)$
0.05	$3.81E+02$	$1.31E-05$	$2.32E-04$	$2.71E-03$	$1.41E+00$
0.1	$3.54E+02$	$1.21E-05$	$2.33E-04$	$3.68E-03$	$1.33E+00$
0.15	$3.35E+02$	$1.09E-05$	$2.32E-04$	$3.93E-03$	$1.27E+00$
0.2	$3.22E+02$	$1.01E-05$	$2.30E-04$	$4.25E-03$	$1.23E+00$
0.25	$3.13E+02$	$9.64E-06$	$2.28E-04$	$4.54E-03$	$1.21E+00$

Table 2.2 Properties of N-type BiTe Material at 550K

x(m)	$T_{avg,plate}(K)$	$\rho_n(\Omega.m)$	$\alpha_n(V/K)$	$Z_n(K^{-1})$	$K_n\left(\frac{W}{m.K}\right)$
0.05	$3.81E+02$	$1.37E-05$	$2.21E-04$	$2.00E+00$	$1.77E+00$
0.1	$3.54E+02$	$1.28E-05$	$2.24E-04$	$2.56E-03$	$1.67E+00$
0.15	$3.35E+02$	$1.19E-05$	$2.25E-04$	$2.88E-03$	$1.60E+00$
0.2	$3.22E+02$	$1.13E-05$	$2.25E-04$	$3.35E-03$	$1.56E+00$
0.25	$3.13E+02$	$1.09E-05$	$2.25E-04$	$3.67E-03$	$1.53E+00$

In Tables 2.1 and 2.2, the values provided are for 0.25m along the x axis, though the assumed dimension of the plate was 0.5m. Note that $T_{avg,plate}$ is decreasing drastically from $381.5K$ at $x = 0.05m$ to $312.9K$ at $x = 0.25$. Further down the plate along the x axis, $T_{avg,plate}$ is not large enough. Thus, the Seebeck effect will not be observed, and will be negligible for the selected BiTe based material.

Also note that electrical resistivity for p-type decreases with decrease in average temperature. This is due to decrease in the number of holes in the valence band with decrease in temperature. The electrical resistivity for n-type also decreases with decrease in average temperature. This is due to decreased number of electrons in the conduction band with decrease in temperature. Thermal conductivity decreases as well in both p-type and n-type material. The Seebeck coefficient and figure of merit show values similar to the graphs provided in Figure 2.7 and Figure 2.8.

2.4 Efficiency of Individual Thermocouple for Selected TEG

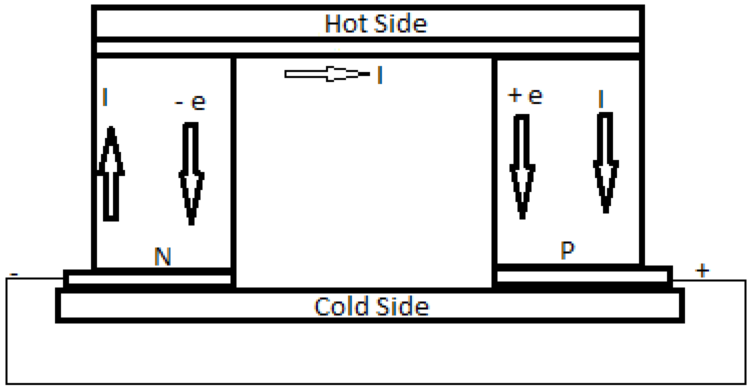

Figure 2.9 Schematic Diagram of Thermocouple

Figure 2.9 shows a TEG working under a temperature gradient. In n-type material, electrons on the hot side get excited and move faster towards the colder side, compared to electrons on cold side. This causes the cold side to be negatively charged and the hot side to be positively charged. The electrons on the cold side flow into the wire/load and obtain substitute holes in the p-type. Electrons in the p-type move from the hot end towards the cold end, creating opposite polarity compared to the n-type. Thus, connecting the n-type and p-type in a series will combine the voltage generated by each.

The efficiency of chosen thermocouples is evaluated at 424.1K on the hot side, which is the bulk exhaust gas temperature from the turbine, and 293K on the cool side, which is assumed to be at a constant surface temperature (Refer Section 3.2). Table 2.3 shows properties of BiTe based materials at an average temperature of 358.5K.

Table 2.3 Properties at 358.5K

$\rho_p(\Omega m)$	1.1928E-05
$\alpha_p(V/k)$	*2.3340E-04*
$K_p(W/K.m)$	1.3408E+00
$\rho_n(\Omega m)$	1.2935E-05
$\alpha_n(V/k)$	2.2352E-04
$K_n(W/K.m)$	1.6858E+00

Equation 1.2 describes the figure of merit for a single thermo element. For combination of n-type and p-type thermo elements, the maximum figure of merit is given as,

$$Z_{pn} = \frac{[|\alpha_n|+|\alpha_p|]^2}{\left[(\rho_n.K_n)^{1/2}+(\rho_p.K_p)^{1/2}\right]^2} = 2.7744\text{E-}03 \qquad (2.4.1)^{[16]}$$

Z_{pn} provides the maximum figure of merit as the product of internal resistance and thermal conductivity is minimized by taking the derivative with respect to the geometrical ratio $\left(\frac{\Upsilon_n}{\Upsilon_p}\right)$ of both types of thermo elements (equation 2.4.1). In addition, the Seebeck effects from both elements are added as all the elements are connected and they act as a source cell in series.

$$(R.K)_{minimized} = \left[(\rho_n.K_n)^{1/2} + (\rho_p.K_p)^{1/2}\right]^2 \qquad (2.4.2)^{[16]}$$

Where,

$\Upsilon_p = \frac{A_p}{t_p}$, $\Upsilon_n = \frac{A_n}{t_n}$

A = cross-sectional area of the element

t = thickness of the element

$$\Upsilon_{\mathrm{p}} = \frac{\mathrm{A_p}}{\mathrm{t_p}} = \left(\frac{1.4 \times 1.4}{1.14}\right) mm = 1.72mm$$

$$\Upsilon_{\mathrm{n}} = \frac{\mathrm{A_n}}{\mathrm{t_n}} = \left(\frac{1.4 \times 1.4}{1.14}\right) mm = 1.72mm$$

Thus, the optimizing factor in the case of selected thermocouples with assumed dimensions is 1.

Thermal Conductance,

$$K_{eq} = \frac{\mathrm{A_p} \times K_p}{\mathrm{t_p}} + \frac{\mathrm{A_n} \times K_n}{\mathrm{t_n}} = 5.2058\mathrm{E} - 03 \text{ W/K} \qquad (2.4.3)^{[16]}$$

Internal Resistance,

$$R = \frac{\rho_n}{\Upsilon_{\mathrm{n}}} + \frac{\rho_p}{\Upsilon_{\mathrm{p}}} = 1.4455\text{E-}02\ \Omega \qquad (2.4.4)^{[16]}$$

In similar fashion the ratio of internal and load resistance m' for the thermocouple has been optimized, to obtain equation 2.4.5.

$$m' = \left(1 + Z_{pn}.T_{avg}\right)^{1/2} = 1.4124 \qquad (2.4.5)^{[16]}$$

The external resistance R_{ext}, is obtained by the product of equations 2.4.4 and 2.4.5. Thus R_{ext} obtained is 2.0416E-02 Ω. Also the open circuit voltage due to the thermocouple is obtained by the product of the Seebeck coefficient and the temperature difference.

$$V_{OC} = \left(|\ \alpha_n\ | + |\ \alpha_p\ |\right) \times \Delta T = 5.9902\mathrm{E} - 02 \text{ V} \qquad (2.4.6)^{[16]}$$

Optimum current,

$$I_{opt} = \frac{(|\alpha_n| + |\alpha_p|) \times \Delta T}{R(m'+1)} = 1.7178 \text{ Amp.} \qquad (2.4.7)^{[16]}$$

Electrical power output,

$P_{output} = {I_{opt}}^2 \times R_{ext}$ =9.9403E-01 Watts. (2.4.8)[16]

Applying the law of the conservation of energy to the hot and cold sides of the thermo elements, four factors contribute to the transport of energy and are given below:

Hot Junction:

1. Heat Input ($Q_L$turbine exhaust heat supplied to the hot thermocouple junctions along the TEG heat exchanger plate)
2. Heat Input due to Joule Heating ($\frac{1}{2} \times {I_{opt}}^2 \times R$, where R is the internal resistance and is assumed to have a linear temperature profile across the element)
3. Power out due to thermoelectric effect ($P_{output} = \left(\mid \alpha_n \mid + \mid \alpha_p \mid\right) \times T_h \times I_{opt},$)
4. Heat out due to conduction of charge carriers from hot junction toward the cold junction.

   Or, $Q_L = \left(\mid \alpha_n \mid + \mid \alpha_p \mid\right) \times T_h \times I_{opt} + K_{eq} \times \Delta T - \frac{1}{2} \times {I_{opt}}^2 \times R)$ (2.4.9)[18]

Cold Junction:

1. Heat Output (Q_{1L} is the remaining amount of heat removed from cold junction by the water).
2. Heat Input due to Joule Heating ($\frac{1}{2} \times {I_{opt}}^2 \times R$, where R is the internal resistance and is assumed to have a linear temperature profile across the element).
3. Power in due to thermoelectric effect ($P_{output} = \left(\mid \alpha_n \mid + \mid \alpha_p \mid\right) \times T_c \times I_{opt}$)
4. Heat in due to conduction of charge carriers from the hot junction toward the cold junction.

$$\text{Or, } Q_{1,L} = \left(|\ \alpha_n\ | + |\ \alpha_p\ |\right) \times T_c \times I_{opt} + K_{eq} \times \Delta T + \frac{1}{2} \times {I_{opt}}^2 \times R) \text{ (2.4.10)[18]}$$

Therefore, electrical power output can be calculated by: $P_{output} = Q_L - Q_{1L}$. This treats thermocouples like a heat engine, where one-dimensional heat transfer is allowed across the thermo elements and all other side are insulated (Refer Figure 2.9). The Seebeck coefficient obtained from the graph is equal to the values obtained using the average integral for a given temperature range. Contact resistance of the aluminum strips and ceramic plates has not been considered due to its small value compared to resistance offered by thermocouple. These equations were derived by treating the Seebeck effect, thermal conductivity, and joule heating with the energy balance equation with boundary condition of hot and cold temperatures applied on either side of the thermocouple. The first term in equation 2.4.9 and 2.4.10 is the Seebeck coefficient which represents the heat dissipated at the ends of thermocouple and through it (Peltier and Thomson effect). The second term is the heat transported due to thermal conductance of the thermocouple at a given thermal gradient. The third term defines joule heating due to internal resistance of the thermocouple to the flow of current. Efficiency of the thermocouple can be obtained by the ratio of electrical power output to the amount of heat supplied at the hot junction.

Efficiency,

$$\eta_{max} = \frac{{I_{opt}}^2 \times R_{ext}}{(|\alpha_n| + |\alpha_p|) \times T_h \times I_{opt} + K_{eq} \times \Delta T - \frac{1}{2} \times {I_{opt}}^2 \times R} = 6.06\% \qquad \text{(2.4.11)[18]}$$

Thus selected BiTe-based thermo-electric material will work at 6.06 percent efficiency when exposed to an average temperature of 358.5K.

Similarly, formulae indicated in the above discussion will be used later in section 3.4 to calculate the total power generated from n number of thermocouples arranged in a series connection, as shown in section 1.6.

Chapter 3: Sizing of TEG Module for 10 KW Brayton Cycle

The size of the Brayton cycle chosen is sufficient for supplying power to individual homes. The exhaust heat available from the turbine can be reused in a TEG heat exchanger to generate additional electricity. Thus, application of this heat exchanger can generate additional power and supply warm water for other household purposes. Implementation of this concept can help the Brayton cycle be more efficient.

3.1 10KW Baseline Brayton Cycle

Assume: Isentropic flow, Change in Kinetic Energy/Potential Energy ΔK.E./ΔP.E.≈0, Mass Flow rate $\dot{m}$ is constant, Pressure is low and Temperature is high, Pressure ratio of the cycle (compressor and turbine) = 13, Specific heat of gas is not a function of temperature.

Given: Specific Heat Ratio of gas, $K = 1.4$ at $T_1 = 300K$

Process 1-2 isentropic compression

$$\left(\frac{T_2}{T_1}\right) = \left(\frac{P_2}{P_1}\right)^{\frac{K-1}{K}} \qquad (3.1.1)^{[2]}$$

Pressure Ratio of the cycle, $\left(\frac{P_2}{P_1}\right) = 13.$

Substituting the values for specific heat ratio, pressure ratio and inlet ambient air temperature T_1 in equation 3.1.1 provides an exit temperature from the compressor at stage 2, $T_2 = 624.30K$.

Process 3-4 isentropic expansion

$$\left(\frac{T_3}{T_4}\right) = \left(\frac{P_3}{P_4}\right)^{\frac{K-1}{K}} \qquad (3.1.2)\text{ [2]}$$

Substituting the values for specific heat ratio, pressure ratio and exit gas temperature from the turbine exhaust $T_4 = 550K$[Refer. Table 1.1] provides inlet temperature to the turbine, $T_3 = 1144.5K$.

Specific Turbine Work, $\mathrm{w_T}$

$$w_T = (h_3 - h_4)\frac{KJ}{Kg} \qquad (3.1.3)\text{ [2]}$$

Specific enthalpy of gas at turbine inlet, $h_3 = 1212.8\ \frac{KJ}{Kg}@1144.5K[19]$

Specific enthalpy of gas at turbine exit, $h_4 = 555.74\ \frac{KJ}{Kg}@550K[19]$

Substituting the values for enthalpy of gas at 1144.5K and 550K provides specific turbine work of $657.08\frac{KJ}{Kg}$.

Specific Compressor Work, $\mathrm{w_c}$

$$w_c = (h_2 - h_1)\frac{KJ}{Kg} \qquad (3.1.4)\text{ [2]}$$

Specific enthalpy of gas at compressor exit, $h_2 = 632.61\ \frac{KJ}{Kg}@624.30K[19]$

Specific enthalpy of gas at turbine exit, $h_1 = 300.19\ \frac{KJ}{Kg}@300K[19]$

Substituting the values for specific enthalpy of gas, compressor work obtained is $332.42\frac{KJ}{Kg}$.

Net work from Turbine, W_{Net}

$$w_{Net} = w_T - w_C \qquad (3.1.5)$$ [2]

Substituting values from equation 3.1.3 and 3.1.4 net work from turbine obtained is $324.66 \frac{KJ}{Kg}$.

Mass flow rate in the cycle is given by equation 3.1.6

$$W_{Net,T} = w_{Net} * \dot{m} \qquad (3.1.6)$$ [2]

$$W_{Net,T} = 10\ KW$$

Substituting the value of specific net work form the turbine and total net work from the turbine, the mass flow rate of the gas in the cycle is obtained, $\dot{m} = 3.08 \times 10^{-2} \frac{Kg}{s}$.

Heat Input to the Heat Exchanger, Q_H

$$Q_H = \dot{m}(h_3 - h_2)KW \qquad (3.1.7)$$ [2]

Furthermore, substituting mass flow rate of the gas, specific enthalpy of gas at turbine inlet and compressor exit, and the rate of heat input to the combustion chamber, $Q_H = 17.87\ KW$

Heat dissipated Q_L from the cycle

$$Q_L = Q_H - W_{Net,T} \qquad (3.1.8)$$ [2]

Substituting the value of rate of heat input to the combustion chamber and rate of total net work performed by the turbine in equation 3.1.8, the total rate of heat dissipated from the cycle is equal to, $\dot{Q}_L = 7.87KW$.

Heat Dissipated from Baseline 10KW Brayton cycle

Figure 3.1 illustrates the Brayton cycle, where stages 1 to 2 indicate adiabatic reversible compression, stages 2 to 3 indicate constant pressure heat addition and stages 3 to 4 indicate adiabatic reversible expansion. Pressure and temperature at each stage is given below:

$T_1 = 300K$

$P_1 = 1\ atm$

$T_2 = 624.30K$

$P_2 = 13\ atm$

$T_3 = 1144.5K$

$P_3 = 13\ atm$

$T_4 = 550K$

$P_4 = 1\ atm$

Thermal Efficiency of the cycle $\eta = \frac{W_{Net,T}}{Q_H} = \frac{10\ KW}{17.87\ KW} = 0.55\ or\ 55\%$

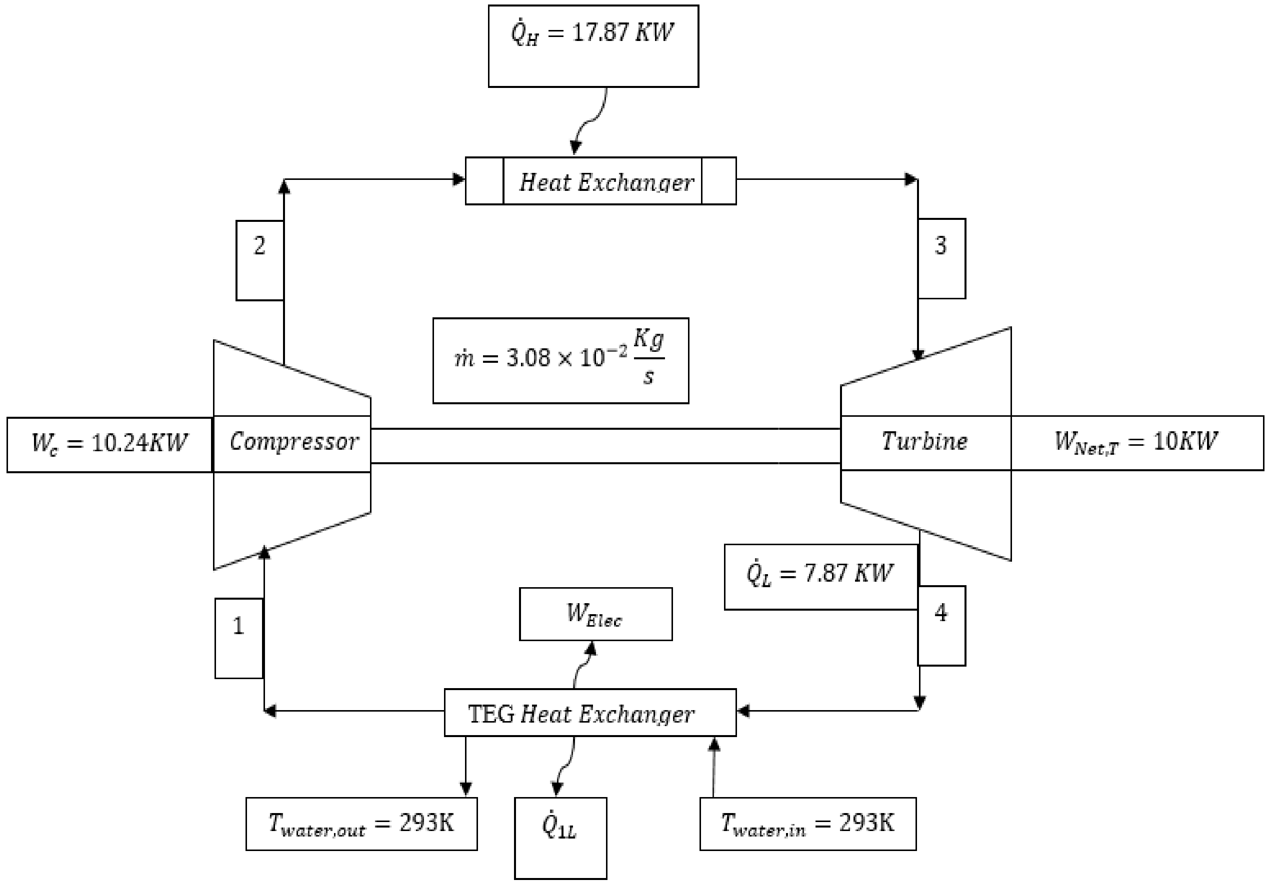

Figure 3.1 Schematic Diagram of Proposed Cycle

3.2 Determination of Overall Heat Exchanger Area

Heat is transferred from hot fluid to the ceramic wall by convection, through the wall by conduction and into the semiconductor legs by conduction. Again heat flows towards the cold fluid by convection. Any radiation effects are negligible in determining the overall heat transfer coefficient as its contribution due to the air gap between thermo elements is low.

Assume: Heat transfer occurs in normal direction to the flat plate surface. Ceramic walls on the hot and cold sides are nearly isothermal. Lateral heat flow is zero: all sides are well insulated. The temperature of water and gas is constant, thus it is 1-d heat transfer process.

Energy balance

Rate of heat transfer into the ceramic hot side – Rate of heat transfer out of the ceramic cold side = Rate of electrical work produced from TEG heat exchanger

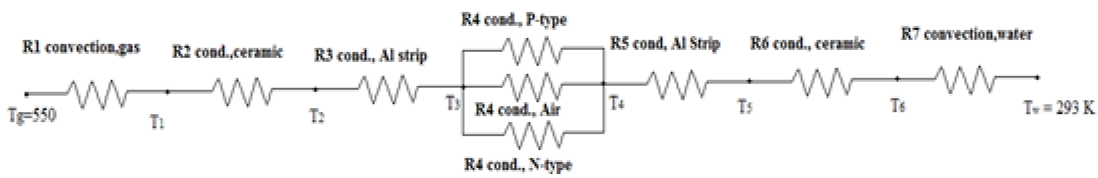

Figure 3.2 Thermal Resistance Circuit for TEG Heat Exchanger

Convection resistance for flow of hot gas, $R_1 = \frac{1}{h_1 A_1}$

Conduction resistance for ceramic plate, $R_2 = \frac{t_2}{K_2 A_2}$

Conduction resistance for aluminum strip, $R_3 = \frac{t_3}{K_3 A_3}$

Conduction resistance for P-type thermo element, $R_4 = \frac{t_4}{K_4 A_4}$

Conduction resistance for air gap between thermo elements, $R_4{}' = \frac{t_4{}'}{K_4{}' A_4{}'}$

Conduction resistance for N-type thermo elements, $R_4{}'' = \frac{t_4{}''}{K_4{}'' A_4{}''}$

Conduction resistance for aluminum strip, $R_5 = \frac{t_5}{K_5 A_5}$

Conduction resistance for ceramic plate, $R_6 = \frac{t_6}{K_6 A_6}$

Convection resistance for flow of cooling water, $R_7 = \frac{1}{h_7 A_7}$

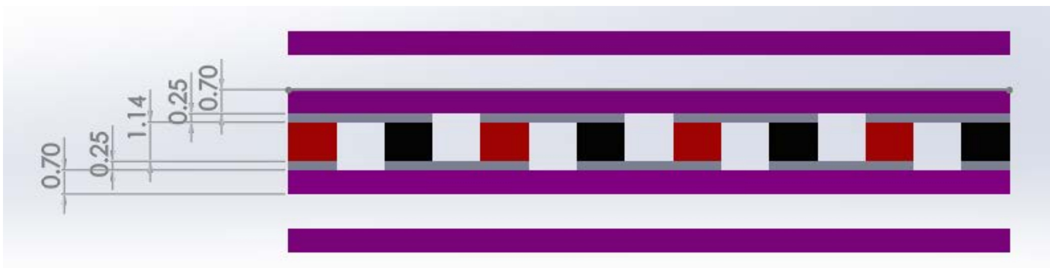

Figure 3.3 Side View of TEG module

As shown in figure 3.3, the gap between parallel ceramic plate is 1.4mm, thickness of the ceramic plate is $t_2 = t_6 = 0.7mm$, thickness of the aluminum conducting strip is $t_3 = t_5 = 0.25mm$, thickness of the thermo elements $t_4 = t_4'' = 1.14mm$, thickness of the air gap between thermo element is $t_4' = (1.14 + 0.25)\text{mm} = 1.39\text{mm}$. Using these assumed values based on a survey of the literature on the geometry of thermo electric modules, the overall heat transfer coefficient can be calculated provided all the thermo physical properties are available.

Parameters for all thermal resistance from R_1 to R_7 are known except their corresponding areas and the convection/conduction coefficient.

1. Convection coefficient for flow of hot gas ,h_1

   The Dittus-Boelter equation used for turbulent flow is used to calculate the Nusselt number. This equation provides less accurate values if the bulk fluid temperature difference between cold and hot is large. The exhaust temperature from the turbine at T_4 is the inlet temperature for the TEG heat exchanger, as $T_{hot,in}$ for TEG heat exchanger,$T_{hot,in} = 550K$.

Given: mass flow rate of hot gas, $\dot{m} = 3.08 \times 10^{-2} \frac{Kg}{s}$

Specific heat at constant pressure $C_p = 1034.85 \frac{J}{Kg.K}$ [19]

$T_{hot,out} = ?$

$$Q_L = \dot{m} \times C_p \times (T_{hot,in} - T_{hot,out}) \quad (3.2.1)$$

Thus, substituting the values in equation 3.2.1 ,$T_{hot,out}$for the TEG heat exchanger is $298.2K$.

Bulk fluid temperature is the average of $T_{hot,in}$ and $T_{hot,out}$, i.e 424.1K

Properties at Bulk Fluid Temperature 424.1K [19]

1	Density of hot gas, ρ_{air}	$0.8328 \frac{Kg}{m^3}$
2	Dynamic viscosity of hot gas, μ_{air}	$2.393 \times 10^{-5} \frac{Kg}{ms}$
3	Prandtl number, Pr	0.7026
4	Thermal Conductivity	$0.034557 \frac{W}{mK}$

Assumed flat plate size for flow of gas,

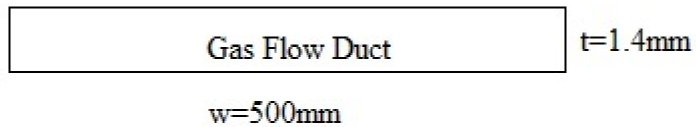

Figure 3.4 Flat Plate for Hot Exhaust Gas

Hydraulic Diameter, $D_h = 2 \times t = 2.8mm$

Gas Velocity,

$$V_{avg} = \frac{\dot{m}}{A_c \times \rho_{air}} \tag{3.2.2}$$

Substituting the values for mass flow rate, flat plate cross sectional area and density of gas at bulk fluid temperature provides $52.83\frac{m}{s}$.

Reynolds Number,

$$Re = \frac{\rho_{air} \times V_{avg} \times D_h}{\mu_{air}} \tag{3.2.3}$$

Substituting the values for density of gas, velocity from equation 3.2.2, hydraulic diameter, and viscosity, the Reynolds number obtained is 5148. Thus the flow of gas on the hot side is turbulent.

The Nusselt number is given by equation 3.2.4:

$$Nu = 0.023 \times Re^{0.8} \times Pr^n \tag{3.2.4}$$

Where $n = 0.3$ for cooling [20].

Substituting values for Re and Pr in equation 3.2.4, the Nusselt number obtained is 19.27.

The convective heat transfer coefficient is $h_1 = \frac{K_1 \times Nu}{D_h} = 237.84 \frac{W}{m^2 \times K}$

2. Conduction coefficient for ceramic plate, K_2

   Thermal conductivity for ceramic plate at bulk fluid temperature of 424.1K on hot side is $24.63\ \frac{W}{m.K}$ [21]

3. Conduction coefficient for aluminum strip, K_3

   Thermal conductivity for aluminum conducting strip at bulk fluid temperature of 424.1K on hot side is $239.03\ \frac{W}{m.K}$ [22]

4. Conduction coefficient for P-type thermo element ,K_4

   Because the thermo element is exposed to two different hot and cold bulk fluid temperatures, thermal conductivity is determined by averaging the temperature of the two sides, $T_{avg} = \frac{(424.1+293)K}{2} = 358.55K$.

   $K_4 = 1.3395 \frac{W}{m.K}$ [17]

5. Conduction coefficient for N-type thermo element, K_4''

   Thermal conductivity at $T_{avg} = 358.55K$

   $K_4'' = 1.6971 \frac{W}{m.K}$ [17]

6. Conduction coefficient for air gap between thermo element, K_4'

Air gap is exposed to two different hot and cold bulk fluid temperatures: thermal conductivity is determined by averaging the temperature of the two sides,

$T_{avg} = 358.55K$.

$K_4{}' = 0.0302 \frac{W}{m.K}$ [21]

7. Conduction resistance for aluminum strip, K_5

Thermal conductivity for aluminum conducting strip at cold fluid temperature of 293K on cold side is $236.72 \frac{W}{m.K}$ [22]

8. Conduction resistance for ceramic plate, K_6

Thermal conductivity for ceramic plate near cold fluid at temperature of 293K is $35.11 \frac{W}{m.K}$ [21]

9. Convection resistance for flow of cooling water, h_7

Bulk fluid temperature is used to apply Dittus-Boelter equation to calculate the convective heat transfer coefficient on cold side.

Assume ΔT_w on cool side to be 10K.

Average efficiency of TEG at $358.55K$ obtained with calculation similar to section 2.4 is 6.066%. Thus approximate electrical power generated at T_{avg} is 6.066% of $\dot{Q}_L$, which is equal to $474.5W$

Specific heat at constant pressure for water, $C_{p,w} = 4194 \frac{J}{Kg.K}$ [19]

Mass flow rate of cooling water in TEG heat exchanger,

$$\dot{m}_w = \frac{(\dot{Q}_L - 474.5)W}{C_{p,w} \times \Delta T_w} \tag{3.2.5}$$

Thus $\dot{m}_w$ for TEG heat exchanger is $0.1763 \frac{Kg}{s}$

Properties at bulk fluid temperature $\left[\frac{(283+293)K}{2}\right] 288K$ and 1 atm [19].

1	Density of water, ρ_{water}	$999 \ \frac{Kg}{m^3}$
2	Dynamic viscosity of cold water, μ_{water}	$1.138 \times 10^{-3} \frac{Kg}{ms}$
3	Thermal Conductivity, K_w	$0.589 \ \frac{W}{mK}$

Assumed duct size for flow of water,

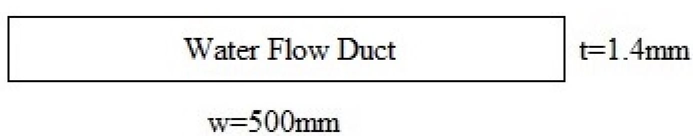

Figure 3.5 Duct for Cooling Water

Hydraulic Diameter, $D_h = 2 \times t = 2.8mm$

Gas Velocity,

$$V_{avg} = \frac{\dot{m}}{A_c \times \rho_{water}} \tag{3.2.6}$$

Substituting the values for mass flow rate, flat plate cross sectional area and density of gas at bulk fluid temperature provides $0.2521\frac{m}{s}$.

Reynolds Number,

$$Re = \frac{\rho_{air} \times V_{avg} \times D_h}{\mu_{air}} \tag{3.2.7}$$

Substituting the values for density of gas, velocity from equation 3.2.6, hydraulic diameter and viscosity, the Reynolds number obtained is 619.6. Thus the flow of gas on the cold side is laminar. For laminar flow inside the rectangular duct, the Nusselt number $Nu = 7.54$ [20, Table 8-1]. The convective heat transfer coefficient for flow of water, $h_w = \frac{K_w \times Nu}{D_h} = 1586.09\frac{W}{m^2 \times K}$.

The relation for the overall heat transfer coefficient is given by equation 3.2.8

$$Q_L = U_{overall} \times A_{Total} \times \Delta T_{LMTD} \tag{3.2.8}$$

A_{Total} is the total area required to transfer 7870 W of heat from the TEG heat exchanger. Equation 3.2.8 is also given as $Q_L = \frac{\Delta T_{LMTD}}{R_{total}}$.

$$\therefore R_{total} = \frac{1}{U_{overall} \times A_{Total}} = \frac{1}{h_1 A_1} + \frac{t_2}{K_2 A_2} + \frac{t_3}{K_3 A_3} + R_{eq,module} + \frac{t_5}{K_5 A_5} + \frac{t_6}{K_6 A_6} + \frac{1}{h_7 A_7} \tag{3.2.9}$$

$R_{eq,module}$ is total thermal resistance due to P-type, N-type and air gap between thermo elements. All the thermo elements are arranged thermally in parallel orientation and electrically in series. First $R_{eq,couple}$ is obtained,

$$\frac{1}{R_{eq,couple}} = \frac{1}{R_4} + \frac{1}{R_4{}'} + \frac{1}{R_4{}''}$$

$$\frac{1}{R_{eq,couple}} = \frac{K_4 A_4}{t_4} + \frac{K_4{}' A_4{}'}{t_4{}'} + \frac{K_4{}'' A_4{}''}{t_4{}''}$$

Given, $t_4{}' = 1.39\text{mm}, t_4 = t_4{}'' = 1.14\text{mm}$

$\therefore\ let\ t_4 = t_4{}'' = t$

$$\frac{1}{R_{eq,couple}} = \frac{K_4 A_4 + K_4{}'' A_4{}''}{t} + \frac{K_4{}' A_4{}'}{t_4{}'}$$

$$R_{eq,couple} = \frac{t \times t_4{}'}{t_4{}'(K_4 A_4 + K_4{}'' A_4{}'') + t \times K_4{}' A_4{}'} \tag{3.2.10}$$

Each module has 71 thermocouple. The thermal conductance for n number of thermocouple is given by equation 3.2.11

$$K = n \times (K_P + K_N) \tag{3.2.11}$$

Similarly equivalent thermal resistance for n thermocouples in a module is given by equation 3.2.12.

$$R_{eq,module} = \frac{1}{n} \times \left[\frac{t \times t_4{}'}{t_4{}'(K_4 A_4 + K_4{}'' A_4{}'') + t \times K_4{}' A_4{}'}\right] \tag{3.2.12}$$

Substituting equation 3.2.12 into equation 3.2.9 gives equation 3.2.13:

$$\therefore R_{total} = \frac{1}{U_{overall} \times A_{Total}} = \frac{1}{h_1 A_1} + \frac{t_2}{K_2 A_2} + \frac{t_3}{K_3 A_3} + \frac{1}{71} \times \left[\frac{t \times t_4{}'}{t_4{}'(K_4 A_4 + K_4{}'' A_4{}'') + t \times K_4{}' A_4{}'}\right] + \frac{t_5}{K_5 A_5} + \frac{t_6}{K_6 A_6} + \frac{1}{h_7 A_7} \tag{3.2.13}$$

Note: The relation between total area and individual area of resistance for each material is developed based on assumed dimension for a single module to obtain the overall heat transfer coefficient (Refer Figure 1.5 & 3.6).

1. $A_{Total} = A_1$=A_2=A_6=A_7 (uniform areas across each thermal resistance in module)

2. A_3 is the area of the lower Aluminum strip (Refer Figure 3.3).

   Let a be the area equivalent to the cross-sectional area of each thermo element. For each thermoelectric module consisting of 71 thermocouples (Refer Figure 1.4) the relation between area of required ceramic plate or A_{Total} and A_3 for a module is given by equation 3.2.16. The number of thermo elements along the x axis is 15, and 17 along the y axis (Refer Figure 1.4). Thus, $A_{Total} = 15 \times 17 \times a = 255a$.

   $$\therefore a = \frac{A_{Total}}{255} \tag{3.2.14}$$

   $$A_3 = 107a$$

   $$\therefore a = \frac{A_3}{107} \tag{3.2.15}$$

   Equating 3.2.14 and 3.2.15 gives equation 3.2.16.

   $$A_3 = \frac{A_{Total} \times 107}{255} \tag{3.2.16}$$

   Note: The above relationship exists for the entire TEG heat exchanger plate, as multiple numbers of modules in serial arrangement builds the plate.

3. $A_4 = A_4{}' = A_4{}'' = a$ is cross-sectional area of n-type, p-type and air gap in between.

$$\therefore R_{eq,module} = \left(\frac{1}{71\times a}\right)\times\left[\frac{t\times t_4'}{t_4'(K_4+K_4'')+t\times K_4'}\right] \tag{3.2.17}$$

Equation 3.2.14 and 3.2.17 give equation 3.2.18.

$$\therefore R_{eq,module} = \left(\frac{255}{71\times A_{Total}}\right)\times\left[\frac{t\times t_4'}{t_4'(K_4+K_4'')+t\times K_4'}\right] \tag{3.2.18}$$

4. A_5 is area of upper aluminum strip (Refer 3.3).

   $A_5 = 3\times 36\times a = 108a$ (Each thermocouple junction formed by upper aluminum strip is 3 times area of each thermo element and each module has 36 thermocouple as seen from the top)

   $$A_5 = 108a \tag{3.2.19}$$

   Equation 3.2.14 and 3.2.19 gives equation 3.2.20.

   $$A_5 = \frac{108\times A_{Total}}{255} \tag{3.2.20}$$

   Substitute all the relation obtained from 1 to 4 gives final equation for overall thermal resistance as shown in equation 3.2.21.

$$\therefore R_{total} = \frac{1}{U_{overall}\times A_{Total}} = \frac{1}{h_1 A_{Total}} + \frac{t_2}{K_2 A_{Total}} + \frac{t_3\times 255}{K_3\times A_{Total}\times 107} + \left(\frac{255}{71\times A_{Total}}\right)\times \left[\frac{t\times t_4'}{t_4'(K_4+K_4'')+t\times K_4'}\right] + \frac{t_5\times 255}{K_5\times 108\times A_{Total}} + \frac{t_6}{K_6 A_{Total}} + \frac{1}{h_7 A_{Total}} \tag{3.2.21}$$

$$\therefore R_{total} = \frac{1}{U_{overall}} = \frac{1}{h_1} + \frac{t_2}{K_2} + \frac{t_3\times 255}{K_3\times 107} + \left(\frac{255}{71}\right)\times\left[\frac{t\times t_4'}{t_4'(K_4+K_4'')+t\times K_4'}\right] + \frac{t_5\times 255}{K_5\times 108} + \frac{t_6}{K_6} + \frac{1}{h_7}$$

$$= \frac{1}{U_{overall}} = (0.004204 + 0.00002842 + 0.000002492 + 0.001341 + 0.000001056 + 0.00001993 + 0.0006304)\frac{m^2\times K}{W}$$

Substituting the corresponding heat transfer coefficients and thickness, values obtained in the second, third, fifth, sixth, and seventh terms are negligible compared to values in the first and fourth terms. Thus, the value of the overall heat transfer coefficient obtained is $180.34\frac{W}{m^2.K}$

Assume Parallel TEG Heat Exchanger

A counter flow heat exchanger can transfer more energy than a parallel heat exchanger, as the exit temperature of the cooling fluid can get close to high temperature of the hot fluid (parallel temperature profile). In a parallel heat exchanger, the temperature difference is high at the entrance region, but later the two fluids tend to reach the same temperature at the exit region (converging temperature profile), depending on the design parameters.

Thus, temperature differences in parallel heat exchangers at the entrance region is high. If thermo electric generators are placed in the region of higher temperature difference more electrical power is obtained. Also note that the efficiency of TEG is directly proportional to temperature difference across the two junctions of the TEG material. Thus, a parallel heat exchanger is selected and log-mean temperature difference is used to find the total area required for the TEG heat exchanger.

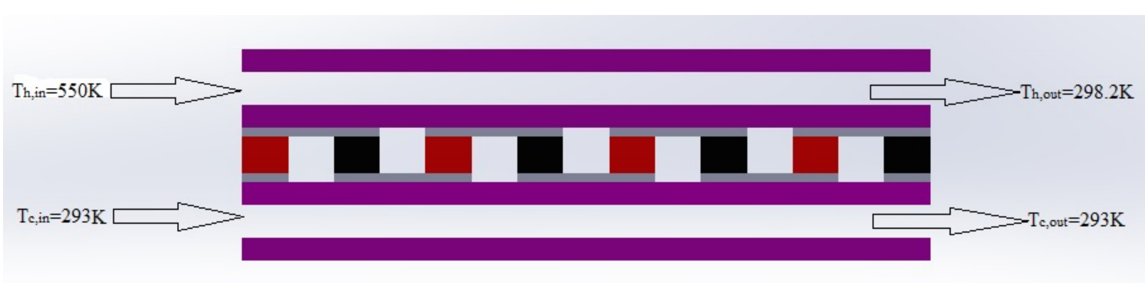

Using equation 3.2.8, the total area required for the heat transfer can be obtained.

$$7870W = 180.34\frac{W}{m^2.K} \times A_{Total,plate} \times \frac{(T_{h,o} - T_{c,o}) - (T_{h,in} - T_{c,in})}{ln\left[\frac{(T_{h,o}-T_{c,o})}{(T_{h,in}-T_{c,in})}\right]}$$

$$7870W = 180.34\frac{W}{m^2.K} \times A_{Total,plate} \times \frac{[(298.2 - 293) - (550 - 293)]K}{ln\left[\frac{(298.2-293)}{(550-293)}\right]}$$

$$\therefore A_{Total,plate} = 0.676\, m^2$$

3.3 Temperature Profile Across TEG Heat Exchanger Plate

The temperature profile of water across the plate on the cool side is assumed to be constant at 293K. Hence, the temperature profile for exhaust gas on the hot side can be obtained using the constant wall temperature method.

$$\dot{Q}_{conv,gas} = \dot{m} \times C_p \times dT_m \qquad (3.3.1)$$

Also, Newton's law of cooling, $\dot{Q}_{conv,gas} = h_g \times (T_s - T_m) \times dA$ and $(T_s - T_m)$ the temperature difference between the surface and the fluid. Since $T_s < T_m$ as the exhaust gas cools, it gives equation 3.3.2:

$$-\left(h_g \times (T_m - T_s) \times dA\right) = \dot{m} \times C_p \times dT_m$$

$$-\left(h_g \times (T_m - T_s) \times p \times dx\right) = \dot{m} \times C_p \times dT_m \qquad (3.3.2)$$

Where,

Perimeter of the duct, $= 2 \times (w \times t)$, but $(w \gg t)$ (Refer Figure 3.4). $\therefore p = 2w$

T_s= Constant wall temperature

T_m = Mean hot exhaust gas temperature

h_g = Average convective heat transfer coefficient of hot exhaust gas

dT_m = Decrease in mean temperature of hot exhaust gas

T = Temperature at any point along the plate in x axis

Integrate from $x = 0$ (Refer Figure 1.4) where $T_m = T_{h,in} = 550K$ to any point x along x axis, where $T_m = T$

$$\int_0^x -\left(h_g \times (T_m - T_s) \times p \times dx\right) = \int_{T_m}^T \dot{m} \times C_p \times dT_m \tag{3.3.3}$$

Solving equation 3.3.3 gives equation 3.3.4

$$\therefore T = (550 - T_s) \times e^{\left(\frac{-h_g \times p \times x}{\dot{m} \times C_p}\right)} + T_s \tag{3.3.4}$$

Here,

$\dot{m} = 3.08 \times 10^{-2} \frac{Kg}{s}$

$C_p = 1034.85 \frac{J}{Kg.K}$[20]

$p = 2w = 2 \times 0.5m = 1m$

$h_g = 237.84 \frac{W}{m^2.K}$

$T_s = 293K$

Substituting corresponding values in equation 3.3.4 provides Table 3.1, which gives average temperatures across the plate.

Table 3.1 Temperature Profile for Exhaust Gas

x(m)	$T(K)$	$T_s(K)$	$T_{avg,plate}(K)$
0.05	4.70E+02	293	3.81E+02
0.1	4.15E+02	293	3.54E+02
0.15	3.77E+02	293	3.35E+02
0.2	3.51E+02	293	3.22E+02
0.25	3.33E+02	293	3.13E+02
0.3	3.20E+02	293	3.07E+02
0.35	3.12E+02	293	3.02E+02
0.4	3.06E+02	293	2.99E+02
0.45	3.02E+02	293	2.97E+02
0.5	2.99E+02	293	2.96E+02

3.4 Thermocouple Configuration

The total area of the TEG heat exchanger plate consists of 10 segments with 0.05m width (x axis) and 1.352m length (y axis) which give the total area of the plate obtained in section 3.2. Each segment has a constant temperature profile depending on the values obtained in Table 3.1.

1. Number of Thermocouples along x axis:

With reference to Figure 1.4, the total breadth of the plate (x axis) with significant $T_{avg,plate}(K)$ is 0.25m for the selected BiTe-based material. This conclusion was drawn from 1-d heat transfer analysis along the x-axis to obtain the temperature profile. Each segment can fit 2 modules along the x axis. Thus the total number of modules along the x axis is 10, as 5 out of 10 segments contribute to generate power.

$$\therefore N_x = 5(segments) \times \frac{2(modules)}{1(segments)} = 10\ modules$$

Thus, every row (x axis) in the heat exchanger plate has $10\ modules \times \frac{71(thermocouple)}{1\ module} = 710\ thermocouple.$

2. Number of Thermocouples along y axis:

   To determine the number of thermocouple along the y axis, the trial and error method (Refer Section 3.5) will be used to determine the distance along the y axis that can be used to incorporate thermocouples out of 1.352 m.

3.5 Efficiency of TEG Heat Exchanger Plate

The parameters calculated in section 2.4 will be obtained for the entire array of thermocouples to obtain total power output, and total heat input to the TEG heat exchanger plate. In addition, the product of overall heat transfer coefficient and the area (obtained by using log-mean temperature difference for a parallel-flow heat exchanger in section 3.2) will provide total heat input to the entire heat exchanger plate.

The efficiency of the plate can be obtained in two ways:

1. Ratio of electrical power output to total heat input as shown in section 2.4
2. Ratio of electrical power output obtained as mentioned in section 2.4 to total heat input obtained, using the overall heat-transfer coefficient mentioned in section 3.2.

Close values of efficiency obtained by both methods for all the selected temperature profiles across the plate in section 3.3 indicate the validity of the approach.

Method 1

Efficiency of thermocouple is evaluated at the temperatures shown in Table 3.2.

Table 3.2 Temperature Values

x(m)	T_h (K)	T_c (K)	ΔT(K)	Tavg (K)
0	5.50E+02	2.93E+02		
0.05	4.70E+02	2.93E+02	1.77E+02	3.81E+02
0.1	4.15E+02	2.93E+02	1.22E+02	3.54E+02
0.15	3.77E+02	2.93E+02	8.39E+01	3.35E+02
0.2	3.51E+02	2.93E+02	5.78E+01	3.22E+02
0.25	3.33E+02	2.93E+02	3.98E+01	3.13E+02

Equation 2.4.1 describes figure of merit for a single thermocouple. For n number of thermocouples, the maximum figure of merit is given by equation 3.5.1.

$$Z_{pn} = \frac{\left[|\alpha_n|+|\alpha_p|\right]^2}{K_p \times \rho_p \left(1+\frac{1}{x \times K_{total,pn}}+\frac{x}{\rho_{total,pn}}+\frac{1}{K_{total,pn} \times \rho_{total,pn}}\right)} \qquad (3.5.1)^{[18]}$$

Z_{pn} provides the maximum figure of merit as the product of internal resistance and thermal conductivity is minimized by taking the derivative with respect to the geometrical ratio of both types of thermo elements (equation 3.5.2). Due to the assumed dimensions, the geometrical ratio is equal to 1. Also, note that the Seebeck effect from both elements is added, as all the elements are connected in a series and act as a source cell in series.

$$(R.K)_{minimized} = n^2 \times K_p \times \rho_p \left(1 + \frac{1}{x \times K_{total,pn}} + \frac{x}{\rho_{total,pn}} + \frac{1}{K_{total,pn} \times \rho_{total,pn}}\right) \qquad (3.5.2)^{[18]}$$

Geometric ratio is $\frac{\Upsilon_n}{\Upsilon_p}$ where $\Upsilon_p = \frac{A_p}{t_p}$ and$\Upsilon_n = \frac{A_n}{t_n}$,

A= Cross-sectional Area of the Element

T= Thickness of Element

$$\Upsilon_p = \frac{A_p}{t_p} = \left(\frac{1.4 \times 1.4}{1.14}\right) mm = 1.72mm$$

$$\Upsilon_n = \frac{A_n}{t_n} = \left(\frac{1.4 \times 1.4}{1.14}\right) mm = 1.72mm$$

Thus the geometrical ratio in the selected thermocouple with assumed dimensions is 1.

Thermal conductance,$K_{total,pn} = n \times \left(\frac{A_p \times K_p}{t_p} + \frac{A_n \times K_n}{t_n}\right) \qquad (3.5.3)^{[18]}$

Internal resistance, $R_{total,pn} = n \times \left(\frac{\rho_n}{\Upsilon_n} + \frac{\rho_p}{\Upsilon_p}\right) \qquad (3.5.4)^{[18]}$

As discussed in section 2.4, the ratio of internal resistance and load resistance m' for the array of thermocouples is given in equation 2.4.5.

The external resistance is given in equation 3.5.5.

$$R_{ext} = m' \times R_{total,pn} \quad (3.5.5)^{[18]}$$

Open circuit voltage due to the array of thermocouples in series is obtained as shown by equation 3.5.6, which is the product of the combined Seebeck coefficient, temperature difference, and number of thermocouples n as voltage in series arrangements adds to increase the voltage.

$$V_{OC} = (|\ \alpha_n\ | + |\ \alpha_p\ |) \times \Delta T \times n \quad (3.5.6)^{[18]}$$

Optimum current is obtained from equation 3.5.7, and the current stays constant even with increase in number of thermocouple. This is due to increases in the Seebeck voltage and the internal resistance by the same factor.

$$I_{opt} = \frac{(|\alpha_n| + |\alpha_p|) \times \Delta T \times n}{R(m'+1)} \quad (3.5.7)^{[18]}$$

Electrical power output is obtained by the product of optimum current and load resistance.

$$P_{output} = {I_{opt}}^2 \times R_{ext} \quad (3.5.8)^{[18]}$$

Factors contributing to the transport of energy in ‘n’ number of thermocouples in series stay the same except for the thermo electric effect and total conductance, which consist of ‘n’ as well. Hot junction heat input is given in equation 3.5.9.

$$\therefore Q_L = n \times (\mid \alpha_n \mid + \mid \alpha_p \mid) \times T_h \times I_{opt} + K_{eq} \times \Delta T - \frac{1}{2} \times I_{opt}{}^2 \times R) \qquad (3.5.9)^{[18]}$$

Cold junction heat removed is given in equation 3.5.10.

$$\therefore Q_{1,L} = n \times (\mid \alpha_n \mid + \mid \alpha_p \mid) \times T_c \times I_{opt} + K_{eq} \times \Delta T + \frac{1}{2} \times I_{opt}{}^2 \times R) \qquad (3.5.10)^{[18]}$$

Efficiency of the thermocouple can be obtained by the ratio of electrical power output to the amount of heat supplied at the hot junction as given in equation 3.5.11.

$$\text{Efficiency, } \eta_{max} = \frac{I_{opt}{}^2 \times R_{ext}}{n \times (|\alpha_n| + |\alpha_p|) \times T_h \times I_{opt} + K_{eq} \times \Delta T - \frac{1}{2} \times I_{opt}{}^2 \times R)} \qquad (3.5.11)^{[18]}$$

Values of property in Table 3.3 correspond to the temperature profile along the plate as shown in Table 3.2. Note that the TEG heat exchanger plate has been divided into 5 segments based on dimensions assumed along the x axis. Moreover, the average temperature of each segment corresponds to T_{avg} at each 0.05 m segment.

Table 3.3 Properties at T_{avg} for BiTe material

x(m)	Tavg (K)	$\rho_{p(\Omega m)}$	$\rho_{n(\Omega m)}$	$\alpha_{p(V/k)}$	$\alpha_{n(V/k)}$	$Z_{p(1/k)}$	$Z_{n(1/k)}$	$K_{p(Watts/K.m)}$	$K_{n(Watts/K.m)}$
0.05	3.8148E+02	1.3074E-05	1.3746E-05	2.3173E-04	2.2073E-04	2.7050E-03	2.0000E+00	1.4073E+00	1.7700E+00
0.1	3.5393E+02	1.2125E-05	1.2830E-05	2.3337E-04	2.2392E-04	3.6790E-03	2.5560E-03	1.3274E+00	1.6698E+00
0.15	3.3496E+02	1.0875E-05	1.1943E-05	2.3194E-04	2.2499E-04	3.9306E-03	2.8750E-03	1.2724E+00	1.6040E+00
0.2	3.2189E+02	1.0095E-05	1.1324E-05	2.2975E-04	2.2518E-04	4.2460E-03	3.3520E-03	1.2345E+00	1.5586E+00
0.25	3.1289E+02	9.6447E-06	1.0869E-05	2.2766E-04	2.2506E-04	4.5420E-03	3.6730E-03	1.2084E+00	1.5274E+00

Based on the properties obtained in Table 3.3 and equation 3.5.4, the total internal combined resistance of p/n-type is calculated, and addition of the Seebeck effect for both types provides the Seebeck coefficient. Equation 3.5.3 gives the total combined thermal conductance, and equation 3.5.1 provides the combined figures of merit, which are independent of the number of thermocouples and temperature values at each segment. Equation 2.4.5 provides the resistance ratio. Repeated calculation for each segment gives all the values for that particular segment of the heat exchanger plate.

Thus, as mention in section 3.4, the trial and error method will be used to find justifiable values for the efficiency of the module with both methods.

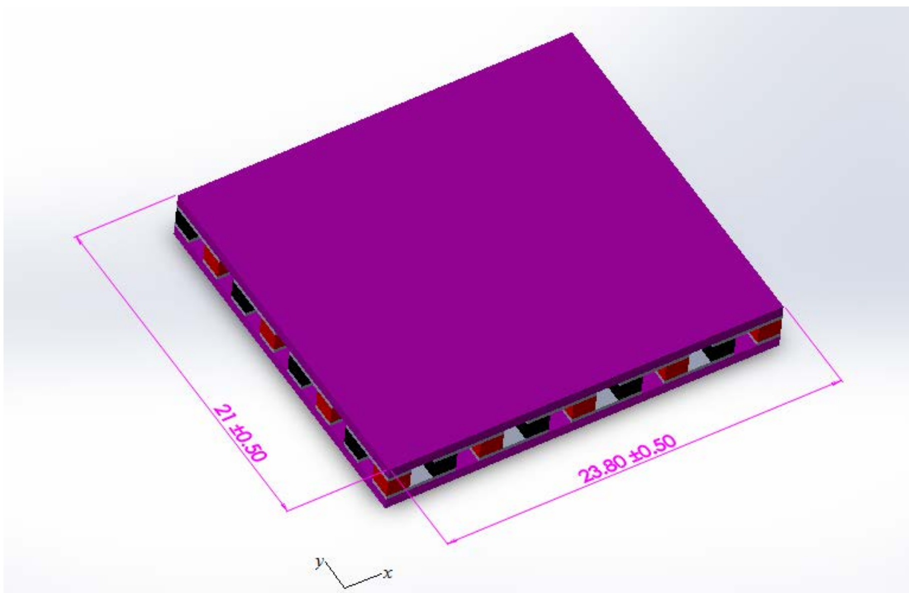

Figure 3.6 Dimension of Each module

Trial 1:

Let the total number of rows of modules along the y axis be 16. Since each module is 21mm in length along the y axis, $(16 \times 21)mm$ or $0.336m$ out of 1.352m will be used to generate power.

The total number of thermocouples when 0.05m of x axis and 0.336m of y axis for each segment is used to generate power, $n = 2 \times 71 \times 16 = 2272$.

Table 3.4 Calculated values at 2272 Thermocouple per Segment

x(m)	$R_{total,pn}(\Omega)$	α_{pn}(V/k)	$K_{total,pn}$(W/K)	$Z_{pn}(K^{-1})$	m'
0.05	3.5428E+01	3.5478E+01	1.2416E+01	2.4023E-03	1.3844E+00
0.1	3.2964E+01	3.3064E+01	1.1713E+01	2.7958E-03	1.4105E+00
0.15	3.0140E+01	3.0290E+01	1.1240E+01	3.1811E-03	1.4372E+00
0.2	2.8292E+01	2.8492E+01	1.0915E+01	3.4595E-03	1.4538E+00
0.25	2.7097E+01	2.7347E+01	1.0691E+01	3.6521E-03	1.4638E+00

Similarly, equation 3.5.6 provides open-circuit voltage, 3.5.7 provides optimum current generated by the thermocouple, 3.5.5 provides external resistance, 3.5.8 provides power output from each segment, and equation 3.5.9 provides the heat input required for each segment at given temperature. Thus, from all of above parameters efficiency is obtained as given in equation 3.5.11.

Table 3.5Calacuated values at 2272 Thermocouple per Segment

x(m)	V_{oc}(v)	I_{opt}(Amp)	$R_{ext.}$(ohm)	P_{output}(W)	$Q_{L,Elect.}$(W)	η_{max} %
0.05	1.8192E+02	2.1536E+00	4.9045E+01	2.2747E+02	3.1556E+03	7.20842508
0.1	1.2661E+02	1.5934E+00	4.6496E+01	1.1804E+02	2.0722E+03	5.69643732
0.15	8.7112E+01	1.1859E+00	4.3318E+01	6.0918E+01	1.3860E+03	4.39517666
0.2	5.9723E+01	8.6027E-01	4.1132E+01	3.0440E+01	9.3212E+02	3.26565029
0.25	4.0926E+01	6.1301E-01	3.9665E+01	1.4905E+01	6.3012E+02	2.36545415
					8.1761E+03	4.5862287

With reference to Table 3.5, it can be concluded that 5 segments of the TEG heat exchanger plate (each segment consisting of 32 (16×2) thermo modules or 2272 $(16 \times 2 \times 71)$ thermocouples in series arrangement) require total heat input of $\dot{Q}_{L,Elect} = 8176.1\,W$. But the exhaust heat available from the turbine is given as, $\dot{Q}_L = 7870\,W$. Hence, the number of thermocouples should be decreased further to match the exhaust heat available from the turbine.

Trial 2:

Tables 3.2 and 3.3 do not change, as they are independent of the number of thermocouples used. In trial 1, 32 modules were used, which exceeded the exhaust heat available, compared to required heat input to the thermocouples. Tables 3.6 and 3.7 are obtained in same way as Trial 1, except with 2130 thermocouples.

Table 3.6 Calculated Values at 2130 Thermocouples per Segment

x(m)	$R_{total,pn}(\Omega)$	$\alpha_{pn}(V/k)$	$K_{total,pn}(W/K)$	$Z_{pn}(K^{-1})$	m'
5.0000E-02	3.3214E+01	4.5245E-04	1.1640E+01	2.4023E-03	1.3844E+00
1.0000E-01	3.0904E+01	4.5729E-04	1.0980E+01	2.7958E-03	1.4105E+00
1.5000E-01	2.8257E+01	4.5693E-04	1.0538E+01	3.1811E-03	1.4372E+00
2.0000E-01	2.6524E+01	4.5493E-04	1.0233E+01	3.4595E-03	1.4538E+00
2.5000E-01	2.5404E+01	4.5272E-04	1.0023E+01	3.6521E-03	1.4638E+00

Table 3.7 Calculated Values at 2130 Thermocouples per Segment

x(m)	$V_{oc}(v)$	$I_{opt}(Amp)$	$R_{ext.}(ohm)$	$P_{output}(W)$	$Q_{L,Elect.}(W)$	η [illegible] %
0.05	1.7055E+02	2.1536E+00	4.5979E+01	2.1325E+02	2.9584E+03	7.20842508
0.1	1.1869E+02	1.5934E+00	4.3590E+01	1.1066E+02	1.9427E+03	5.69643732
0.15	8.1668E+01	1.1859E+00	4.0611E+01	5.7111E+01	1.2994E+03	4.39517666
0.2	5.5990E+01	8.6027E-01	3.8561E+01	2.8537E+01	8.7387E+02	3.26565029
0.25	3.8368E+01	6.1301E-01	3.7186E+01	1.3974E+01	5.9074E+02	2.36545415
					7.6651E+03	4.5862287

As shown in Table 3.7, $30\,(15 \times 2)$ thermo modules (or $2130\,(15 \times 2 \times 71)$ thermocouples placed in series arrangement) requires total heat input of $\dot{Q}_{L,Elect} = 7665.1\,W$. The exhaust heat available from the turbine is $\dot{Q}_L = 7870\,W$ which is sufficient. However, this trial cannot be verified until the heat transfer value for these segments, or the area used to incorporate the thermocouples, transmits enough heat to fulfill the heat requirement for all the thermocouples in use.

Method 2

In this method the electrical power output obtained is as shown in Method 1, but the rate of heat input to the plate is obtained using the overall heat transfer coefficient obtained in section 3.2.

Total Area of the TEG Heat Exchanger Plate $= 0.676\ m^2$.

Area of Each Segment, $A_s = \frac{0.676m^2}{10} = 0.0676\ m^2$.

Breadth of Each Segment, $b = 0.05m$

Length of Each Segment, $l = \frac{0.0676m^2}{0.05m} = 1.352m$

Thus, from the product of the overall heat transfer coefficient, area of each segment, and logarithmic temperature difference across the TEG heat exchanger plate, heat transfer across all segments with thermocouples can be obtained as shown in Table 3.8 (Refer equation 3.2.8)

Table 3.8QL, Overall for Each Segment

x(m)	LMTD(K)	$U_{overall}$(W/m^2.K	A_s(m^2)	$Q_{L,overall}$(W)	η_{max} %
0.05	2.1450E+02	1.8034E+02	6.7600E-02	2616.923988	7.2084251
0.1	1.4771E+02	1.8034E+02	6.7600E-02	1802.001988	5.6964373
0.15	1.0171E+02	1.8034E+02	6.7600E-02	1240.850395	4.3951767
0.2	7.0036E+01	1.8034E+02	6.7600E-02	854.4439538	3.2656503
0.25	4.8227E+01	1.8034E+02	6.7600E-02	588.3662309	2.3654542
				7102.586556	4.5862287

Table 3.8 shows that a total of 7102.58 Watts of heat will be transferred from all 5 segments consisting of TEG. Remaining heat $\dot{Q}_L - Q_{L,overall} = (7870 - 7102.58) Watts$ will be transferred from the last five segments, which is equivalent to 767.42 Watts.

Therefore, comparison between Tables 3.7 and 3.8 indicates that $Q_{L,Elect.}$in the case of 2130 thermocouples exceeds the heat transfer capacity of 5 segments, which is 7102.58 Watts. Thus, the number of thermocouples in these 5 segments needs to be trimmed further, considering the heat transfer capacity of 5 segments. The array of modules required for optimum power output and less heat input than $Q_{L,overall}$ is obtained when the number of thermocouples is 1917(27 thermo modules). This number can be obtained when 27 thermo modules are arranged in series in each segment. Table 3.9 summarizes all the calculated values using both approaches.

Table 3.9 Calculated Values for 1917 Thermocouples per Segment

Method1						
x(m)	**$R_{total,pn}(\Omega)$**	**$\alpha_{pn}(V/k)$**	**$K_{total,pn}(W/K)$**	**$Z_{pn}(K^{-1})$**	**m'**	
0.05	3.32E+01	4.52E-04	1.16E+01	2.40E-03	1.38E+00	
0.1	3.09E+01	4.57E-04	1.10E+01	2.80E-03	1.41E+00	
0.15	2.83E+01	4.57E-04	1.05E+01	3.18E-03	1.44E+00	
0.2	2.65E+01	4.55E-04	1.02E+01	3.46E-03	1.45E+00	
0.25	2.54E+01	4.53E-04	1.00E+01	3.65E-03	1.46E+00	
x(m)	**$V_{oc}(V)$**	**$I_{opt}(Amp)$**	**$R_{ext}(ohm)$**	**$P_{output}(W)$**	**$Q_{L,Elect.}(W)$**	**$\eta_{[illegible]}$ %**
0.05	1.53E+02	2.15E+00	4.14E+01	1.92E+02	2.66E+03	7.21E+00
0.1	1.07E+02	1.59E+00	3.92E+01	9.96E+01	1.75E+03	5.70E+00
0.15	7.35E+01	1.19E+00	3.65E+01	5.14E+01	1.17E+03	4.40E+00
0.2	5.04E+01	8.60E-01	3.47E+01	2.57E+01	7.86E+02	3.27E+00
0.25	3.45E+01	6.13E-01	3.35E+01	1.26E+01	5.32E+02	2.37E+00
	8.37E+01	**1.28E+00**	**3.71E+01**	**3.81E+02**	**6.90E+03**	**4.59E+00**
Method2						
x(m)	**LMTD(K)**	**$U_{overall}(W/m^2.K)$**	**$A_s(m^2)$**	**$P_{output}(W)$**	**$Q_{L,overall}$**	**$\eta_{[illegible]}$ %**
0.05	2.15E+02	1.80E+02	6.76E-02	1.92E+02	2.62E+03	7.21E+00
0.1	1.48E+02	1.80E+02	6.76E-02	9.96E+01	1.80E+03	5.70E+00
0.15	1.02E+02	1.80E+02	6.76E-02	5.14E+01	1.24E+03	4.40E+00
0.2	7.00E+01	1.80E+02	6.76E-02	2.57E+01	8.54E+02	3.27E+00
0.25	4.82E+01	1.80E+02	6.76E-02	1.26E+01	5.88E+02	2.37E+00
				3.81E+02	**7.10E+03**	**4.59E+00**

Thus, from Table 3.9, it can be shown that both approaches are in agreement on average efficiency. $Q_{L,Elect.}$is less than $Q_{L,overall}$, which means sufficient heat input is available to the thermocouples. Total electric power obtained by the use of BiTe-based thermocouples is 381 Watts. Table 3.9 also shows that by arranging all the thermocouples in series, the average voltage generated by 5 segments is 83.7 V, and the average current generated is 1.28 amps.

3.6 Combined Efficiency of Baseline 10KW Brayton Cycle

Table 3.9 shows that 381Watts could be saved using the TEG Heat Exchanger. In addition, section 3.1 shows that the efficiency of a simple 10KW reversible Brayton cycle is 55%.

Total power output using work output from the turbine and electrical power output from the TEG heat exchanger is $(10000 + 381)\ 10381$ Watts.

Total heat input to 10KW Brayton cycle = 17870 Watts.

$$\eta_{combined} = \frac{total\ power\ output}{total\ heat\ intput} = \frac{10381}{17870} Watts = 0.58 \text{ or } 58\%$$

Thus with the use of thermocouples overall efficiency has increased by 3%.

Chapter 4: Conclusion

4.1 Summary

In closing, medium-quality exhaust heat was selected based on a survey of the literature. Among all other waste heat recovery devices, a flat-plate heat exchanger with built-in thermo modules arranged in series was selected. Based on the temperature profile across the flat plate, bismuth telluride-based material was selected. The effect of temperature on the properties of such materials was found to be significant. Calculations show that the efficiency of individual thermocouples decreases with decrease in temperature. Because the temperature profile across the flat plate decreases, the entire flat plate of the heat exchanger could not be used for power generation.

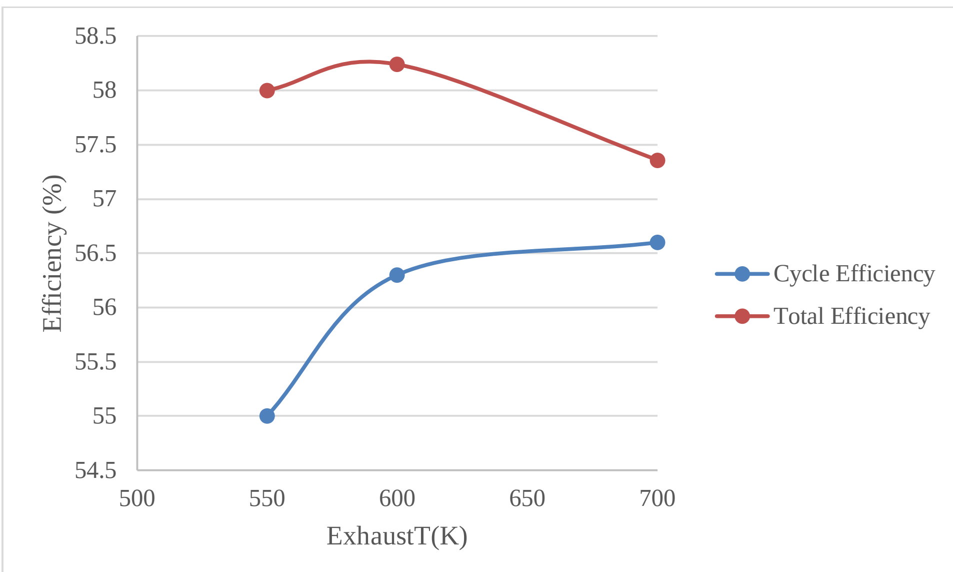

Figure 4.1 Comparison of Efficiency at Various Turbine Exhaust Temperatures

Figure 4.1 shows that heat recovered by the use of a TEG heat exchanger for electrical power generation contributes to increased efficiency of a 10 KW baseline Brayton cycle from 55% to 58% when exhaust temperature is 550K. The optimum number of thermocouples incorporated in the TEG heat exchanger was found to be 1917 per segment. 27 modules were found to fit in each segment. Again, at turbine exhaust of 600K the efficiency of Brayton cycle was found to be 56.3%, and it increased to 58.24% with the TEG heat exchanger. The optimum number of thermocouples that could fit in each segment was 1420, or 20 modules in each segment. For a turbine exhaust temperature of 700K, the efficiency of the Brayton cycle was found to be 56.6%, and it increased to 57.36% with the TEG heat exchanger. The number of thermocouples that could fit at this temperature was 355 or 5 modules per segment.

As shown in Figure 4.1, the total efficiency of the cycle decreases with increase in temperature, as electrical power contributed by the TEG heat exchanger decreases. This is due to increase in thermal conductivity and electrical resistivity with increase in temperature for the selected BiTe-based material as shown in Figures 2.7 and 2.8. This decreases the figure of merit. Thus, it can also be concluded that the selected material performs better at lower temperatures.

Regarding the variation of electrical power, voltage, and current generated across each segments across the plate, it can be concluded that all of the parameters drop with decrease in average temperature across the plate. It can be concluded that most of the calculations performed were specific to the chosen material. Heat input required for these thermocouples did not exceed the available exhaust heat source, and efficiency of each segment is in agreement with both methods mentioned in section 3.5.

Such systems can be used to generate small amounts of electric power and supply heat to the cooling fluid, while at the same time being used for house hold applications. For example, generated power can be used to run small water pumps or other devices, increasing overall cycle efficiency.

Repeated calculation at turbine exhaust temperatures of 550K, 600K and 700 K can be found in Appendix A.

4.2 Contribution

Many researchers have made contributions to improving the power generating capacity of thermoelectric material. As mentioned in Chapter 1, an approach was developed to show the incorporation of thermo-electric generators to recover exhaust heat from the Brayton cycle. Equations used in section 2.4 are derived from Decher who treated thermocouples as a heat engines. This was also verified by calculating the overall heat transfer coefficient across the heat exchanger [18]. Parametric plots for efficiency at three different exhaust temperatures suitable for the selected BiTe-based material was obtained.

4.3 Future Work

Many issues remain unsolved regarding this research, and a number of topics can be raised to answer more questions. Some of the topics to explore are listed as follows,

- Selected semiconductor used in TEG has low efficiency due to low figure of merit. The contradicting nature of electrical resistivity and thermal conductivity with increase in temperature is the fundamental problem researchers are working to overcome. If both factor could be reduced with increase in temperature, the figure of merit would increases beyond unity, thus increasing efficiency.

- Study of proper configuration of thermocouples inside TEG heat exchanger to avoid corrosion effects, reduce thermal stress, and optimize geometry would guarantee longer hours of maintenance-free operation.
- Considering the irreversible factors occurring in the Brayton cycle, a TEG heat exchanger will provide accurate values.
- Lastly, implementation of computer simulations based on changes in various parameters affecting the property and efficiency of TEG will help to develop a generalized mathematical model and validate analytical values obtained.

References

[1] Second Law of Thermodynamics, Available: http://en.wikipedia.org/wiki/Second_law_of_thermodynamics, Date accessed: 2/26/13

[2] James A. Fay and Dan S. Golomb, 2002, Energy and the Environment, Oxford University Press;New York, NY.

[3] Kehlhofer and Rolf, 1991, Combined-Cycle Gas & Steam Turbine Power Plants, Page 7.

[4] D.M. Rowe (Ed), 1994, Handbook of Thermoelectrics, CRC Press; Boca Raton, USA.

[5] "Efficiency by the Numbers" by Lee S. Langston

[6] Available: http://www.electronics-cooling.com/2006/11/the-seebeck-coefficient/#respond, Date accessed: 3/21/13

[7] Available: http://physicsworld.com/cws/article/news/2011/may/05/multiple-valleys-boost-thermoelectric-performance, Date accessed: 4/27/13

[8] Z.H. Dughaish, 2002, "Lead telluride as a thermoelectric material for thermoelectric power generation", Physica B: Physics of Condensed Matter, Vol.332, Page 205 - 223.

[9] Available: http://www.komatsu.com.sg/CompanyInfo/profile/report/pdf/152-05_E.pdf, Date accessed: 8/21/12

[10] Heikes, Robert R., 1961,Thermoelectricity Science and Engineering, Interscience Publishers; New York,NY

[11] Snyder, G. Jeffrey, 2008, “Complex thermoelectric materials”, Nature Materials, Vol.7, Page 105 – 114.

[12] Available: http://www.energyefficiencyasia.org, Date accessed: 7/14/12

[13] Available: http://www.sciencedaily.com/releases/2007/06/070603225026.htm, Date accessed: 5/31/2012

[14] Available: http://www.learnthermo.com/T1-tutorial/ch09/lesson-E/pg04.php, Date accessed: 2/3/2014

[15] Available: http://sounak4u.weebly.com, Date accessed: 2/3/2014

[16] Stanley W. Angrist, 1982. Direct Energy Conversion (Fourth Edition). 470 Atlantic Aveneue,Boston, Massachusetts 02210: Allyn and Bacon.

[17] Yamashita, Osamu and Tomiyoshi, Shoichi and Makita, Ken, 2003,"Bismuth telluride compounds with high thermoelectric figures of merit", Journal of Applied Physics, Vol. 93, Page 368-374.

[18] Reiner Decher,1996, Direct Energy Conversion: Fundamentals of Electric Power Production, Oxford University Press.

[19] Yunus A. Çengel, Michael A. Boles,2004, Thermodynamics: An Engineering Approach, McGraw-Hill.

[20] Yunus A.Cengel, Afshin J. Ghajar, 2010, "Heat and Mass Transfer Fundamentals & Applications", 4th Edition, McGraw-Hill Higher Education.

[21] Available: http://e-collection.library.ethz.ch/eserv/eth:5708/eth-5708-02.pdf, Date accessed: 4/10/2013

[22] Available: https://www.efunda.com, Date accessed: 1/12/2013

[23] Available: http://facstaff.cbu.edu/rprice/lectures/htcoeff.html, Date accessed: 1/14/2014

Appendix

Calculation for assumed turbine exhaust of 600K

1 Sizing of TEG Module for 10 KW Brayton Cycle

1.1 10KW Baseline Brayton Cycle

Assume:- Isentropic flow, Change in Kinetic Energy/Potential Energy ΔK.E./ΔP.E.≈0, Mass Flow rate $\dot{m}$ is constant, Ideal air assumptions applicable for gas in the cycle, Pressure Ratio of the cycle(compressor and turbine) = 13, Specific heat of gas is not a function of temperature.

Given, Specific Heat Ratio of air, $K = 1.4$ at $T_1 = 300K$

Process 1-2 isentropic compression

$$\left(\frac{T_2}{T_1}\right) = \left(\frac{P_2}{P_1}\right)^{\frac{K-1}{K}} \tag{1.1.1}$$

Pressure Ratio of the cycle, $\left(\frac{P_2}{P_1}\right) = 13$.

Substituting the values for specific heat ratio, pressure ratio and inlet ambient air temperature T_1 in equation 1.1.1 provides exit temperature from the compressor at stage 2, $T_2 = 624.30K$

Process 3-4 isentropic expansion

$$\left(\frac{T_3}{T_4}\right) = \left(\frac{P_3}{P_4}\right)^{\frac{K-1}{K}} \tag{1.1.2}$$

Substituting the values for specific heat ratio, pressure ratio and exit gas temperature from the turbine exhaust $T_4 = 600K$ inlet temperature to the turbine, $T_3 = 1248.6K$.

Specific Turbine Work, $\mathrm{w_T}$

$$w_T = (h_3 - h_4)\frac{KJ}{Kg} \qquad (1.1.3)$$

Specific enthalpy of gas at turbine inlet,$h_3 = 1335.09\ \frac{KJ}{Kg}$@$1248.6K$[19]

Specific enthalpy of gas at turbine exit,$h_4 = 607.02\ \frac{KJ}{Kg}$@$600K$[19]

Substituting the values for enthalpy of gas at 1248.6K and 600K provides specific turbine work of $728.07\frac{KJ}{Kg}$.

Specific Compressor Work,$\mathrm{w_c}$

$$w_c = (h_2 - h_1)\frac{KJ}{Kg} \qquad (1.1.4)$$

Specific enthalpy of gas at compressor exit,$h_2 = 632.61\ \frac{KJ}{Kg}$@$624.30K$[19]

Specific enthalpy of gas at turbine exit,$h_1 = 300.19\ \frac{KJ}{Kg}$@$300K$[19]

Substituting the values for specific enthalpy of gas, compressor work $w_c = (h_2 - h_1)\frac{KJ}{Kg} = 332.42\frac{KJ}{Kg}$.

Network from Turbine, $\mathrm{W_{Net}}$

$$w_{Net} = w_T - w_C \qquad (1.1.5)$$

Substituting values from equation 1.1.3 and 1.1.4 network from turbine obtained is $395.65\frac{KJ}{Kg}$.

Mass flow rate in the cycle is given by equation 1.1.6

$$W_{Net,T} = w_{Net} * \dot{m} \tag{1.1.6}$$

$$W_{Net,T} = 10\ KW$$

Substituting the value of specific network form the turbine and total network from the turbine, the mass flow rate of the gas in the cycle is obtained, $\dot{m} = 2.53 \times 10^{-2}\frac{Kg}{s}$.

Heat Input to the Heat Exchanger, Q_H

$$Q_H = \dot{m}(h_3 - h_2)KW \tag{1.1.7}$$

Substituting mass flow rate of the gas, specific enthalpy of gas at turbine inlet and compressor exit, the rate of heat input to the combustion chamber, $Q_H = 17.77\ KW$

Heat dissipated Q_L from the cycle

$$Q_L = Q_H - W_{Net,T} \tag{1.1.8}$$

Substituting the value of rate of heat input to the combustion chamber and rate of total network performed by the turbine in equation 1.1.8, the total rate of heat dissipated from the cycle, $\dot{Q}_L = 7.77KW$.

Heat Dissipated from Baseline 10KW Brayton cycle

Figure 1.1 illustrates the Brayton cycle, where stage 1 to 2 indicate adiabatic reversible compression, stage 2 to 3 indicate constant pressure heat addition and stage 3 to 4 indicate adiabatic reversible expansion. Pressure and temperature at each stage is given below,

$T_1 = 300K$

$P_1 = 1\ atm$

$T_2 = 624.30K$

$P_2 = 13\ atm$

$T_3 = 1248.6K$

$P_3 = 13\ atm$

$T_4 = 600K$

$P_4 = 1\ atm$

Thermal Efficiency of the cycle $\eta = \frac{W_{Net,T}}{Q_H} = \frac{10\ KW}{17.77\ KW} = 0.563\ or\ 56.3\%$

Note: TEG heat exchanger discards most of the heat from turbine and produces some electrical work while constant temperature cooling water flows at $293K$on cooling side.

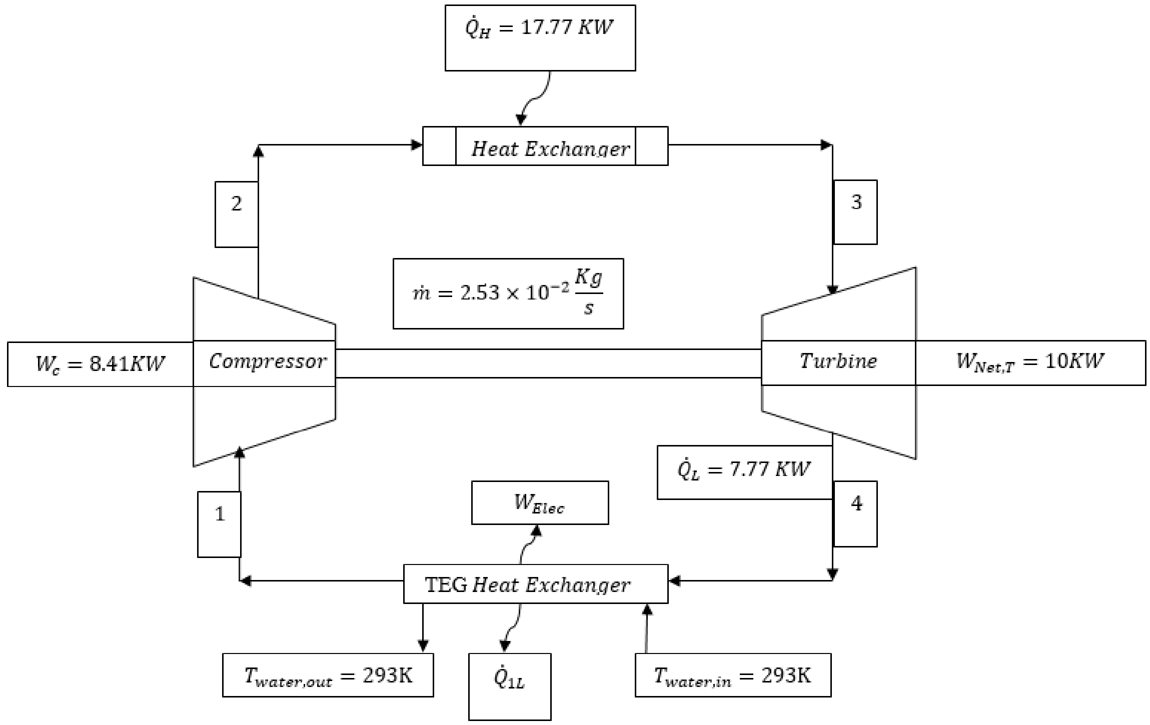

Figure 6.1 Schematic Diagram of Proposed Cycle

1.2 Determination of Overall Heat Exchanger Area

Heat is transferred from hot fluid to the ceramic wall by convection and through the wall by conduction and into the semiconductor legs by conduction. Again heat flows towards the cold fluid by convection. Any radiation effects are neglected in determining the overall heat transfer coefficient.

Assume: Heat transfer is in normal direction to the flat plate surface. Ceramic walls on the hot and cold side are nearly isothermal. Lateral heat flow is zero, all sides are well insulated. The temperature of water and gas is constant thus it is 1-d heat transfer process.

Energy balance

Rate of heat transfer into the ceramic hot side – Rate of heat transfer out of the ceramic cold side = Rate of electrical work produced from TEG heat exchanger

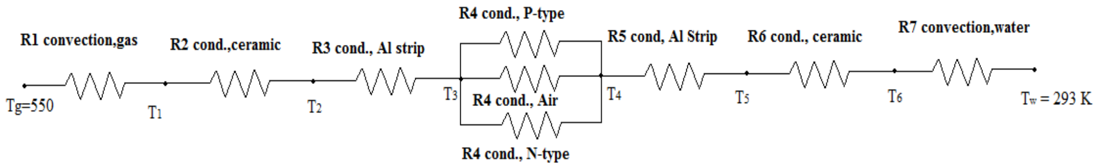

Figure 6.2 Thermal Resistance Circuit for TEG Heat Exchanger

Convection resistance for flow of hot gas, $R_1 = \frac{1}{h_1 A_1}$

Conduction resistance for ceramic plate, $R_2 = \frac{t_2}{K_2 A_2}$

Conduction resistance for aluminum strip, $R_3 = \frac{t_3}{K_3 A_3}$

Conduction resistance for P-type thermo element, $R_4 = \frac{t_4}{K_4 A_4}$

Conduction resistance for air gap between thermo elements, $R_4{}' = \frac{t_4{}'}{K_4{}' A_4{}'}$

Conduction resistance for N-type thermo elements, $R_4{}'' = \frac{t_4{}''}{K_4{}'' A_4{}''}$

Conduction resistance for aluminum strip, $R_5 = \frac{t_5}{K_5 A_5}$

Conduction resistance for ceramic plate, $R_6 = \frac{t_6}{K_6 A_6}$

Convection resistance for flow of cooling water, $R_7 = \frac{1}{h_7 A_7}$

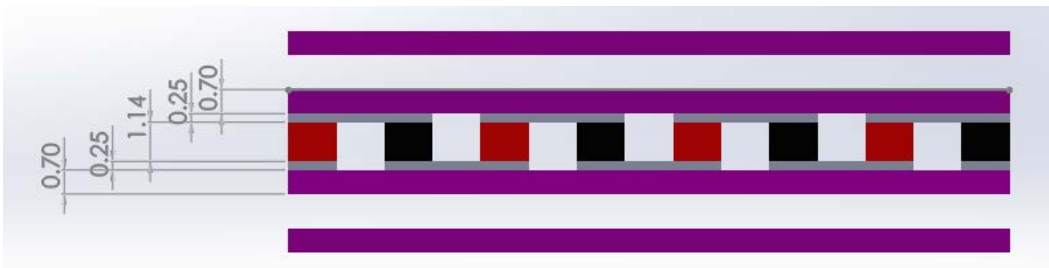

Figure 6.3Side View of TEG module

As shown in figure 1.3 gap between parallel ceramic plate is 1.4mm, thickness of ceramic plate is $t_2 = t_6 = 0.7mm$, thickness of aluminum conducting strip is $t_3 = t_5 = 0.25mm$, thickness of thermo elements$t_4 = t_4'' = 1.14mm$, thickness of air gap between thermo element is $\boldsymbol{t_4}' = (1.14 + 0.25)\text{mm} = 1.39\text{mm}$. Using these assumed value based on literature survey on geometry of thermo electric module overall heat transfer coefficient can be calculated provided all the thermo physical properties are available.

Parameters for all thermal resistance from R_1 to R_7 are known except their corresponding area and convection/conduction coefficient.

1. Convection coefficient for flow of hot gas, h_1

   The Dittus-Boelter equation used for turbulent flow is used to calculate Nusselt number. This equation provides less accurate values if the bulk fluid temperature difference between cold and hot fluid is large. Exhaust temperature from turbine at T_4 is inlet temperature for TEG heat exchanger as $T_{hot,in}$ for TEG heat exchanger, $T_{hot,in} = 600K$.

Given mass flow rate of hot gas, $\dot{m} = 2.53 \times 10^{-2} \frac{Kg}{s}$

Specific heat at constant pressure $C_p = 1034.85 \frac{J}{Kg.K}$ [20]

$T_{hot,out} = ?$

$$Q_L = \dot{m} \times C_p \times (T_{hot,in} - T_{hot,out}) \tag{1.2.1}$$

Thus substituting values in equation 1.2.1, $T_{hot,out}$ for TEG heat exchanger is $303.23K$

Bulk fluid temperature is average of $T_{hot,in}$ and $T_{hot,out}$ i.e. 451.61K

Properties at Bulk fluid temperature 451.61K

1	Density of hot gas, ρ_{air}[20]	$0.782 \frac{Kg}{m^3}$
2	Dynamic viscosity of hot gas, μ_{air}[20]	$2.501 \times 10^{-5} \frac{Kg}{ms}$
3	Prandtlnumber, Pr[19]	0.7815
4	Thermal Conductivity[20]	$0.03633 \frac{W}{mK}$

Assumed duct size for flow of gas,

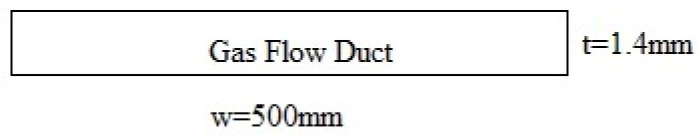

Figure 6.4Duct for Hot Exhaust Gas

Hydraulic Diameter, $D_h = 2 \times t = 2.8mm$

Gas Velocity,

$$V_{avg} = \frac{\dot{m}}{A_c \times \rho_{air}} \tag{1.2.2}$$

Substituting the values for mass flow rate, flat plate cross sectional area and density of gas at bulk fluid temperature provides $46.2\frac{m}{s}$.

Reynolds Number,

$$Re = \frac{\rho_{air} \times V_{avg} \times D_h}{\mu_{air}} \tag{1.2.3}$$

Substituting the values for density of gas, velocity from equation 1.2.2, hydraulic diameter and viscosity Reynolds number obtained is 4044.8. Thus the flow of gas on the hot side is turbulent.

Nusselt number is given by equation 1.2.4.

$$Nu = 0.023 \times Re^{0.8} \times Pr^n \tag{1.2.4}$$

Where $n = 0.3$ for cooling [20].

Substituting values for Re and Pr number in equation 1.2.4, nusselt number obtained is 16.4.

Also, Convective heat transfer coefficient $h_1 = \frac{K_1 \times Nu}{D_h} = 212.8 \frac{W}{m^2 \times K}$

2. Conduction coefficient for ceramic plate,K_2

   Thermal conductivity for ceramic plate at bulk fluid temperature of 451.61K on hot side is $22.88\ \frac{W}{m.K}$[21]

3. Conduction coefficient for aluminum strip,K_3

   Thermal conductivity for aluminum conducting strip at bulk fluid temperature of 451.61K on hot side is $238 \frac{W}{m.K}$[22]

4. Conduction coefficient for P-type thermo element,K_4

   Since the thermo element is exposed to two different hot and cold bulk fluid temperatures, thermal conductivity is determined at average temperature of two sides, $T_{avg} = \frac{(451.61+293)K}{2} = 372.3K$.

   $K_4 = 1.4 \frac{W}{m.K}$[17]

5. Conduction coefficient for N-type thermo elements,$K_4{}''$

   Thermal conductivity at $T_{avg} = 372.3K$

   $K_4{}'' = 1.7 \frac{W}{m.K}$[17]

6. Conduction coefficient for air gap between thermo elements,$K_4{}'$

Air gap is exposed to two different hot and cold bulk fluid temperatures, thermal conductivity is determined at average temperature of two sides, $T_{avg} = 372.3K$.

$K_4{}' = 0.0311\ \frac{W}{m.K}$[21]

7. Conduction resistance for aluminum strip, K_5

   Thermal conductivity for aluminum conducting strip at cold fluid temperature of 293K on cold side is $236.72\frac{W}{m.K}$[22]

8. Conduction resistance for ceramic plate, K_6

   Thermal conductivity for ceramic plate at cold fluid temperature of 293K is $35.11\frac{W}{m.K}$[21]

9. Convection resistance for flow of cooling water, h_7

   Bulk fluid temperature is used to apply Dittus-Boelter equation for calculating the convective heat transfer coefficient on cold side.

   Assume ΔT_w on cool side to be 10K.

   Average efficiency of TEG at $372.3K$ obtained with calculation similar to section 2.4 shows to be 6.81%. Thus approximate electrical power generated at T_{avg} is $6.81\%\ of\ \dot{Q}_L = 0.0681 \times 7.77KW = 529.13W$

   Specific heat at constant pressure $C_{p,w} = 4194\frac{J}{Kg.K}$ [19]

   Mass flow rate of cooling water in TEG heat exchanger,

$$\dot{m}_w = \frac{(\dot{Q}_L - 529.13)W}{C_{p,w} \times \Delta T_w} \tag{1.2.5}$$

Thus $\dot{m}_w$ for TEG heat exchanger is $0.17 \ \frac{Kg}{s}$

Properties at bulk fluid temperature $\left[\frac{(283+293)K}{2}\right] 288K$ [20].

1	Density of water, ρ_{water}	$999 \ \frac{Kg}{m^3}$
2	Dynamic viscosity of cold water, μ_{water}	$1.138 \times 10^{-3} \ \frac{Kg}{ms}$
3	Thermal Conductivity, K_{water}	$0.589 \ \frac{W}{mK}$

Assumed duct size for flow of water,

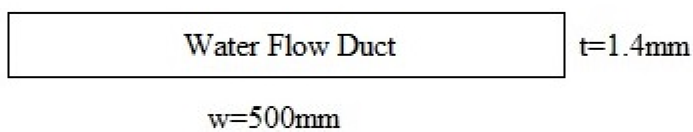

Figure 6.5Duct for Cooling Water

Hydraulic Diameter, $D_h = 2 \times t = 2.8mm$

Gas Velocity,

$$V_{avg} = \frac{\dot{m}}{A_c \times \rho_{water}} \tag{1.2.6}$$

Substituting the values for mass flow rate, flat plate cross sectional area and density of gas at bulk fluid temperature provides $0.24 \frac{m}{s}$.

Reynolds Number,

$$Re = \frac{\rho_{air\times}V_{avg\times}D_h}{\mu_{air}} \tag{1.2.7}$$

Substituting the values for density of gas, velocity from equation 1.2.6, hydraulic diameter and viscosity reynolds number obtained is 590.Thus the flow of gas on the cold side is laminar. For laminar flow inside rectangular duct the nusselt number $Nu = 7.54$ [20, Table 8-1].Also convective heat transfer coefficient for flow of water, $h_w = \frac{K_w \times Nu}{D_h} = 1586.09 \frac{W}{m^2 \times K}$.

The relation for Overall heat transfer coefficient is given by equation 1.2.8

$$Q_L = U_{overall} \times A_{Total} \times \Delta T_{LMTD} \tag{1.2.8}$$

A_{Total} is the total area required to transfer 7770 W of heat from the TEG heat exchanger.

Equation 1.2.8 is also given as $Q_L = \frac{\Delta T_{LMTD}}{R_{total}}$.

$$\therefore R_{total} = \frac{1}{U_{overall} \times A_{Total}} = \frac{1}{h_1 A_1} + \frac{t_2}{K_2 A_2} + \frac{t_3}{K_3 A_3} + R_{eq,module} + \frac{t_5}{K_5 A_5} + \frac{t_6}{K_6 A_6} + \frac{1}{h_7 A_7} \tag{1.2.9}$$

$R_{eq,module}$ is total thermal resistance due to P-type, N-type and air gap between thermo elements. All the thermo elements are arranged thermally in parallel orientation whereas electrically in series. First $R_{eq,couple}$ is obtained,

$$\frac{1}{R_{eq,couple}} = \frac{1}{R_4} + \frac{1}{R_4{}'} + \frac{1}{R_4{}''}$$

$$\frac{1}{R_{eq,couple}} = \frac{K_4 A_4}{t_4} + \frac{K_4{}' A_4{}'}{t_4{}'} + \frac{K_4{}'' A_4{}''}{t_4{}''}$$

Given, $t_4{}' = 1.39\text{mm}, t_4 = t_4{}'' = 1.14\text{mm}$

$\therefore\ let\ t_4 = t_4'' = t$

$$\frac{1}{R_{eq,couple}} = \frac{K_4 A_4 + K_4'' A_4''}{t} + \frac{K_4' A_4'}{t_4'}$$

$$R_{eq,couple} = \frac{t \times t_4'}{t_4'(K_4 A_4 + K_4'' A_4'') + t \times K_4' A_4'} \tag{1.2.10}$$

Each module has 71 thermocouple. The thermal conductance for n number of thermocouple is given by equation 1.2.11.

$$K = n \times (K_P + K_N) \tag{1.2.11}$$

Similarly equivalent thermal resistance for n thermocouple in a module is given by equation 1.2.12.

$$R_{eq,module} = \frac{1}{n} \times \left[\frac{t \times t_4'}{t_4'(K_4 A_4 + K_4'' A_4'') + t \times K_4' A_4'}\right] \tag{1.2.12}$$

Substituting equation 1.2.12 and equation 1.2.9 gives equation 1.2.13

$$\therefore R_{total} = \frac{1}{U_{overall} \times A_{Total}} = \frac{1}{h_1 A_1} + \frac{t_2}{K_2 A_2} + \frac{t_3}{K_3 A_3} + \frac{1}{71} \times \left[\frac{t \times t_4'}{t_4'(K_4 A_4 + K_4'' A_4'') + t \times K_4' A_4'}\right] + \frac{t_5}{K_5 A_5} + \frac{t_6}{K_6 A_6} + \frac{1}{h_7 A_7} \tag{1.2.13}$$

Note: Relation between total area and individual resistance area for each material is developed based on assumed dimension for a single module to obtain overall heat transfer coefficient (Refer chapter 1 and chapter 3).

5. $A_{Total} = A_1 = A_2 = A_6 = A_7$ (uniform areas across each thermal resistance in module)

6. A_3 is area of lower Aluminum strip (Refer figure 3.3 chapter 3).

Let a be area equivalent to cross-sectional area of each thermo element. For each thermoelectric module consisting of 71 thermocouple (Refer figure 1.4 chapter 1) the relation between area of required ceramic plate or A_{Total} and $A_3$for a module is given underneath.

$A_{Total} = 15 \times 17 \times a = 255a$

Number of thermo elements along x axis is 15 and 17 along y axis (Refer figure 1.4 chapter 1).

$$\therefore a = \frac{A_{Total}}{255} \tag{1.2.14}$$

$A_3 = 107a$

$$\therefore a = \frac{A_3}{107} \tag{1.2.15}$$

Equating1.2.14 and 1.2.15gives equation 1.2.16.

$$A_3 = \frac{A_{Total} \times 107}{255} \tag{1.2.16}$$

Note: Above relationship exists for entire TEG heat exchanger plate as multiple numbers of modules in series arrangement builds the plate.

7. $A_4 = A_4{}' = A_4{}'' = a$ is cross sectional area of n-type, p-type and air gap in between.

$$\therefore R_{eq,module} = \left(\frac{1}{71 \times a}\right) \times \left[\frac{t \times t_4{}'}{t_4{}'(K_4 + K_4{}'') + t \times K_4{}'}\right] \tag{1.2.17}$$

Equation1.2.14 and 1.2.17 give equation 1.2.18.

$$\therefore R_{eq,module} = \left(\frac{255}{71 \times A_{Total}}\right) \times \left[\frac{t \times t_4{}'}{t_4{}'(K_4 + K_4{}'') + t \times K_4{}'}\right] \tag{1.2.18}$$

8. $A_5$is area of upper Aluminum strip (Refer 3.3 chapter 3).

$A_5 = 3 \times 36 \times a = 108a$ (Each thermocouple junction formed by upper aluminum strip is 3 times area of each thermo element and each module has 36 thermocouple as seen from the top)

$$A_5 = 108a \tag{1.2.19}$$

Equation 1.2.14 and 1.2.19gives equation 1.2.20.

$$A_5 = \frac{108 \times A_{Total}}{255} \tag{1.2.20}$$

Substitute all the relation obtained from 1 to 4 gives final equation for overall thermal resistance as shown in equation 1.2.21.

$$\therefore R_{total} = \frac{1}{U_{overall} \times A_{Total}} = \frac{1}{h_1 A_{Total}} + \frac{t_2}{K_2 A_{Total}} + \frac{t_3 \times 255}{K_3 \times A_{Total} \times 107} + \left(\frac{255}{71 \times A_{Total}}\right) \times \left[\frac{t \times t_4'}{t_4'(K_4 + K_4'') + t \times K_4'}\right] + \frac{t_5 \times 255}{K_5 \times 108 \times A_{Total}} + \frac{t_6}{K_6 A_{Total}} + \frac{1}{h_7 A_{Total}} \tag{1.2.21}$$

$$\therefore R_{total} = \frac{1}{U_{overall}}$$

$$= \frac{1}{h_1} + \frac{t_2}{K_2} + \frac{t_3 \times 255}{K_3 \times 107} + \left(\frac{255}{71}\right) \times \left[\frac{t \times t_4'}{t_4'(K_4 + K_4'') + t \times K_4'}\right]$$

$$+ \frac{t_5 \times 255}{K_5 \times 108} + \frac{t_6}{K_6} + \frac{1}{h_7} = \frac{1}{U_{overall}}$$

$$= (0.0047 + 0.0000306 + 0.0000025 + 0.00131 + 0.000001056$$

$$+ 0.00001993 + 0.0006304)\frac{m^2 \times K}{W}$$

Substitute corresponding heat transfer coefficients and thickness, values obtained in second, third, fifth, sixth and seventh terms are negligible compared to values in first and fourth terms. Thus the value of overall heat transfer coefficient obtained is $166.4 \frac{W}{m^2.K}$

Assume Parallel TEG Heat Exchanger

Counter flow heat exchanger can transfer more energy than parallel heat exchanger as the exit temperature of the cooling fluid can get close to high temperature of the hot fluid (parallel temperature profile). In case of parallel heat exchanger the temperature difference is high at the entrance region and later the two fluids tend to meet same temperature point at exit region (converging temperature profile) depending on the design parameters.

Thus temperature difference in case of parallel heat exchanger at entrance region is high. If thermo electric generators are placed in the region of higher temperature difference more electrical power is obtained. Also note that efficiency of TEG is directly proportional to temperature difference across the two junctions of the TEG material. Thus parallel heat exchanger is selected and log mean temperature difference is used to find the total area required for the TEG heat exchanger.

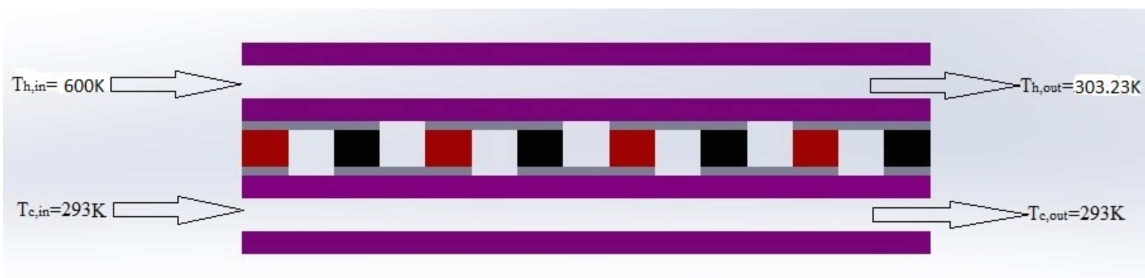

Using equation 1.2.8, the total area required for the heat transfer can be obtained.

$$7870W = 166.4\frac{W}{m^2.K} \times A_{Total,plate} \times \frac{(T_{h,o} - T_{c,o}) - (T_{h,in} - T_{c,in})}{ln\left[\frac{(T_{h,o}-T_{c,o})}{(T_{h,in}-T_{c,in})}\right]}$$

$$7770W = 166.4\frac{W}{m^2.K} \times A_{Total,plate} \times \frac{[(303.23-293)-(600-293)]K}{ln\left[\frac{(303.23-293)}{(600-293)}\right]}$$

$$\therefore A_{Total,plate} = 0.535\,m^2$$

1.3 Temperature Profile across TEG Heat Exchanger Plate

Temperature profile of water across the plate on cool side is assumed to be constant at 293K. Thus the temperature profile for exhaust gas on the hot side can be obtained using constant wall temperature method.

$$\dot{Q}_{conv,gas} = \dot{m} \times C_p \times dT_m \qquad (1.3.1)$$

Also from Newton's law of cooling $\dot{Q}_{conv,gas} = h_g \times (T_s - T_m) \times dA$ and $(T_s - T_m)$ is the temperature difference between the surface and the fluid. Since $T_s < T_m$ or the exhaust gas will cool thus it gives equation 1.3.2.

$$-\left(h_g \times (T_m - T_s) \times dA\right) = \dot{m} \times C_p \times dT_m$$

$$-\left(h_g \times (T_m - T_s) \times p \times dx\right) = \dot{m} \times C_p \times dT_m \qquad (1.3.2)$$

Where,

Perimeter of the duct, $p = 2 \times (w \times t)$, but $(w \gg t)$ (Refer figure 3.4) $\therefore p = 2w$

T_s= Constant wall temperature

T_m = Mean hot exhaust gas temperature

h_g = Average convective heat transfer coefficient of hot exhaust gas

dT_m = Decrease in mean temperature of hot exhaust gas

T = Temperature at any pointalong the plate in x axis

Integrate from $x = 0$ (Refer figure 1.4 chapter 1) where $T_m = T_{h,in} = 600K$ to any point x along x axis, where $T_m = T$

$$\int_0^x -\left(h_g \times (T_m - T_s) \times p \times dx\right) = \int_{T_m}^{T} \dot{m} \times C_p \times dT_m \tag{1.3.3}$$

Solving equation 1.3.3 gives equation 1.3.4

$$\therefore T = (600 - T_s) \times e^{\left(\frac{-h_g \times p \times x}{\dot{m} \times C_p}\right)} + T_s \tag{1.3.4}$$

Here,

$\dot{m} = 2.53 \times 10^{-2} \frac{Kg}{s}$

$C_p = 1046.23 \frac{J}{Kg.K}$[20]

$p = 2w = 2 \times 0.5m = 1m$

$h_g = 212.8 \frac{W}{m^2.K}$

$T_s = 293K$

Substituting corresponding values in equation 1.3.4, provides table 1.1.

Table 6.1Temperatue Profile for Exhaust Gas

x(m)	$T(K)$	$T_s(K)$	$T_{avg,plate}(K)$,
5.00E-	4.98E+02	2.93E+02	3.96E+02
1.00E-	4.30E+02	2.93E+02	3.62E+02
1.50E-	3.85E+02	2.93E+02	3.39E+02
2.00E-	3.54E+02	2.93E+02	3.24E+02
2.50E-	3.34E+02	2.93E+02	3.14E+02
3.00E-	3.21E+02	2.93E+02	3.07E+02
3.50E-	3.11E+02	2.93E+02	3.02E+02
4.00E-	3.05E+02	2.93E+02	2.99E+02
4.50E-	3.01E+02	2.93E+02	2.97E+02
5.00E-	2.99E+02	2.93E+02	2.96E+02

1.4 Thermocouple configuration

The total area of TEG heat exchanger plate consists of 10 segments with 0.05m width (x axis) and 1.07m length (y axis) which give the total areas of the plate obtained in section 1.2. Each segment has constant temperature profile depending on the values obtained in Table 1.1.

3. Number of Thermocouples along x axis

   With reference to figure 1.4 (chapter 1) the total breadth of the plate (x axis) with significant $T_{avg,plate}(K)$ is 0.25m for the selected BiTe based material. This conclusion was drawn from 1-d heat transfer analysis along x-axis to obtain the temperature profile. Each segment can fit 2 modules along x axis. Thus the total number of modules along x axis is 10 as 5 out of 10 segments contribute to generate power.

$$\therefore N_x = 5(segments) \times \frac{2(modules)}{1(segments)} = 10\ modules$$

Thus every row (x axis) in heat exchanger plate has10 $modules \times \frac{71(thermocouple)}{1\,module} = 710\ thermocouple.$

4. Number of Thermocouples along y axis

   To determine the number of thermocouple along y axis trial and error method (Refer Section 1.5) will be used to determine the distance along y axis that can be useful to incorporate thermocouples out of 1.07 m.

1.5 Efficiency of TEG Heat Exchanger Plate

The parameters calculated in section 2.4 (chapter 2) will be obtained for entire array of thermocouple to obtain total power output and total heat input to the TEG heat exchanger plate. Also the product of overall heat transfer coefficient, area and log mean temperature difference for parallel flow heat exchanger in section 1.2will provide total heat input to the entire heat exchanger plate.

Again the efficiency of plate can be obtained in two ways,

3. Electrical Power Output to total heat input as shown in section 2.4(chapter 2)
4. Electrical Power Output obtained as mentioned in section 2.4 to total heat input obtained using overall heat transfer coefficient mentioned in section1.2

Close values of efficiency obtained by both the ways for all the selected temperature profile across the plate in section 1.3would indicate the validity of the approach.

Method 1

Efficiency of thermocouple is evaluated at average temperatures as shown in Table1.2.

Table 6.2 Temperature Values

x(m)	Th (K)	Tc (K)	ΔT(K)	Tavg (K)
0	6.0000E+02	2.93E+02		
0.05	4.9838E+02	2.93E+02	2.0538E+02	3.9569E+02
0.1	4.3040E+02	2.93E+02	1.3740E+02	3.6170E+02
0.15	3.8492E+02	2.93E+02	9.1922E+01	3.3896E+02
0.2	3.5450E+02	2.93E+02	6.1496E+01	3.2375E+02
0.25	3.3414E+02	2.93E+02	4.1141E+01	3.1357E+02

Equation 2.4.1(chapter 2) describes figure of merit for single thermocouple. For n number of thermocouple, maximum figure of merit is given by equation 1.5.1

$$Z_{pn} = \frac{\left[|\alpha_n|+|\alpha_p|\right]^2}{K_p \times \rho_p \left(1+\frac{1}{x \times K_{total,pn}}+\frac{x}{\rho_{total,pn}}+\frac{1}{K_{total,pn} \times \rho_{total,pn}}\right)} \qquad (1.5.1)^{[18]}$$

Z_{pn}provides maximum figure of merit as the product of internal resistance and thermal conductivity is minimized by taking derivative with respect to the geometrical ratio of both type of thermo elements to obtain equation 1.5.2. Due to the assumed dimensions geometrical ratio is equal to 1.Also note that the see beck effect from both the elements are added as all the elements are connected in series and they act as a source cell in series.

$$(R.K)_{minimized} = n^2 \times K_p \times \rho_p \left(1+\frac{1}{x \times K_{total,pn}}+\frac{x}{\rho_{total,pn}}+\frac{1}{K_{total,pn} \times \rho_{total,pn}}\right) \qquad (1.5.2)^{[18]}$$

Geometric ratio is $\frac{\Upsilon_n}{\Upsilon_p}$ where,$\Upsilon_p = \frac{A_p}{t_p}$ and$\Upsilon_n = \frac{A_n}{t_n}$,

A= Cross sectional Area of the Element

T= Thickness of Element

$$\Upsilon_{\mathrm{p}} = \frac{\mathrm{A_p}}{\mathrm{t_p}} = \left(\frac{1.4 \times 1.4}{1.14}\right) mm = 1.72mm$$

$$\Upsilon_{\mathrm{n}} = \frac{\mathrm{A_n}}{\mathrm{t_n}} = \left(\frac{1.4 \times 1.4}{1.14}\right) mm = 1.72mm$$

Thus the geometrical ratio in case of selected thermocouple with assumed dimension is 1.

Thermal Conductance, $K_{total,pn} = n \times \left(\frac{\mathrm{A_p} \times K_p}{\mathrm{t_p}} + \frac{\mathrm{A_n} \times K_n}{\mathrm{t_n}}\right)$ (1.5.3)[18]

Internal Resistance, $R_{total,pn} = n \times \left(\frac{\rho_n}{\Upsilon_{\mathrm{n}}} + \frac{\rho_p}{\Upsilon_{\mathrm{p}}}\right)$ (1.5.4)[18]

As discussed in section 2.4 (chapter 2) the ratio of internal and load resistance m' for array of thermocouple is given same as in equation 2.4.5 (chapter 2).

Also external resistance is given as in equation 2.5.5.

$R_{ext} = m' \times R_{total,pn}$ (1.5.5)[18]

Open circuit voltage due to the array of thermocouples in series is obtained as shown by equation 1.5.6 which is the product of combined see beck coefficient, temperature difference and number of thermocouple n as voltage in series arrangements adds to increase the voltage.

$V_{OC} = (\mid \alpha_n \mid + \mid \alpha_p \mid) \times \Delta T \times n$ (1.5.6)[18]

Optimum current is given by equation 1.5.7 and the current stays the same as increase in number of thermocouple increases see beck voltage and internal resistance by same factor.

$$I_{opt} = \frac{(|\alpha_n|+|\alpha_p|)\times \Delta T \times n}{R(m'+1)} \qquad (1.5.7)^{[18]}$$

Electrical power output is obtained by the product of optimum current and load resistance.

$$P_{output} = {I_{opt}}^2 \times R_{ext} \qquad (1.5.8)^{[18]}$$

Factors contributing to transport of energy in case of ‘n’ number thermocouple in series stays the same except for thermo electric effect and total conductance which consists ‘n’ as well. For hot junction heat input is given as in equation 1.5.9.

$$\therefore Q_L = n \times \left(|\ \alpha_n\ | + |\ \alpha_p\ |\right) \times T_h \times I_{opt} + K_{eq} \times \Delta T - \frac{1}{2} \times {I_{opt}}^2 \times R) \qquad (1.5.9)^{[18]}$$

For cold junction heat removed is given as in equation 1.5.10.

$$\therefore Q_{1,L} = n \times \left(|\ \alpha_n\ | + |\ \alpha_p\ |\right) \times T_c \times I_{opt} + K_{eq} \times \Delta T + \frac{1}{2} \times {I_{opt}}^2 \times R) \qquad (1.5.10)^{[18]}$$

Efficiency of thermocouple can be obtained by the ratio of electrical power output to the amount of heat supplied at the hot junction as given in equation 1.5.11.

$$\text{Efficiency, } \eta_{max} = \frac{{I_{opt}}^2 \times R_{ext}}{n \times (|\alpha_n|+|\alpha_p|)\times T_h \times I_{opt} + K_{eq} \times \Delta T - \frac{1}{2} \times {I_{opt}}^2 \times R)} \qquad (1.5.11)^{[18]}$$

Tabulated values of property in table 1.3 correspond to the temperature profile along the plate as shown in Table 1.2. Note that the TEG heat exchanger plate has been divided into 10 segment based on dimension assumed along x axis. Also the average temperature of each segment corresponds to T_{avg}obtain at each 0.05 m segment.

Table 6.3 Properties at Tavg for BiTe material

x(m)	T(avg)K	$\rho_{p(\Omega m)}$	$\rho_{n(\Omega m)}$	α_p(V/k)	α_n(V/k)	K_p(W/K.m)	K_n(W/K.m)
5.00E-02	3.9569E+02	1.3785E-05	1.4172E-05	2.2917E-04	2.1832E-04	1.4485E+00	1.8147E+00
1.00E-01	3.6170E+02	1.2085E-05	1.3056E-05	2.3335E-04	2.2322E-04	1.3499E+00	1.6968E+00
1.50E-01	3.3896E+02	1.0948E-05	1.2122E-05	2.3241E-04	2.2484E-04	1.2840E+00	1.6179E+00
2.00E-01	3.2375E+02	1.0187E-05	1.1415E-05	2.3012E-04	2.2518E-04	1.2399E+00	1.5651E+00
2.50E-01	3.1357E+02	9.6785E-06	1.0904E-05	2.2783E-04	2.2508E-04	1.2104E+00	1.5598E+00

Based on properties obtained in Table 1.3 and equation 1.5.4 the total internal combined resistance of p/n-type is calculated, addition of see beck effect for both the type provides combines see beck coefficient, equation 1.5.3 gives total combined thermal conductance, equation 1.5.1 provides combined figure of merit which is independent of number of thermocouples and temperature values at each segment. Equation 2.4.5 (chapter 2) provided resistance ratio. Repeated calculation for each segment provides all the values for that particular segment of the heat exchanger plate.

Thus as mention in section 1.4 trial and error method will be used until justifiable values for efficiency of module with both method agrees to obtain number of thermocouples along y-axis.

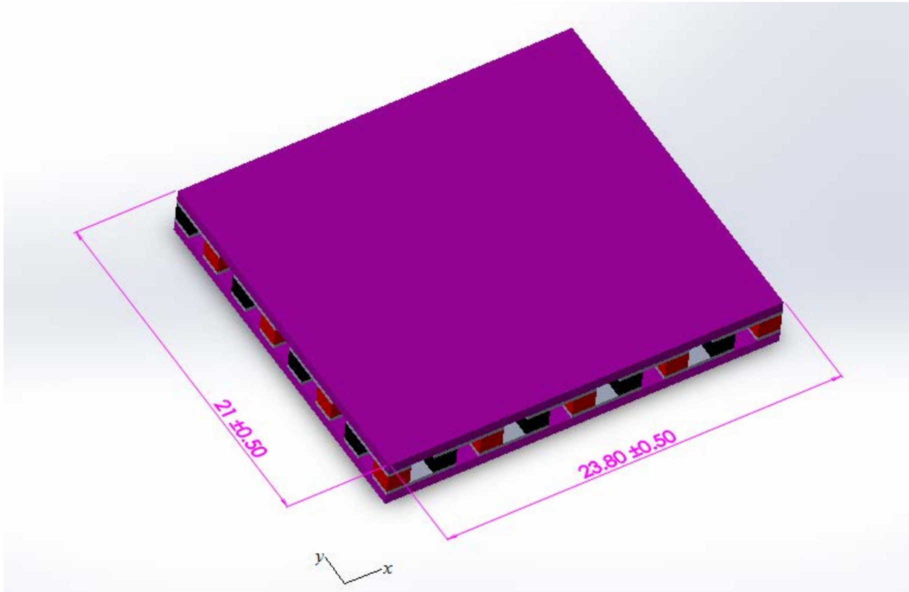

Figure 6.6Dimension of Each module

Trial1:

Let the total number of rows of modules along y axis be 14, $(14 \times 21)mm$ or $0.294m$ out of 1.07m will be used to generate power.

Total number of thermocouples when 0.05m of x axis and 0.294m of y axis for each segment is used to generate power,$n = 2 \times 71 * 14 = 1988$. Also one more module is reduced thus making 1917 thermocouples.

Table 6.4Calculated values at 1917 Thermocouple per Segment

x(m)	$R_{total,pn}(\Omega)$	$\alpha_{pn}(V/k)$	$K_{total,pn}(W/K)$	$Z_{pn}(K^{-1})$	m'
5.0000E-02	3.1159E+01	4.4748E-04	1.0760E+01	2.1950E-03	1.3669E+00
1.0000E-01	2.8020E+01	4.5657E-04	1.0046E+01	2.7215E-03	1.4087E+00
1.5000E-01	2.5713E+01	4.5725E-04	9.5681E+00	3.1231E-03	1.4348E+00
2.0000E-01	2.4076E+01	4.5530E-04	9.2485E+00	3.4212E-03	1.4518E+00
2.5000E-01	2.2940E+01	4.5291E-04	9.1337E+00	3.5978E-03	1.4588E+00

Similarly equation 1.5.6 provides open circuit voltage, 1.5.7 provides optimum current generated by the thermocouple, 1.5.5 provides external resistance, 1.5.8 provides power output from each segment, equation 1.5.9 provides the heat input required for each segment at given temperature. Thus from all of above parameters efficiency is obtained as given in equation 1.5.11.

Table 6.5Calacuated results at 1917 Thermocouple per Segment

x(m)	$V_{oc}(v)$	$I_{opt}(Amps)$	$R_{ext}(ohm)$	$P_{output}(W)$	$Q_{L,Elect.}(W)$	$\eta_{(max)}(\%)$
5.0000E-02	1.7618E+02	2.3889E+00	4.2592E+01	2.4307E+02	3.1422E+03	7.7354E+00
1.0000E-01	1.2026E+02	1.7818E+00	3.9471E+01	1.2532E+02	2.0070E+03	6.2440E+00
1.5000E-01	8.0574E+01	1.2870E+00	3.6892E+01	6.1109E+01	1.2925E+03	4.7281E+00
2.0000E-01	5.3674E+01	9.0928E-01	3.4953E+01	2.8899E+01	8.4013E+02	3.4398E+00
2.5000E-01	3.5720E+01	6.3327E-01	3.3465E+01	1.3421E+01	5.5489E+02	2.4186E+00
				4.7181E+02	7.8367E+03	4.9132E+00

With reference to Table 1.5 it can be concluded that 5 segments of TEG heat exchanger plate each segment consisting of 27 thermo modules or 1917(27×71) thermocouples in series arrangement requires total heat input of$\dot{Q}_{L,Elect} = 7836.7\ W$. But the exhaust heat available from the turbine, $\dot{Q}_L = 7770\ W$. Thus the number of thermocouples should be decreased further to match the exhaust heat available from the turbine.

Trial 2:

Table 1.2 and 1.3 does not change as it is independent of number of thermocouples used. In trial 1, 27 modules were used that exceeded the exhaust heat available compared to required heat input to the thermocouples. Table 1.6 and 1.7 can be obtained in same way as mentioned in Trial 1.

Table 6.6 Calculated Values at 1846 Thermocouple per Segment

x(m)	$R_{total,pn}(\Omega)$	α_{pn}(V/k)	$K_{total,pn}$(W/K)	$Z_{pn}(K^{-1})$	m'
5.0000E-02	3.0005E+01	4.4748E-04	1.0361E+01	2.1950E-03	1.3669E+00
1.0000E-01	2.6982E+01	4.5657E-04	9.6736E+00	2.7215E-03	1.4087E+00
1.5000E-01	2.4761E+01	4.5725E-04	9.2137E+00	3.1231E-03	1.4348E+00
2.0000E-01	2.3185E+01	4.5530E-04	8.9060E+00	3.4212E-03	1.4518E+00
2.5000E-01	2.2090E+01	4.5291E-04	8.7954E+00	3.5978E-03	1.4588E+00

Table 6.7 Calculated Values at 1846 Thermocouple per Segment

x(m)	V_{oc}(v)	I_{opt}(Amps)	R_{ext}(ohm)	P_{output}(W)	$Q_{L,Elect.}$(W)	$\eta_{(max)}$(%)
5.0000E-02	1.6966E+02	2.3889E+00	4.1015E+01	2.3406E+02	3.0259E+03	7.7354E+00
1.0000E-01	1.1580E+02	1.7818E+00	3.8009E+01	1.2068E+02	1.9327E+03	6.2440E+00
1.5000E-01	7.7590E+01	1.2870E+00	3.5526E+01	5.8846E+01	1.2446E+03	4.7281E+00
2.0000E-01	5.1686E+01	9.0928E-01	3.3658E+01	2.7828E+01	8.0901E+02	3.4398E+00
2.5000E-01	3.4397E+01	6.3327E-01	3.2226E+01	1.2924E+01	5.3433E+02	2.4186E+00
				4.5434E+02	7.5465E+03	4.9132E+00

As shown in Table 3.7 for $26\ (13 \times 2)$ thermo modules or $1846\ (13 \times 2 \times 71)$ thermocouples placed in series arrangement requires total heat input of $\dot{Q}_{L,Elect} = 7546.5\ W$ .The exhaust heat available from the turbine, $\dot{Q}_L = 7770\ W$ is sufficient enough to fulfill heat requirement. But this trial cannot be verified until the heat transfer value for these segments or area used to incorporate thermocouple transmits enough heat to fulfill the heat requirement for all the thermocouples in use.

Method 2

In this method the electrical power output obtained is as shown in method 1 but the rate of heat input to the plate is obtained using overall heat transfer coefficient obtained in section 3.2.

Total Area of the TEG Heat Exchanger Plate $= 0.535\ m^2$.

Area of Each Segment, $A_s = \frac{0.535m^2}{10} = 0.0535\ m^2$.

Breadth of Each Segment, $b = 0.05m$

Length of Each Segment, $l = \frac{0.0535m^2}{0.05m} = 1.07m$

Thus from the product of overall heat transfer coefficient, area of each segment and logarithmic temperature difference across the TEG heat exchanger plate heat transfer across all the segment with thermocouples can be obtained as shown in Table 1.8(Refer equation 1.2.5)

Table 6.8QL, overall for Each Segment

x(m)	LMTD(K)	$U_{overall}(W/m^2.K$	$A_s(m^2)$	$Q_{L,Overall}(W)$	$\eta_{(max)}(\%)$
5.0000E-02	2.5280E+02	1.6640E+02	5.3500E-02	2.2505E+03	1.0400E+01
1.0000E-01	1.6912E+02	1.6640E+02	5.3500E-02	1.5056E+03	8.0154E+00
1.5000E-01	1.1314E+02	1.6640E+02	5.3500E-02	1.0072E+03	5.8423E+00
2.0000E-01	7.5692E+01	1.6640E+02	5.3500E-02	6.7384E+02	4.1298E+00
2.5000E-01	5.0638E+01	1.6640E+02	5.3500E-02	4.5080E+02	2.8668E+00
				5.8880E+03	3.1255E+01

Note: Table 1.8 shows total of 5888 Watts of heat will be transferred from all 5 segments consisting of TEG. Remaining heat $\dot{Q}_L - Q_{L,overall} = (7770 - 5888) Watts$ will be transferred from last five segments which is equivalent to 1882 watts.

Also comparison between Table 1.7 and 1.8 indicates that $Q_{L,Elect.}$ in case of 1846 thermocouples exceeds the heat transfer capacity of 5 segments which is 5888 Watts. Thus the number of thermocouple in these 5 segments further needs to be trimmed considering the heat transfer capacity of 5 segments. Array of module required for optimum power output that requires less heat input than $Q_{L,overall}$ is obtained when number of thermocouple is 1420 (20 modules each segment). It can be obtained when 20 thermo modules are arranged in series in each segment. Table 1.9 below shows all the calculated values using both the approach.

Table 6.9Calculated values for 1420 thermocouples per segment

Method1						
x(m)	**$R_{total,pn}$(Ω)**	**α_{pn}(V/k)**	**$K_{total,pn}$(W/K)**	**$Z_{pn}(K^{-1})$**	**m'**	
5.0000E-02	2.3081E+01	4.4748E-04	7.9700E+00	2.1950E-03	1.3669E+00	
1.0000E-01	2.0756E+01	4.5657E-04	7.4412E+00	2.7215E-03	1.4087E+00	
1.5000E-01	1.9047E+01	4.5725E-04	7.0874E+00	3.1231E-03	1.4348E+00	
2.0000E-01	1.7834E+01	4.5530E-04	6.8508E+00	3.4212E-03	1.4518E+00	
2.5000E-01	1.6993E+01	4.5291E-04	6.7657E+00	3.5978E-03	1.4588E+00	
x(m)	**V_{oc}(v)**	**I_{opt}(Amps)**	**R_{ext}(ohm)**	**P_{output}(W)**	**$Q_{L,Elect.}$(W)**	**$\eta_{(max)}$(%)**
5.0000E-02	1.3051E+02	2.3889E+00	3.1550E+01	1.8005E+02	2.3276E+03	7.7354E+00
1.0000E-01	8.9081E+01	1.7818E+00	2.9238E+01	9.2829E+01	1.4867E+03	6.2440E+00
1.5000E-01	5.9685E+01	1.2870E+00	2.7328E+01	4.5266E+01	9.5738E+02	4.7281E+00
2.0000E-01	3.9759E+01	9.0928E-01	2.5891E+01	2.1406E+01	6.2232E+02	3.4398E+00
2.5000E-01	2.6459E+01	6.3327E-01	2.4789E+01	9.9412E+00	4.1103E+02	2.4186E+00
	6.9098E+01	1.4001E+00	2.7759E+01	**3.4949E+02**	**5.8050E+03**	**4.9132E+00**
Method2						
x(m)	**LMTD(K)**	**$U_{overall}$(W/m^2.K**	**A_s(m^2)**	**P_{output}(W)**	**$Q_{L,Overall}$(W**	**$\eta_{(max)}$(%)**
5.0000E-02	2.5280E+02	1.6640E+02	5.3500E-02	1.8005E+02	2.2505E+03	8.0004E+00
1.0000E-01	1.6912E+02	1.6640E+02	5.3500E-02	9.2829E+01	1.5056E+03	6.1657E+00
1.5000E-01	1.1314E+02	1.6640E+02	5.3500E-02	4.5266E+01	1.0072E+03	4.4941E+00
2.0000E-01	7.5692E+01	1.6640E+02	5.3500E-02	2.1406E+01	6.7384E+02	3.1768E+00
2.5000E-01	5.0638E+01	1.6640E+02	5.3500E-02	9.9412E+00	4.5080E+02	2.2052E+00
				3.4949E+02	**5.8880E+03**	**4.8084E+00**

Thus from Table 1.9 it can be shown that average efficiency using both the approach agrees.$Q_{L,Elect.}$is less than $Q_{L,overall}$ which means sufficient heat input is available to the thermocouples. Total electrical power obtained by the use of BiTe based thermocouple is 349.5 Watts. Table 1.9 also shows that arranging all the thermocouple in series the average voltage generated by 5 segments is 69 V and average current generated is 1.4 amps.

1.6 Combined Efficiency of Baseline 10KW Brayton Cycle

Thus table 1.9 shows 349.5 Watts could be saved using TEG heat exchanger. Also section 1.1 shows that efficiency of simple 10KW reversible Brayton cycle is 56.3%.

Total power output using work output from the turbine and electrical power output from the TEG Heat Exchanger is $(10000 + 349.5)\ 10349.5\ Watts$.

Total Heat Input to 10KW Brayton cycle = 17770 Watts.

$$\eta_{combined} = \frac{total\ power\ output}{total\ heat\ intput} = \frac{10349.5}{17770} Watts = 0.5824 \text{ or} 58.24\%$$

Thus with the use of thermocouple overall efficiency has increased by 1.94%.

Calculation for assumed turbine exhaust of 700K

2 Sizing of TEG Module for 10 KW Brayton Cycle

2.1 10KW Baseline Brayton Cycle

Assume:- Isentropic flow, Change in Kinetic Energy/Potential Energy ΔK.E./ΔP.E.≈0, Mass Flow rate $\dot{m}$ is constant, Ideal air assumptions applicable for gas in the cycle, Pressure Ratio of the cycle(compressor and turbine) = 13, Specific heat of gas is not a function of temperature.

Given, Specific Heat Ratio of air, $K = 1.4$ at $T_1 = 300K$

Process 1-2 isentropic compression

$$\left(\frac{T_2}{T_1}\right) = \left(\frac{P_2}{P_1}\right)^{\frac{K-1}{K}} \tag{2.1.1}$$

Pressure Ratio of the cycle, $\left(\frac{P_2}{P_1}\right) = 13.$

Substituting the values for specific heat ratio, pressure ratio and inlet ambient air temperature T_1 in equation 2.1.1 provides exit temperature from the compressor at stage 2, $T_2 = 624.30K$

Process 3-4isentropicexpansion

$$\left(\frac{T_3}{T_4}\right) = \left(\frac{P_3}{P_4}\right)^{\frac{K-1}{K}} \tag{2.1.2}$$

Substituting the values for specific heat ratio, pressure ratio and exit gas temperature from the turbine exhaust $T_4 = 700K$inlet temperature to the turbine,$T_3 = 1456.7K$.

Specific Turbine Work, $\mathrm{w_T}$

$$w_T = (h_3 - h_4)\frac{KJ}{Kg} \tag{2.1.3}$$

Specific enthalpy of gas at turbine inlet,$h_3 = 1582.9\ \frac{KJ}{Kg}@1456.7K[19]$

Specific enthalpy of gas at turbine exit, $h_4 = 713.27\ \frac{KJ}{Kg}@700K[19]$

Substituting the values for enthalpy of gas at 1456.7K and 700K provides specific turbine work of $869.6\frac{KJ}{Kg}$.

Specific Compressor Work, $\mathrm{w_c}$

$$w_c = (h_2 - h_1)\frac{KJ}{Kg} \tag{2.1.4}$$

Specific enthalpy of gas at compressor exit, $h_2 = 632.61\ \frac{KJ}{Kg}@624.30K[19]$

Specific enthalpy of gas at turbine exit, $h_1 = 300.19\ \frac{KJ}{Kg}@300K[19]$

Substituting the values for specific enthalpy of gas, compressor work $w_c = (h_2 - h_1)\frac{KJ}{Kg} = 332.42\frac{KJ}{Kg}$.

Network from Turbine, $\mathrm{W_{Net}}$

$$w_{Net} = w_T - w_C \tag{2.1.5}$$

Substituting values from equation 2.1.3 and 2.1.4 network from turbine obtained is$537.18\frac{KJ}{Kg}$.

Mass flow rate in the cycle is given by equation 2.1.6

$$W_{Net,T} = w_{Net} * \dot{m} \tag{2.1.6}$$

$$W_{Net,T} = 10KW$$

Substituting the value of specific network form the turbine and total network from the turbine, the mass flow rate of the gas in the cycle is obtained, $\dot{m} = 1.86 \times 10^{-2}\frac{Kg}{s}$.

Heat Input to the Heat Exchanger,Q_H

$$Q_H = \dot{m}(h_3 - h_2)KW \tag{2.1.7}$$

Substituting mass flow rate of the gas, specific enthalpy of gas at turbine inlet and compressor exit, the rate of heat input to the combustion chamber,$Q_H = 17.67\ KW$

Heat dissipated Q_L from the cycle

$$Q_L = Q_H - W_{Net,T} \tag{2.1.8}$$

Substituting the value of rate of heat input to the combustion chamber and rate of total network performed by the turbine in equation 2.1.8, the total rate of heat dissipated from the cycle, $\dot{Q}_L = 7.67KW$.

Heat Dissipated from Baseline 10KW Brayton cycle

Figure 2.1 illustrates the Brayton cycle, where stage 1 to 2 indicate adiabatic reversible compression, stage 2 to 3 indicate constant pressure heat addition and stage 3 to 4 indicate adiabatic reversible expansion. Pressure and temperature at each stage is given below,

$T_1 = 300K$

$P_1 = 1\ atm$

$T_2 = 624.30K$

$P_2 = 13\ atm$

$T_3 = 1456.7K$

$P_3 = 13\ atm$

$T_4 = 700K$

$P_4 = 1\ atm$

Thermal Efficiency of the cycle $\eta = \frac{W_{Net,T}}{Q_H} = \frac{10\ KW}{17.67\ KW} = 0.566\ or\ 56.6\%$

Note: TEG heat exchanger discards most of the heat from turbine and produces some electrical work while constant temperature cooling water flows at $293K$on cooling side.

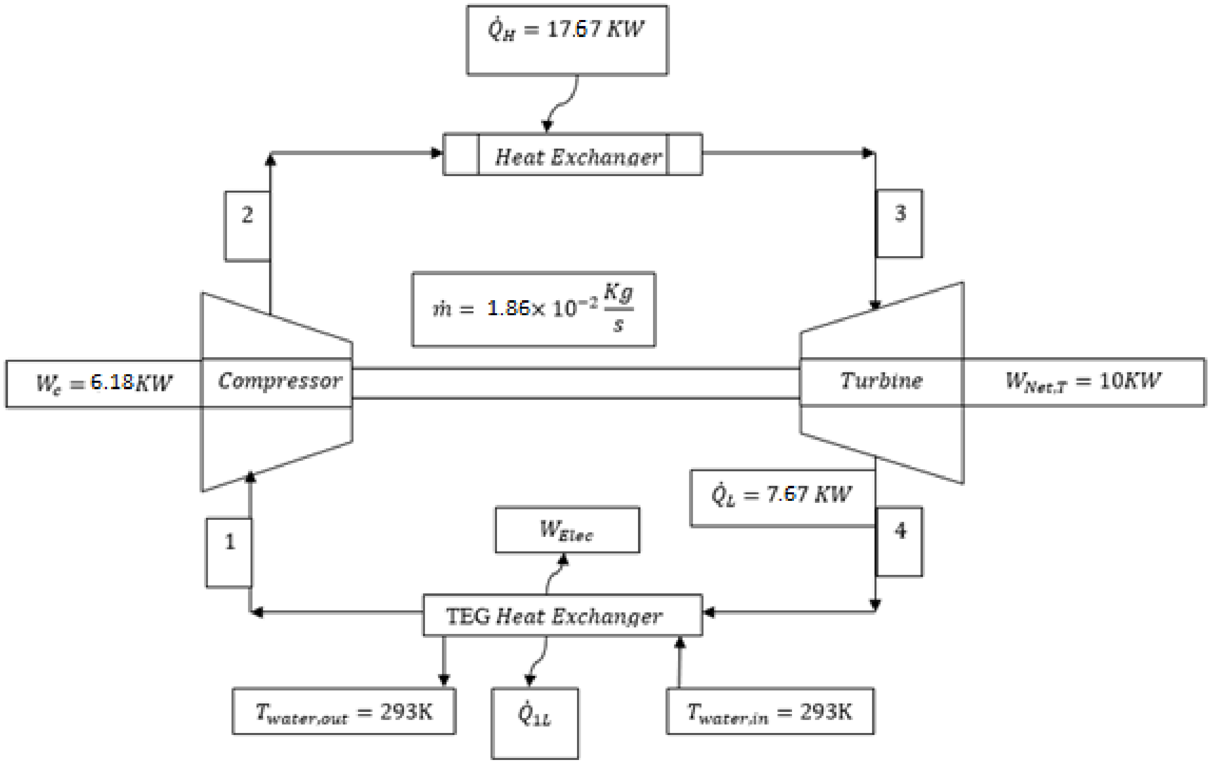

Figure 6.7Schematic Diagram of Proposed Cycle

2.2 Determination of Overall Heat Exchanger Area

Heat is transferred from hot fluid to the ceramic wall by convection and through the wall by conduction and into the semiconductor legs by conduction. Again heat flows towards the cold fluid by convection. Any radiation effects are neglected in determining the overall heat transfer coefficient.

Assume: Heat transfer is in normal direction to the flat plate surface. Ceramic walls on the hot and cold side are nearly isothermal. Lateral heat flow is zero, all sides are well insulated. The temperature of water and gas is constant thus it is 1-d heat transfer process.

Energy balance

Rate of heat transfer into the ceramic hot side – Rate of heat transfer out of the ceramic cold side = Rate of electrical work produced from TEG heat exchanger

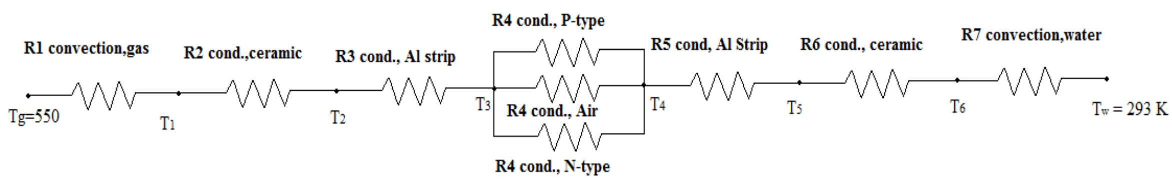

Figure 6.8Thermal Resistance Circuit for TEG Heat Exchanger

Convection resistance for flow of hot gas,$R_1 = \frac{1}{h_1 A_1}$

Conduction resistance for ceramic plate,$R_2 = \frac{t_2}{K_2 A_2}$

Conduction resistance for aluminum strip,$R_3 = \frac{t_3}{K_3 A_3}$

Conduction resistance for P-type thermo element,$R_4 = \frac{t_4}{K_4 A_4}$

Conduction resistance for air gap between thermo elements,$R_4{}' = \frac{t_4{}'}{K_4{}' A_4{}'}$

Conduction resistance for N-type thermo elements,$R_4{}'' = \frac{t_4{}''}{K_4{}'' A_4{}''}$

Conduction resistance for aluminum strip, $R_5 = \frac{t_5}{K_5 A_5}$

Conduction resistance for ceramic plate, $R_6 = \frac{t_6}{K_6 A_6}$

Convection resistance for flow of cooling water, $R_7 = \frac{1}{h_7 A_7}$

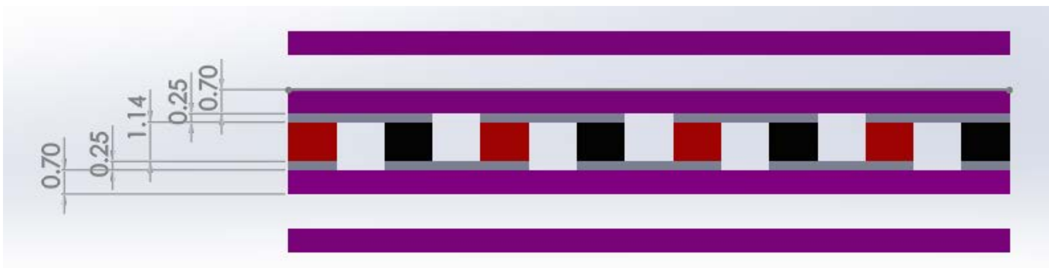

Figure 6.9Side View of TEG module

As shown in figure 2.3 gap between parallel ceramic plate is 1.4mm, thickness of ceramic plate is $t_2 = t_6 = 0.7mm$, thickness of aluminum conducting strip is $t_3 = t_5 = 0.25mm$, thickness of thermo elements $t_4 = t_4'' = 1.14mm$, thickness of air gap between thermo element is $\boldsymbol{t_4}' = (1.14 + 0.25)\text{mm} = 1.39\text{mm}$. Using these assumed value based on literature survey on geometry of thermo electric moduleoverall heat transfer coefficient can be calculated provided all the thermo physical properties are available.

Parameters for all thermal resistance from R_1 to R_7 are known except their corresponding area and convection/conduction coefficient.

1. Convection coefficient for flow of hot gas, h_1

   The Dittus-Boelter equation used for turbulent flow is used to calculate Nusselt number. This equation provides less accurate values if the bulk fluid temperature difference between cold and hot fluid is large. Exhaust temperature from turbine at T_4 is inlet temperature for TEG heat exchanger as $T_{hot,in}$ for TEG heat exchanger, $T_{hot,in} = 700K$.

Given mass flow rate of hot gas, $\dot{m} = 1.86 \times 10^{-2} \frac{Kg}{s}$

Specific heat at constant pressure $C_p = 1034.85 \frac{J}{Kg.K}$ [20]

$T_{hot,out} = ?$

$$Q_L = \dot{m} \times C_p \times (T_{hot,in} - T_{hot,out}) \tag{2.2.1}$$

Thus substituting values in equation 2.2.1, $T_{hot,out}$ for TEG heat exchanger is $500.76K$

Bulk fluid temperature is average of $T_{hot,in}$ and $T_{hot,out}$ i.e. 500.76K

Properties at Bulk fluid temperature 500.76K

1	Density of hot gas, ρ_{air} [20]	$0.7053 \frac{Kg}{m^3}$
2	Dynamic viscosity of hot gas, μ_{air} [20]	$2.69 \times 10^{-5} \frac{Kg}{ms}$
3	Prandtl number, Pr [19]	0.6777
4	Thermal Conductivity[20]	$0.03945 \frac{W}{mK}$
5	Dynamic viscosity of hot gas, μ_{air} at 293K	$1.82 \times 10^{-5} \frac{Kg}{ms}$

Assumed duct size for flow of gas,

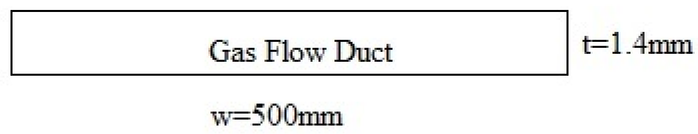

Figure 6.10Duct for Hot Exhaust Gas

Hydraulic Diameter, $D_h = 2 \times t = 2.8mm$

Gas Velocity,

$$V_{avg} = \frac{\dot{m}}{A_c \times \rho_{air}} \tag{2.2.2}$$

Substituting the values for mass flow rate, flat plate cross sectional area and density of gas at bulk fluid temperature provides $37.67\frac{m}{s}$.

Reynolds Number,

$$Re = \frac{\rho_{air} \times V_{avg} \times D_h}{\mu_{air}} \tag{2.2.3}$$

Substituting the values for density of gas, velocity from equation 2.2.2, hydraulic diameter and viscosity Reynolds number obtained is 2765.5. Thus the flow of gas on the hot side is transitional. Levenspiel equation can be used in case of transitional flow[23].

$$Nu = 0.116\left(Re^{\frac{2}{3}} - 125\right)Pr^{1/3}\left(1 + \left(\frac{D_h}{L}\right)^{2/3}\right)\left(\frac{\mu_{bulk\,temp.}}{\mu_{wall\,temp.}}\right) \tag{2.2.4}$$

Substituting values for Re and Pr number in equation 2.2.4, nusselt number obtained is 11.2.

Also, Convective heat transfer coefficient $h_1 = \frac{K_1 \times Nu}{D_h} = 157.8 \frac{W}{m^2 \times K}$

2. Conduction coefficient for ceramic plate, K_2

   Thermal conductivity for ceramic plate at bulk fluid temperature of 500.71K on hot side is $20.1\ \frac{W}{m.K}$[21]

3. Conduction coefficient for aluminum strip, K_3

   Thermal conductivity for aluminum conducting strip at bulk fluid temperature of 500.7K on hot side is $236 \frac{W}{m.K}$[22]

4. Conduction coefficient for P-type thermo element, K_4

   Since the thermo element is exposed to two different hot and cold bulk fluid temperatures, thermal conductivity is determined at average temperature of two sides, $T_{avg} = \frac{(500.71+293)K}{2} = 396.85K$.

   $K_4 = 1.45 \frac{W}{m.K}$[17]

5. Conduction coefficient for N-type thermo elements, K_4''

   Thermal conductivity at $T_{avg} = 396.85K$

   $K_4'' = 1.82 \frac{W}{m.K}$[17]

6. Conduction coefficient for air gap between thermo elements, K_4'

   Air gap is exposed to two different hot and cold bulk fluid temperatures, thermal conductivity is determined at average temperature of two sides, $T_{avg} = 396.85K$.

$K_4{}' = 0.0327 \frac{W}{m.K}$[21]

7. Conduction resistance for aluminum strip, K_5

   Thermal conductivity for aluminum conducting strip at cold fluid temperature of 293K on cold side is $236.72 \frac{W}{m.K}$[22]

8. Conduction resistance for ceramic plate, K_6

   Thermal conductivity for ceramic plate at cold fluid temperature of 293K is $35.11 \frac{W}{m.K}$[21]

9. Convection resistance for flow of cooling water, h_7

   Bulk fluid temperature is used to apply Dittus-Boelter equation for calculating the convective heat transfer coefficient on cold side.

   Assume ΔT_w on cool side to be 10K.

   Average efficiency of TEG at $396.8K$ obtained with calculation similar to section 2.4 (chapter 2) shows to be 7.78%. Thus approximate electrical power generated at T_{avg} is $7.78\%\ of \dot{Q}_L = 0.0778 \times 7.67KW = 596.72W$

   Specific heat at constant pressure $C_{p,w} = 4194 \frac{J}{Kg.K}$ [19]

   Mass flow rate of cooling water in TEG heat exchanger,

   $$\dot{m}_w = \frac{(\dot{Q}_L - 596.72)W}{C_{p,w} \times \Delta T_w} \tag{2.2.5}$$

   Thus $\dot{m}_w$ for TEG heat exchanger is $0.17 \frac{Kg}{s}$

Properties at bulk fluid temperature $\left[\frac{(283+293)K}{2}\right] 288K$ [20].

1	Density of water, ρ_{water}	$999 \frac{Kg}{m^3}$
2	Dynamic viscosity of cold water, μ_{water}	$1.138 \times 10^{-3} \frac{Kg}{ms}$
3	Thermal Conductivity, K_{water}	$0.589 \frac{W}{mK}$

Assumed duct size for flow of water,

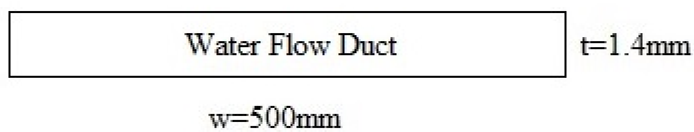

Figure 6.11Duct for Cooling Water

Hydraulic Diameter, $D_h = 2 \times t = 2.8mm$

Gas Velocity,

$$V_{avg} = \frac{\dot{m}}{A_c \times \rho_{water}} \tag{2.2.6}$$

Substituting the values for mass flow rate, flat plate cross sectional area and density of gas at bulk fluid temperature provides $0.24 \frac{m}{s}$.

Reynolds Number,

$$Re = \frac{\rho_{air} \times V_{avg} \times D_h}{\mu_{air}} \tag{2.2.7}$$

Substituting the values for density of gas, velocity from equation 2.2.6, hydraulic diameter and viscosity Reynolds number obtained is 590.Thus the flow of gas on the cold side is laminar. For laminar flow inside rectangular duct the nusselt number $Nu = 7.54$ [20, Table 8-1].Also convective heat transfer coefficient for flow of water, $h_w = \frac{K_w \times Nu}{D_h} = 1586.09 \frac{W}{m^2 \times K}$.

The relation for Overall heat transfer coefficient is given by equation 2.2.8

$$Q_L = U_{overall} \times A_{Total} \times \Delta T_{LMTD} \tag{2.2.8}$$

A_{Total} is the total area required to transfer 7670 W of heat from the TEG heat exchanger. Equation 2.2.8 is also given as $Q_L = \frac{\Delta T_{LMTD}}{R_{total}}$.

$$\therefore R_{total} = \frac{1}{U_{overall} \times A_{Total}} = \frac{1}{h_1 A_1} + \frac{t_2}{K_2 A_2} + \frac{t_3}{K_3 A_3} + R_{eq,module} + \frac{t_5}{K_5 A_5} + \frac{t_6}{K_6 A_6} + \frac{1}{h_7 A_7} \tag{2.2.9}$$

$R_{eq,module}$ is total thermal resistance due to P-type, N-type and air gap between thermo elements. All the thermo elements are arranged thermally in parallel orientation whereas electrically in series. First $R_{eq,couple}$ is obtained,

$$\frac{1}{R_{eq,couple}} = \frac{1}{R_4} + \frac{1}{R_4'} + \frac{1}{R_4''}$$

$$\frac{1}{R_{eq,couple}} = \frac{K_4 A_4}{t_4} + \frac{K_4' A_4'}{t_4'} + \frac{K_4'' A_4''}{t_4''}$$

Given, $t_4' = 1.39\text{mm}, t_4 = t_4'' = 1.14\text{mm}$

$$\therefore let\ t_4 = t_4'' = t$$

$$\frac{1}{R_{eq,couple}} = \frac{K_4 A_4 + K_4'' A_4''}{t} + \frac{K_4' A_4'}{t_4'}$$

$$R_{eq,couple} = \frac{t \times t_4{}'}{t_4{}'(K_4 A_4 + K_4{}'' A_4{}'') + t \times K_4{}' A_4{}'} \quad (2.2.10)$$

Each module has 71 thermocouple. The thermal conductance for n number of thermocouple is given by equation 2.2.11.

$$K = n \times (K_P + K_N) \quad (2.2.11)$$

Similarly equivalent thermal resistance for n thermocouple in a module is given by equation 2.2.12.

$$R_{eq,module} = \frac{1}{n} \times \left[\frac{t \times t_4{}'}{t_4{}'(K_4 A_4 + K_4{}'' A_4{}'') + t \times K_4{}' A_4{}'}\right] \quad (2.2.12)$$

Substituting equation 2.2.12 and equation 2.2.9 gives equation 2.2.13

$$\therefore R_{total} = \frac{1}{U_{overall} \times A_{Total}} = \frac{1}{h_1 A_1} + \frac{t_2}{K_2 A_2} + \frac{t_3}{K_3 A_3} + \frac{1}{71} \times \left[\frac{t \times t_4{}'}{t_4{}'(K_4 A_4 + K_4{}'' A_4{}'') + t \times K_4{}' A_4{}'}\right] + \frac{t_5}{K_5 A_5} + \frac{t_6}{K_6 A_6} + \frac{1}{h_7 A_7} \quad (2.2.13)$$

Note: Relation between total area and individual resistance area for each material is developed based on assumed dimension for a single module to obtain overall heat transfer coefficient (Refer chapter 1 and chapter 3).

1. $A_{Total} = A_1 = A_2 = A_6 = A_7$ (uniform areas across each thermal resistance in module)

2. A_3 is area of lower Aluminum strip (Refer figure 3.3 chapter 3).

   Let a be area equivalent to cross-sectional area of each thermo element. For each thermoelectric module consisting of 71 thermocouple (Refer figure 1.4 chapter 1) the relation between area of required ceramic plate or A_{Total} and $A_3$for a module is given underneath.

$A_{Total} = 15 \times 17 \times a = 255a$

Number of thermo elements along x axis is 15 and 17 along y axis (Refer figure 1.4 chapter 1).

$$\therefore a = \frac{A_{Total}}{255} \quad (2.2.14)$$

$A_3 = 107a$

$$\therefore a = \frac{A_3}{107} \quad (2.2.15)$$

Equating2.2.14 and 2.2.15gives equation 2.2.16.

$$A_3 = \frac{A_{Total} \times 107}{255} \quad (2.2.16)$$

Note: Above relationship exists for entire TEG heat exchanger plate as multiple numbers of modules in series arrangement builds the plate.

3. $A_4 = A_4' = A_4'' = a$ is cross sectional area of n-type, p-type and air gap in between.

$$\therefore R_{eq,module} = \left(\frac{1}{71 \times a}\right) \times \left[\frac{t \times t_4'}{t_4'(K_4 + K_4'') + t \times K_4'}\right] \quad (2.2.17)$$

Equation2.2.14 and 2.2.17 give equation 2.2.18.

$$\therefore R_{eq,module} = \left(\frac{255}{71 \times A_{Total}}\right) \times \left[\frac{t \times t_4'}{t_4'(K_4 + K_4'') + t \times K_4'}\right] \quad (2.2.18)$$

4. $A_5$is area of upper Aluminum strip (Refer 3.3 chapter 3).

$A_5 = 3 \times 36 \times a = 108a$ (Each thermocouple junction formed by upper aluminum strip is 3 times area of each thermo element and each module has 36 thermocouple as seen from the top)

$$A_5 = 108a \tag{2.2.19}$$

Equation 2.2.14 and 2.2.19gives equation 2.2.20.

$$A_5 = \frac{108 \times A_{Total}}{255} \tag{2.2.20}$$

Substitute all the relation obtained from 1 to 4 gives final equation for overall thermal resistance as shown in equation 2.2.21.

$$\therefore R_{total} = \frac{1}{U_{overall} \times A_{Total}} = \frac{1}{h_1 A_{Total}} + \frac{t_2}{K_2 A_{Total}} + \frac{t_3 \times 255}{K_3 \times A_{Total} \times 107} + \left(\frac{255}{71 \times A_{Total}}\right) \times \left[\frac{t \times t_4'}{t_4'(K_4 + K_4'') + t \times K_4'}\right] + \frac{t_5 \times 255}{K_5 \times 108 \times A_{Total}} + \frac{t_6}{K_6 A_{Total}} + \frac{1}{h_7 A_{Total}} \tag{2.2.21}$$

$$\therefore R_{total} = \frac{1}{U_{overall}}$$

$$= \frac{1}{h_1} + \frac{t_2}{K_2} + \frac{t_3 \times 255}{K_3 \times 107} + \left(\frac{255}{71}\right) \times \left[\frac{t \times t_4'}{t_4'(K_4 + K_4'') + t \times K_4'}\right]$$

$$+ \frac{t_5 \times 255}{K_5 \times 108} + \frac{t_6}{K_6} + \frac{1}{h_7} = \frac{1}{U_{overall}}$$

$$= (0.0063 + 0.000035 + 0.0000025 + 0.001242 + 0.000001056$$

$$+ 0.00001993 + 0.0006304) \frac{m^2 \times K}{W}$$

Substitute corresponding heat transfer coefficients and thickness, values obtained in second, third, fifth, sixth and seventh terms are negligible compared to values in first and fourth terms. Thus the value of overall heat transfer coefficient obtained is $132.6 \frac{W}{m^2.K}$

Assume Parallel TEG Heat Exchanger

Counter flow heat exchanger can transfer more energy than parallel heat exchanger as the exit temperature of the cooling fluid can get close to high temperature of the hot fluid (parallel temperature profile). In case of parallel heat exchanger the temperature difference is high at the entrance region and later the two fluids tend to meet same temperature point at exit region (converging temperature profile) depending on the design parameters.

Thus temperature difference in case of parallel heat exchanger at entrance region is high. If thermo electric generators are placed in the region of higher temperature difference more electrical power is obtained. Also note that efficiency of TEG is directly proportional to temperature difference across the two junctions of the TEG material. Thus parallel heat exchanger is selected and log mean temperature difference is used to find the total area required for the TEG heat exchanger.

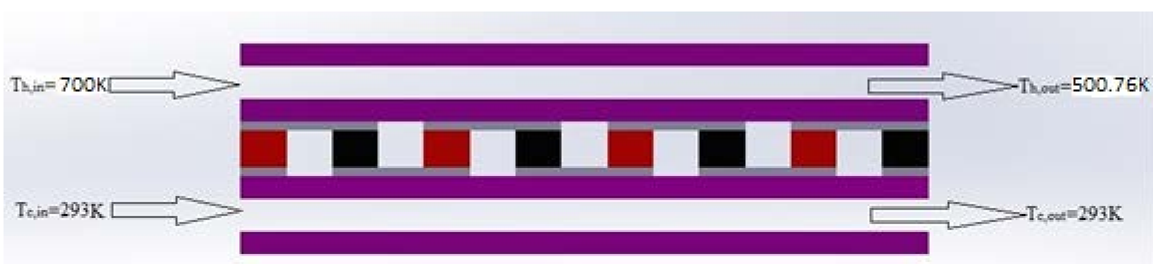

Using equation 2.2.8, the total area required for the heat transfer can be obtained.

$$7670W = 132.6\frac{W}{m^2.K} \times A_{Total,plate} \times \frac{(T_{h,o} - T_{c,o}) - (T_{h,in} - T_{c,in})}{ln\left[\frac{(T_{h,o}-T_{c,o})}{(T_{h,in}-T_{c,in})}\right]}$$

$$7670W = 132.6\frac{W}{m^2.K} \times A_{Total,plate} \times \frac{[(500.76 - 293) - (700 - 293)]K}{ln\left[\frac{(500.76-293)}{(700-293)}\right]}$$

$$\therefore A_{Total,plate} = 0.195\, m^2$$

2.3 Temperature Profile across TEG Heat Exchanger Plate

Temperature profile of water across the plate on cool side is assumed to be constant at 293K. Thus the temperature profile for exhaust gas on the hot side can be obtained using constant wall temperature method.

$$\dot{Q}_{conv,gas} = \dot{m} \times C_p \times dT_m \quad (2.3.1)$$

Also from Newton's law of cooling $\dot{Q}_{conv,gas} = h_g \times (T_s - T_m) \times dA$ and $(T_s - T_m)$ is the temperature difference between the surface and the fluid. Since $T_s < T_m$ or the exhaust gas will cool thus it gives equation 2.3.2.

$$-\left(h_g \times (T_m - T_s) \times dA\right) = \dot{m} \times C_p \times dT_m$$

$$-\left(h_g \times (T_m - T_s) \times p \times dx\right) = \dot{m} \times C_p \times dT_m \quad (2.3.2)$$

Where,

Perimeter of the duct, $p = 2 \times (w \times t)$, but $(w \gg t)$ (Refer figure 3.4) $\therefore p = 2w$

T_s= Constant wall temperature

T_m = Mean hot exhaust gas temperature

h_g = Average convective heat transfer coefficient of hot exhaust gas

dT_m = Decrease in mean temperature of hot exhaust gas

T = Temperature at any pointalong the plate in x axis

Integrate from $x = 0$ (Refer figure 1.4 chapter 1) where $T_m = T_{h,in} = 700K$ to any point x along x axis, where $T_m = T$

$$\int_0^x -\left(h_g \times (T_m - T_s) \times p \times dx\right) = \int_{T_m}^{T} \dot{m} \times C_p \times dT_m \qquad (2.3.3)$$

Solving equation 2.3.3 gives equation 2.3.4

$$\therefore T = (700 - T_s) \times e^{\left(\frac{-h_g \times p \times x}{\dot{m} \times C_p}\right)} + T_s \qquad (2.3.4)$$

Here,

$\dot{m} = 1.86 \times 10^{-2} \frac{Kg}{s}$

$C_p = 1046.23 \frac{J}{Kg.K}$[20]

$p = 2w = 2 \times 0.5m = 1m$

$h_g = 157.8 \frac{W}{m^2.K}$

$T_s = 293K$

Substituting corresponding values in equation 2.3.4, provides table 2.1.

Table 6.10Temperatue Profile for Exhaust Gas

x(m)	$T(K)$	$T_s(K)$	$T_{avg,plate}(K)$,
0.05	5.64E+02	293	4.29E+02
0.1	4.74E+02	293	3.83E+02
0.15	4.14E+02	293	3.53E+02
0.2	3.73E+02	293	3.33E+02
0.25	3.47E+02	293	3.20E+02
0.3	3.29E+02	293	3.11E+02
0.35	3.17E+02	293	3.05E+02
0.4	3.09E+02	293	3.01E+02
0.45	3.04E+02	293	2.98E+02
0.5	3.00E+02	293	2.97E+02

2.4 Thermocouple configuration

The total area of TEG heat exchanger plate consists of 10 segments with 0.05m width (x axis) and 0.39m length (y axis) which give the total areas of the plate obtained in section 2.2. Each segment has constant temperature profile depending on the values obtained in Table 2.1.

1. Number of Thermocouples along x axis

   With reference to figure 1.4(chapter1) the total breadth of the plate (x axis) with significant $T_{avg,plate}(K)$ is 0.3m for selected BiTe based material. This conclusion was drawn from 1-d heat transfer analysis along x-axis to obtain the temperature profile. Each segment can fit 2 modules along x axis. Thus the total number of modules along x axis is 12 as 6 out of 10 segments contribute to generate power.

$$\therefore N_x = 6(segments) \times \frac{2(modules)}{1(segments)} = 12\, modules$$

Thus every row (x axis) in heat exchanger plate

has$12\ modules \times \frac{71(thermocouple)}{1\ module} = 852\ thermocouple$

2. Number of Thermocouples along y axis

   To determine the number of thermocouple along y axis trial and error method (Refer Section 2.5) will be used to determine the distance along y axis that can be useful to incorporate thermocouples out of 0.39 m.

2.5 Efficiency of TEG Heat Exchanger Plate

The parameters calculated in section 2.4(chapter 2) will be obtained for entire array of thermocouple to obtain total power output and total heat input to the TEG heat exchanger plate. Also the product of overall heat transfer coefficient, area and log mean temperature difference for parallel flow heat exchanger in section 2.2 will provide total heat input to the entire heat exchanger plate.

Again the efficiency of plate can be obtained in two ways,

1. Electrical Power Output to total heat input as shown in section 2.4(chapter 2)
2. Electrical Power Output obtained as mentioned in section 2.4 to total heat input obtained using overall heat transfer coefficient mentioned in section 2.2.

Close values of efficiency obtained by both the ways for all the selected temperature profile across the plate in section 2.3would indicate the validity of the approach.

Method 1

Efficiency of thermocouple is evaluated at average temperatures as shown in Table2.2.

Table 6.11 Temperature Values

x(m)	Th (K)	Tc (K)	ΔT(K)	Tavg (K)
0.05	5.64E+02	2.93E+02	2.71E+02	4.29E+02
0.1	4.74E+02	2.93E+02	1.81E+02	3.83E+02
0.15	4.14E+02	2.93E+02	1.21E+02	3.53E+02
0.2	3.73E+02	2.93E+02	8.04E+01	3.33E+02
0.25	3.47E+02	2.93E+02	5.36E+01	3.20E+02
0.3	3.29E+02	2.93E+02	3.57E+01	3.11E+02

Equation 2.4.1(chapter 2) describes figure of merit for single thermocouple. For n number of thermocouple, maximum figure of merit is given by equation 2.5.1.

$$Z_{pn} = \frac{\left[|\alpha_n|+|\alpha_p|\right]^2}{K_p \times \rho_p \left(1+\frac{1}{x \times K_{total,pn}}+\frac{x}{\rho_{total,pn}}+\frac{1}{K_{total,pn} \times \rho_{total,pn}}\right)} \qquad (2.5.1)$$ [18]

Z_{pn} provides maximum figure of merit as the product of internal resistance and thermal conductivity is minimized by taking derivative with respect to the geometrical ratio of both type of thermo elements to obtain equation 2.5.1. Due to the assumed dimensions geometrical ratio is equal to 1.Also note that the see beck effect from both the elements are added as all the elements are connected in series and they act as a source cell in series.

$$(R.K)_{minimized} = n^2 \times K_p \times \rho_p \left(1 + \frac{1}{x \times K_{total,pn}} + \frac{x}{\rho_{total,pn}} + \frac{1}{K_{total,pn} \times \rho_{total,pn}}\right) \quad (2.5.2)$$ [18]

Geometric ratio is $\frac{\Upsilon_n}{\Upsilon_p}$ where, $\Upsilon_p = \frac{A_p}{t_p}$ and $\Upsilon_n = \frac{A_n}{t_n}$,

A= Cross sectional Area of the Element

T= Thickness of Element

$$\Upsilon_p = \frac{A_p}{t_p} = \left(\frac{1.4 \times 1.4}{1.14}\right) mm = 1.72mm$$

$$\Upsilon_n = \frac{A_n}{t_n} = \left(\frac{1.4 \times 1.4}{1.14}\right) mm = 1.72mm$$

Thus the geometrical ratio in case of selected thermocouple with assumed dimension is 1.

Thermal Conductance, $K_{total,pn} = n \times \left(\frac{A_p \times K_p}{t_p} + \frac{A_n \times K_n}{t_n}\right)$ (2.5.3)[18]

Internal Resistance, $R_{total,pn} = n \times \left(\frac{\rho_n}{\Upsilon_n} + \frac{\rho_p}{\Upsilon_p}\right)$ (2.5.4)[18]

As discussed in section 2.4 (chapter 2) the ratio of internal and load resistance m' for array of thermocouple is given same as in equation 2.4.5 (chapter 2).

Also, the external resistance is given as in equation 2.5.5.

$R_{ext} = m' \times R_{total,pn}$ (2.5.5)[18]

Open circuit voltage due to the array thermocouple in series is obtained as shown by equation 2.5.6 which is the product of combined see beck coefficient, temperature difference and number of thermocouple n as voltage in series arrangements adds to increase the voltage.

$$V_{OC} = (|\ \alpha_n\ | + |\ \alpha_p\ |) \times \Delta T \times n \qquad (2.5.6)^{[18]}$$

Optimum current is given by equation 2.5.7 and the current stays the same as increase in number of thermocouple increases see beck voltage and internal resistance by same factor.

$$I_{opt} = \frac{(|\alpha_n| + |\alpha_p|) \times \Delta T \times n}{R(m' + 1)} \qquad (2.5.7)^{[18]}$$

Electrical power output is obtained by the product of optimum current and load resistance.

$$P_{output} = {I_{opt}}^2 \times R_{ext} \qquad (2.5.8)^{[18]}$$

Factors contributing to transport of energy in case of ‘n’ number of thermocouple in series stays the same except for thermo electric effect and total conductance which consists ‘n’ as well. For hot junction heat input is given as in equation 2.5.9.

$$\therefore Q_L = n \times (|\ \alpha_n\ | + |\ \alpha_p\ |) \times T_h \times I_{opt} + K_{eq} \times \Delta T - \frac{1}{2} \times {I_{opt}}^2 \times R) \qquad (2.5.9)^{[18]}$$

For cold junction heat removed is given as in equation 2.5.10.

$$\therefore Q_{1,L} = n \times (|\ \alpha_n\ | + |\ \alpha_p\ |) \times T_c \times I_{opt} + K_{eq} \times \Delta T + \frac{1}{2} \times {I_{opt}}^2 \times R) \qquad (2.5.10)^{[18]}$$

Efficiency of thermocouple can be obtained by the ratio of electrical power output to the amount of heat supplied at the hot junction as given in equation 1.5.11

Efficiency, $\eta_{max} = \frac{I_{opt}{}^2 \times R_{ext}}{n \times (|\alpha_n| + |\alpha_p|) \times T_h \times I_{opt} + K_{eq} \times \Delta T - \frac{1}{2} \times I_{opt}{}^2 \times R)}$ (2.5.11)[18]

Tabulated values of property in table 2.3 corresponds to the temperature profile along the plate as shown in Table 2.2. Note that the TEG heat exchanger plate has been divided into 10 segment based on dimension assumed along x axis. Also the average temperature of each segment corresponds to T_{avg} obtain at each 0.05 m segment.

Table 6.12 Properties at T_{avg} for BiTe material

x(m)	Tavg (K)	ρ_p(Ωm)	ρ_n(Ωm)	α_p(V/k)	α_n(V/k)	K_p(W/K.m)	K_n(W/K.m)
0.05	4.29E+02	1.5433E-05	1.4937E-05	2.1872E-04	2.1073E-04	1.5441E+00	1.9291E+00
0.1	3.83E+02	1.3172E-05	1.3808E-05	2.3144E-04	2.2042E-04	1.4130E+00	1.7722E+00
0.15	3.53E+02	1.1665E-05	1.2728E-05	2.3335E-04	2.2397E-04	1.3256E+00	1.6676E+00
0.2	3.33E+02	1.0660E-05	1.1862E-05	2.3170E-04	2.2504E-04	1.2673E+00	1.5979E+00
0.25	3.20E+02	9.9900E-06	1.1220E-05	2.2930E-04	2.2517E-04	1.2284E+00	1.5514E+00
0.3	3.11E+02	9.5434E-06	1.0763E-05	2.2713E-04	2.2501E-04	1.2025E+00	1.5204E+00

Based on properties obtained in Table 2.3 and equation 2.5.4 the total internal combined resistance of p/n-type is calculated, addition of see beck effect for both the type provides combines see beck coefficient, equation 2.5.3 gives total combined thermal conductance, equation 2.5.1 provides combined figure of merit which is independent of number of thermocouples and temperature values at each segment. Equation 2.4.5 (chapter 2) provided resistance ratio. Repeated calculation for each segment provides all the values for that particular segment of the heat exchanger plate.

Thus as mention in section 2.4 trial and error method will be used until justifiable values for efficiency of module with both method agrees to obtain number of thermocouples along y-axis.

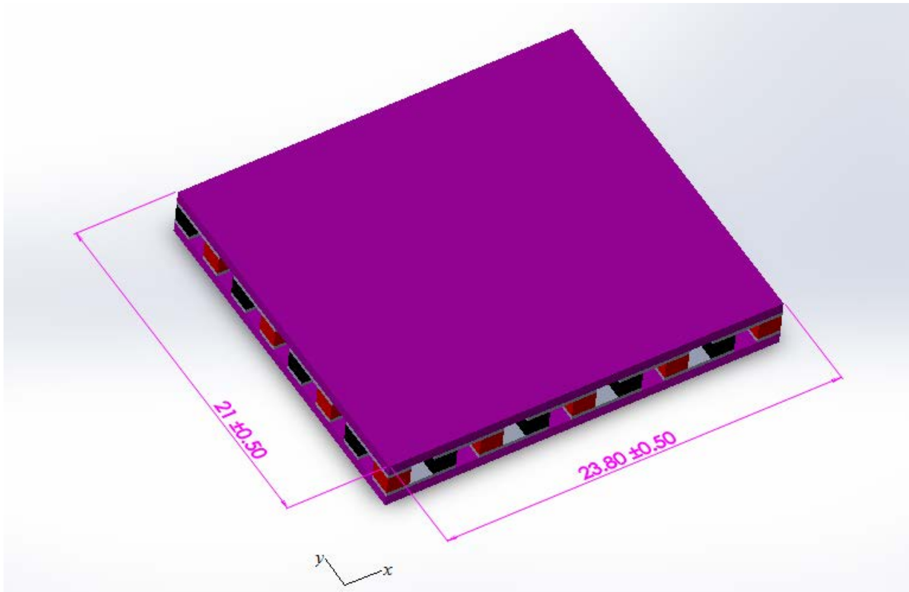

Figure 6.12Dimension of Each module

Trial1:

Let the total number of rows of modules along y axis be 3, $(3 \times 21)mm$ or $0.063m$ out of 0.39m will be used to generate power but last row consists of one less module.

Total number of thermocouples when 0.05m of x axis and 0.063m of y axis is used to generate power,$n = (2 \times 3 - 1) \times 71 = 355$. Also one more module is reduced thus making 355 thermocouples.

Table 6.13Calculated values at 355 Thermocouple per Segment

x(m)	$R_{total,pn}(\Omega)$	$\alpha_{pn}(V/k)$	Ktotal,pn(W/K)	$Z_{pn}(K^{-1})$	m'
0.05	6.2683E+00	4.2945E-04	2.1208E+00	1.7484E-03	1.3227E+00
0.1	5.5687E+00	4.5187E-04	1.9449E+00	2.3759E-03	1.3824E+00
0.15	5.0346E+00	4.5732E-04	1.8276E+00	2.8645E-03	1.4185E+00
0.2	4.6485E+00	4.5674E-04	1.7495E+00	3.2328E-03	1.4412E+00
0.25	4.3777E+00	4.5448E-04	1.7017E+00	3.4943E-03	1.4552E+00
0.3	4.1912E+00	4.5213E-04	1.6626E+00	3.6971E-03	1.4661E+00

Similarly equation 2.5.6 provides open circuit voltage, 2.5.7 provides optimum current generated by the thermocouple, 2.5.5 provides external resistance, 2.5.8 provides power output from each segment, equation 2.5.9 provides the heat input required for each segment at given temperature. Thus from all of above parameters efficiency is obtained as given in equation 2.5.11.

Table 6.14Calacuated results at 355 Thermocouple per Segment

x(m)	$V_{oc}(V)$	$I_{opt}(Amps)$	$R_{ext}(\Omega)$	$P_{output}(W)$	$Q_{L,Elect}.(W)$	$\eta_{(max)}\%$
0.05	4.1366E+01	2.8413E+00	8.2909E+00	6.6930E+01	7.9459E+02	8.4233E+00
0.1	2.9018E+01	2.1872E+00	7.6982E+00	3.6828E+01	5.0477E+02	7.2960E+00
0.15	1.9579E+01	1.6080E+00	7.1414E+00	1.8465E+01	3.2187E+02	5.7368E+00
0.2	1.3036E+01	1.1488E+00	6.6996E+00	8.8412E+00	2.0714E+02	4.2682E+00
0.25	8.6479E+00	8.0461E-01	6.3702E+00	4.1241E+00	1.3479E+02	3.0597E+00
0.3	5.7357E+00	5.5493E-01	6.1446E+00	1.8922E+00	8.8047E+01	2.1491E+00
				1.3708E+02	2.0512E+03	5.1555E+00

With reference to Table 2.5 it can be concluded that 6 segments of TEG heat exchanger plate each segment consisting of 5 thermo modules or 355(5×71) thermocouples in series arrangement requires total heat input of$\dot{Q}_{L,Elect} = 2051.2\ W$. The exhaust heat available from the turbine is $\dot{Q}_L = 7670\ W$. In trial 1, 5 modules were used in each segment that underlie the exhaust heat available from turbine.

As shown in Table 2.5 for 5 thermo modules or 355 thermocouples placed in series arrangement in each segment requires total heat input of $\dot{Q}_{L,Elect} = 2051.2W$.This trial cannot be verified until the heat transfer value for these segments or area used to incorporate thermocouple transmits enough heat to fulfill the heat requirement for all the thermocouples in use.

Method 2

In this method the electrical power output obtained is as shown in method 1 but the rate of heat input to the plate is obtained using overall heat transfer coefficient obtained in section 3.2.

Total Area of the TEG Heat Exchanger Plate $= 0.195\ m^2$.

Area of Each Segment, $A_s = \frac{0.195m^2}{10} = 0.0195\ m^2$.

Breadth of Each Segment, $b = 0.05m$

Length of Each Segment, $l = \frac{0.0195m^2}{0.05m} = 0.39m$

Thus from the product of overall heat transfer coefficient, area of each segment and logarithmic temperature difference across the TEG heat exchanger plate heat transfer across all the segment with thermocouples can be obtained as shown in Table 2.8(Refer equation 2.2.5)

Table 6.15 $Q_{L, overall}$ for Each Segment

x(m)	LMTD(K)	$U_{overall}(W/m^2.K)$	$A_s(m^2)$	$Q_{L,Overall}(W)$	$\eta_{(max)}\%$
0.05	3.3460E+02	1.3260E+02	1.9500E-02	8.6995E+02	7.6936E+00
0.1	2.2307E+02	1.3260E+02	1.9500E-02	5.7998E+02	6.3499E+00
0.15	1.4871E+02	1.3260E+02	1.9500E-02	3.8666E+02	4.7756E+00
0.2	9.9145E+01	1.3260E+02	1.9500E-02	2.5778E+02	3.4298E+00
0.25	6.6097E+01	1.3260E+02	1.9500E-02	1.7185E+02	2.3998E+00
0.3	4.4066E+01	1.3260E+02	1.9500E-02	1.1457E+02	1.6516E+00
				2.3808E+03	4.3834E+00

Note: Table 2.6 shows total of 2380 Watts of heat will be transferred from all 6 segments consisting of TEG. Remaining heat $\dot{Q}_L - Q_{L,overall} = (7670 - 2380) Watts$ will be transferred from last five segments which is equivalent to 5290 watts.

Also comparison between Table 2.5 and 2.6 indicates that $Q_{L,Elect.}$ in case of 355 thermocouples in each segment does not exceed the heat transfer capacity of 6 segments which is 2380 Watts. Array of module required for optimum power output that requires less heat input than $Q_{L,overall}$ is obtained when number of thermocouple is 355 (5 modules each segment). It can be obtained when 5 thermo modules are arranged in series in each segment. It can be shown that average efficiency using both the approach is very close. $Q_{L,Elect.}$ is less than $Q_{L,overall}$ which means sufficient heat input is available to the thermocouples. Total electrical power obtained by the use of BiTe based thermocouple is 137 Watts.

2.6 Combined Efficiency of Baseline 10KW Brayton Cycle

Thus table 2.5 shows 349.5Watts could be saved using TEG heat exchanger. Also section 2.1 shows that efficiency of simple 10KW reversible Brayton cycle is 56.6%.

Total power output using work output from the turbine and electrical power output from the TEG Heat Exchanger is $(10000 + 137)\ 10137\ Watts$.

Total Heat Input to 10KW Brayton cycle = 17670Watts.

$$\eta_{combined} = \frac{total\ power\ output}{total\ heat\ intput} = \frac{10137}{17670} Watts = 0.5736 \text{or} 57.36\%$$

Thus with the use of thermocouple overall efficiency has increased by 0.76%.